Republic of Iraq

Ministry of Higher Education and

Scientific Research

University of Anbar

College of Science

Department of Applied Geology

Engineering applications of the Ground Penetrating Radar method in Fallujah city

A thesis

Submitted to the College of Science / University of Anbar in Partial Fulfillment of the Requirements for the Degree of Master Of Science in Applied Geology

By

Zeyad Najeh Abed Al-Hameed

B. SC. In Applied Geology 2019

Supervised by

Prof. Dr. Ali Mishaal Abed

Dr. Hayder Abdul Zahra Al-dabbagh

2022 A.D **1444 A.H**


قال اللّه تعالى :
يَرْفَعِ اللهُ الَّذِينَ آمَنُوا
مِنكُمْ وَالَّذِينَ
أُوتُوا الْعِلْمَ
دَرَجَاتٍ
(المجادلة : 11)

Supervisor Certification

We certify that the preparation of this thesis entitled " **Engineering applications of the Ground Penetrating Radar method in Fallujah city**" was made under our supervision by **Zeyad Najeh Abed Al-Hameed** and submitted in partial fulfillment of requirements for the degree of Master of Science presented to Department of Applied Geology / Collage of Science / University of Anbar.

Signature:
Name : Dr. Ali Mishaal Abed
Scientific Titled: Professor
Address: College of Science / technology
University of Anbar
Date: / / 2022

Signature:
Name Hayder Abdul Zahra Al-dabbagh
Scientific Titled: Doctor
Address: Ministry of science and
Date: / / 2022

Approved by the head of the Department of Applied Geology.

In view of the available recommendation, I forward this dissertation for debate by the examining committee.

Signature:
Name : Dr. Abed Saleh Faiyad
Scientific Titled: Professor
Address: Department of Applied Geology - College of Science - University of Anbar
Date: / / 2022

Approved by the Dean of the College of Science.

Signature:
Name: Dr. Emad A. M. Salih
Scientific Title: Professor
Address: Dean of the College of Science / University of Anbar
Date: / / 2022

Committee Certification

We attest that we read this thesis, that the student was subjected to a thorough examination of its contents by the examining committee, and that in our opinion it qualifies for the degree of Master of Science in Applied Geology.

Signature:
Name:
Scientific Title: Professor
Address:
Date: / / 2022
(Chairman)

Signature:
Name:
Scientific Title:
Address:
Date: / / 2022
(Member)

Signature:
Name:
Scientific Title:
Address:
Date: / / 2022
(Member)

Signature:
Name:
Scientific Title: Professor
Address:
Date: / / 2022
(Member and Supervisor)

Signature:
Name:
Scientific Title:
Address:
Date: / / 2022
(Member and Supervisor)

Dedication

To my love: my father, mother

To my brothers

To my Teachers

To my Friends

To everyone who thinks and seeks to advance knowledge everywhere

I dedicate this humble effort

Zeyad

Acknowledgments

I thank Allah Almighty for making it possible for me to complete this study, and for making it easy for the worshiper of the weak the possible and the impossible.

Thanking Allah Almighty is not complete except by thanking His servants who helped me a lot so that this work appears in this way, and for this I present:

With sincere thanks and appreciation to Professor Ali Mishaal Abed and Dr. Haider Abed al-Zahra al-Dabbagh, firstly for accepting the assignment of the scientific management of this memorandum, and secondly for making every effort they can for the sake of scientific and literary supervision throughout the study period.

I also extend my sincere thanks and appreciation to the group of respected professors who seemed to me the best by providing a hand of scientific and moral assistance, especially the respected two respected academically and literary gentlemen: Mr. Ahmed Omran Abdul Karim / Ministry of Science and Technology/ Geophysical Center, and Dr. Muhammad Mohsen Ali Al-Hameedawi /General Authority for Ground Water.

I also extend my heartfelt thanks to my father and mother who stood with me and supported me throughout my studies.

Thanks are due to the Dean of the College of Sciences, Prof. Dr. Emad A. M. Salih, the Head of the Applied Geology Department, Prof. Dr. Abed Saleh Faiyad due to the opportunity that was given to me to obtain a master's. And I would like to express my deep gratitude to the teaching staff in department of applied Geology, College of Science, University of Anbar for their kind help and cooperation through the different stages of my study.

To everyone who helped me from near or from a far, a letter of thanks, appreciation and gratitude that I convey to you through this study.

Zeyad

Abstract

Ground Penetrating Radar (GPR) technology has been used in Fallujah, Anbar Governorate as a non-destructive, fast, low cost and powerful method in detecting any change in the components of subsurface materials which can therefore be applied in urban and facility areas. The main objective of this study is to simulate shallow geometry probe GPR data obtained by 250 and 500 MHz antennas. . This work is carried out in five different sites, in each site, 5 lines were selected, and the length and directions of the lines vary from site to site, and the distance between the lines is 5 meters. The collected GPR data was imported and processed using ReflexW^{TM} which is a standalone package program that can import a range of different data types. Depending on the type of antenna, the penetration depth ranges from 3 to 6 meters in the study area. Various buried objects, areas of weakness, and voids were detected at shallow depths. And the discovery of areas of weakness is represented by the fragility of soil and shallow groundwater, which affects the foundations of civil buildings in the city.

After processing the radar data, an anomaly was detected at each survey site. Due to the shallower contact and greater contrast between the loose and compacted soil layers, the first interface becomes more visible in all antenna profiles at 250 and 500 MHz. A characteristic reflection also appears after interpretation of the GPR data and is believed to represent buried objects close to the surface. Due to the shallowness of groundwater and its ascent near the surface, many areas of weakness show, represented by voids.

Table of content

No.	Subject	pages
	Chapter one (Introduction)	1-7
1.1	preface	1
1.2	Location of the study area	1
1.3	Tectonic and Geological of the study area	2
1.4	Previous studies	4
1.4.1	Previous studies in World	4
1.4.2	previous studied in Iraq	5
1.5	Aim of the study	7
	Chapter two (Theoretical background)	8-52
2-1	Preface	8
2.2	GPR Method	9
2.3	Electromagnetic Theory	10
2.3.1	Maxwell's Equations	11
2.3.1.1	Faraday's Law	12
2.3.1.2	Ampere's Circuital Law	12
2.2.1.3	Magnetic Gauss Theorem	13
2.3.1.4	Electric Gaussian Theorem (Gauss's Law in electric)	13
2.4	Propagation of radio wave	13
2.4.1	Velocity	13
2.4.2	Attenuation	14
2.4.3	Scattering	15
2.4.3.1	Spectral reflection	15
2.4.3.2	Refraction	16
2.4.3.3	Diffraction	16
2.4.3.4	Resonant scattering	16
2.4.4	polarization	17

2.4.5	Penetration depth	18
2.4.6	Resolution	20
2.4.6.1	vertical Resolution	22
2.4.6.2	Horizontal Resolution	22
2.5.	Surface-based Reflection of GPR Configuration	23
2.5.1	Velocity analysis by direct wave travel time	24
2.5.2	Central Frequency	25
2.6	GPR Survey parameters	25
2.6.1	Antenna frequency	26
2.6.2	Sample number	27
2.6.3	Sampling interval	28
2.6.4	Trace interval	28
2.6.5	Time window	28
2.7	GPR Data Processing	29
2.7.1	Data Editing	30
2.7.2	Basic Processing	30
2.7.3	Advanced Data Processing	31
2.7.4	Visualization Processing	31
2.8	Filtering Tools	31
2.8.1	Subtract mean (Dewow)	32
2.8.2	Time zero correction	33
2.8.3	Background Removal	33
2.8.4	Bandpass filter	34
2.8.5	Time Gain	35
2.9	Data Display and Interpretation	37
2.10	instrumentation	39
2.10.1	RAMAC/GPR system	39
2.10.1.1	Control Unit CU II	39

2.10.1.2	Shielded antennas	41
2.10.1.3	The MALÅ (RAMAC) XV Monitor	42
2.10.1.4	Rough Terrain cart	44
2.11	Instrument calibration	45
2.12	The modes of GPR	46
2.13	GPS Instrument	46
2.14	Field work	47
	Chapter three (Data Processing and Interpretation)	53-75
3.1	Preface	53
3.2	GPR data processing	53
3.2.1	Data Editing	54
3.2.2	ReflexW software program	54
3.2.3	Basic Processing:	55
3.3	Result and Interpretation of GPR profiles	56
3.3.1	Antenna 250 MHz	57
3.3.2	Antenna 500 MHz	67
3.4	Discussion	74
	Chapter four (conclusion and recommendations)	76-77
4.1	conclusion	76
4.2	recommendations	77
	References	78
	Appendices	I-x

Table of Figures

Fig.No	Figure Title	Pages
1.1	location of study area	2
1.2	Tectonic map of study area	3

2.1	schematic diagram of a GPR System	10
2.2	Propagation of Electromagnetic wave	11
2.3	Scattering mechanisms	17
2.4	Vertical and horizontal polarization of an electromagnetic wave	18
2.5	Two-way travel time of GPR signal	19
2.6	Temporal pulses with half Width W.	21
2.7	Vertical and Horizontal resolution.	22
2.8	Sketch of the Step Size	23
2.9	EM signals paths between transmitting and receiving antennae for the airwave, the ground wave and reflected waves	24
2.10	A typical overview of the GPR dataset flow	30
2.11	Dewow filter correction on a raw GPR trace	32
2.12	Changing in a time-zero position is an example	33
2.13	(A) GPR profile before background removal (B) GPR profile after background removal	34
2.14	Time Gain filter.	36
2.15	Explain how a one-dimensional trace changes when an antenna is relocated and many traces are stacked side-by-side to form a two-dimensional cross section	37
2.16	control unit CU II	40
2.17	control unit CU II battery	41
2.18	RAMAC/GPR antenna (250MHz).	42
2.19	The MALÅ(RAMAC) XV Monitor.	43
2.20	Battery pack and battery bag of the XV Monitor.	43
2.21	Rough Terrain Cart (RTC)	44
2.22	RAMAC/GPR Instrument	45
2.23	Common off set mode	46

2.24	GPS Instrument	47
2.25	Aerial photograph show five sites are chosen within the study area.	48
2.26	Schematic diagram of fieldwork procedure in site one	49
2.27	grid survey within the site one.	49
2.28	Schematic diagram of fieldwork procedure in site two.	50
2.29	Schematic diagram of fieldwork procedure in site three.	51
2.30	**:** Schematic diagram of fieldwork procedure in site four.	51
2.31	Schematic diagram of fieldwork procedure in site five	52
3.1	Raw data of GPR profile (1), before processing.	54
3.2	GPR data processing flow using ReflexW.	55
3.3	show the applying of the basic processing stage for the raw data of antenna 250 MHz.	56
3.4	show radargram profile (1) of antenna 250 MHz for site one.	57
3.5	show profile (2) of antenna 250MHz for site one.	58
3.6	show profile (5) of antenna 250MHz for site one.	58
3.7	Grid survey within the site one	59
3.8	A pool of water flowing through 10 meter deep	60
3.9	(A) show profile (8) and (B) show profile (9)of antenna 250 for site two.	60
3.10	profile (12) of antenna 250MHz for site two.	61
3.11	Profile (14) transverse path of antenna 250 MHz for site two	61

3.12	(A)show profile (15) and (B) profile (16) of antenna 250MHz for site Three.	62
3.13	profile (17) of antenna 250MHz for site Three.	62
3.14	profile (23) of antenna 250MHz for site four.	63
3.15	profile (25) of antenna 250MHz for site four.	64
3.16	profile (26) of antenna 250MHz for site four.	64
3.17	Profile (28) transverse path of antenna 250 MHz for site four	65
3.18	profile (29) of antenna 250MHz for site five.	65
3.19	profile (31) of antenna 250MHz for site five.	66
3.20	profile (32) of antenna 250MHz for site five.	66
3.21	Profile (35) transverse path of antenna 250 MHz fore site five	67
3.22	(A) show profile (36) and (B) show profile (37) of antenna 500 MHz for site one.	68
3.23	profile (38) of antenna 500 MHz for site one.	68
3.24	Profile (41) transverse path of antenna 500 MHz for site one	68
3.25	(A) profile (43) and (B) profile (44) of antenna 500MHz for site two.	69
3.26	profile (47) of antenna 500 MHz for site two.	69
3.27	(A) profile (50) and (B) profile (51) of antenna 500MHz for site three.	70
3.28	Profile (52) of antenna 500 MHz for site three.	71
3.29	Profile (57) of antenna 500 MHz for site four.	71
3.30	(A) profile (58) and (B) profile (60) of antenna 500 MHz for site four.	72
3.31	(A) profile (64) and (B) profile (65) of antenna 500 MHz for site five.	72
3.32	Profile (67) of antenna 500 MHz for site five.	73

3.33	Profile (70) transverse path of antenna 500 MHz for site five	73
3.34	Soil sections of site three.	75

List of tables

Table No.	Title	Pages
2.1	Antenna frequency (MHz), the lower limit of object target size (m), approximate depth range (m) and approximate penetration depth (m) (Operating manual of RAMAC, 2009).	20
2.2	lists the antenna survey parameters (taken from Annan, 2005; MAL, 2005; Ortyl, 2006).	27

Table of Abbreviations

Abbreviations	Description
GPR	Ground Penetrating Radar
EM	Electromagnetic
CMP	Common midpoint
FOM	fixed offset method
WARR	wide-angle Reflection and refraction
H	magnetic field
E	electric field
emf	Electromagnetic field
σ	electrical conductivity
ε	dielectric constant

μ	magnetic permittivity
ρ	electrical resistivity
RDP	Relative Dielectric Permittivity
PRF	Pulse repetition frequency
TWTT	two-way travel time
T0	Time zero
FFT	fast Fourier transform
AGC	Automatic Gain Control
SEC	Spreading & Exponential Calibrated Compensate
SNR	signal-to-noise ratio

chapter one

Introduction

1.1 preface:

Engineering geophysics is the research of subsurface materials and structures that may have engineering implications using geophysical technologies (Reynolds 1997). Geophysics tries to figure out a body's internal composition and structure, as well as the nature of the processes that form the visible features on the surface (Matzner, 2001). Ground penetrating radar (GPR) is a non-destructive geophysical technology for photographing the subsurface at high resolution. It can thus be utilized in urban and sensitive situations (Kearey et al., 2002; Griffin and Pippett 2002). The GPR geophysical technology, which was first developed for high resolution subsurface imaging is now commonly used to assess the condition of foundations, pavements, concrete slabs, and walls.

1.2 Location of the study area:

The study area is located within the administrative boundaries of the Fallujah city it is located between latitudes (33° 21' 9" - 33° 17' 47" N) and longitudes (43° 49' 33" - 43° 44' 58" E) (Figure 1.1). The GPR survey is conducted in five stations were selected within the study.

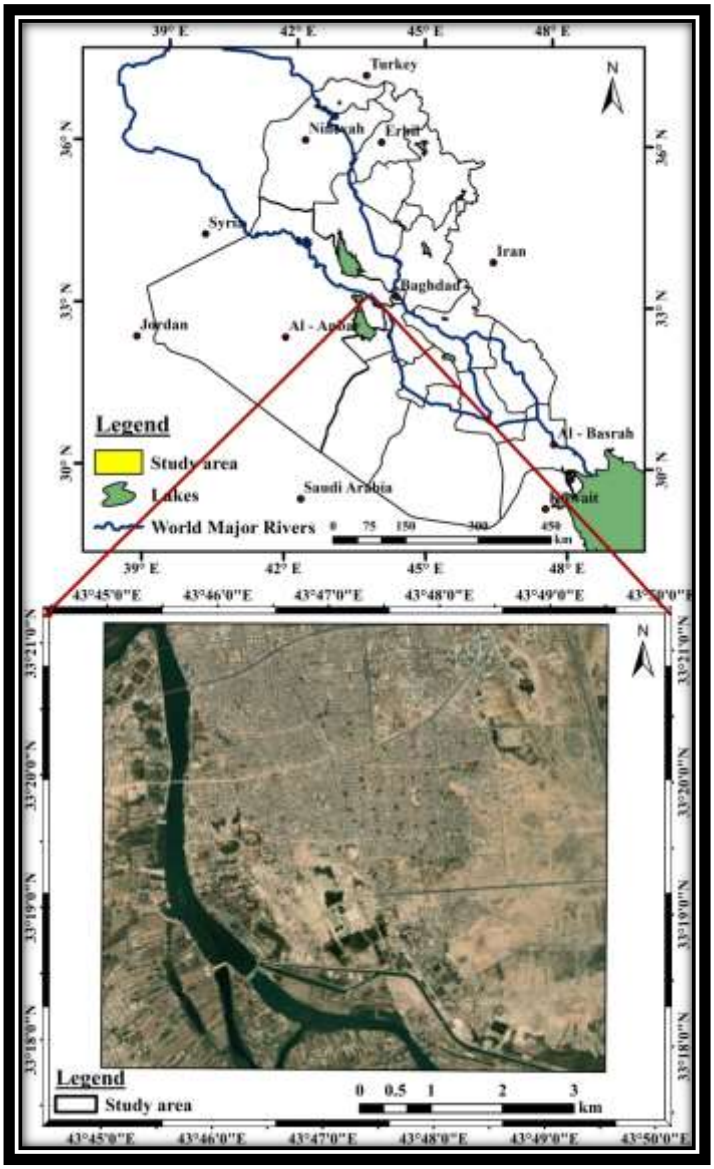

Fig.1.1: location of study area

1.3 Tectonic and Geological of the study area:

According to (Fouad, 2015)the study area is Located with two tectonics platform as a shown in (Fig. 1.2).

• The Inner Platform: Characterized by the no significant Permo Triassic rifting. The Alpine compressional deformation can be recognized in the studied area which represented by the Western Desert Subzone at the Northwest of this part (Fouad, 2015). This classification based on the physiography of the area. At the same time, the study area is at the transition tectonic zone.

• The Outer Platform: The main part of the Mesozoic Arabian plate passive margin and the Late Cretaceous foreland basin. It is significantly involved in the Alpine orogenic deformation (Fouad, 2015).

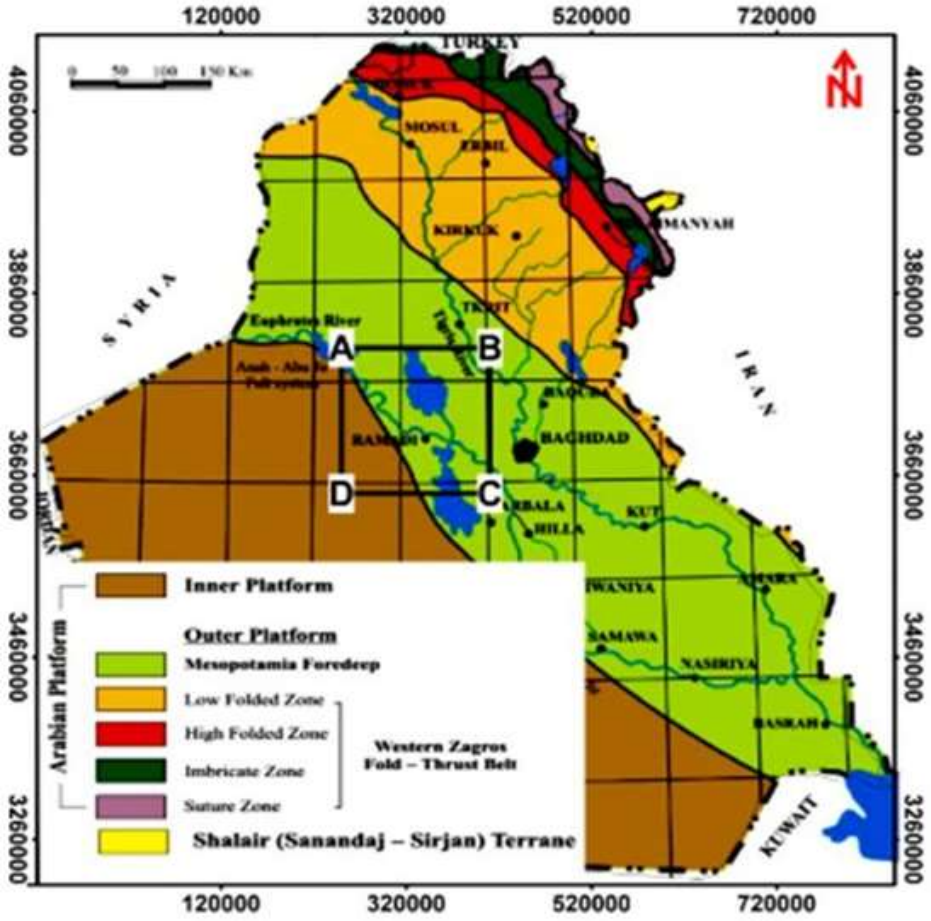

Fig. 1-2: Tectonic map of study area (Buday and Jassim, 1987)

Quaternary Deposits: The deposits of Salah Aldin & Al Anbar governorate outcrops, which reach the Euphrates River and consist of sand, shale, clay, and gravel in some sections, particularly Pleistocene deposits in the northern half of the investigated area. As we got closer to the Euphrates River, the thickness of these deposits changed and rises in density, (Buday and Jassim, 1987).

1.4 Previous studies:

1.4.1 Previous studies in World:

Loulizi, 2001 used GPR method to determine the dielectric properties of concrete over the GPR frequency range, synthesize reflected air-coupled radar signals, and compare them to measured waveforms. He modeled and studied the effects of simulated defects in concrete on the reflected air-coupled and ground-coupled radar signals, and validate the research results in the field by predicting layer thicknesses of flexible pavements.

Harris, 2006 Defined the GPR technique for determining pavement thickness along with evaluating the technique. The findings of this study indicate that the procedure of measuring pavement thickness with GPR has not improved to the point where a qualified GPR interpreter is no longer required. The GPR system used for the investigation included a number of systematic flaws.

Chen, 2006 created simulation software for electromagnetic difficulties including coupling, antenna design, antenna placement analysis, micro strip design, scattering analysis, and so on. In comparison to standard absorptive GPR antennas, the exceptionally low permittivity and conductivity of the expanded polystyrene dielectric region used in this design have demonstrated to have a substantially higher radiation efficiency. From 450MHz onwards, it has an efficiency of 50% or more, but absorptive antennas have a trade-off of losing half their efficiency in order to achieve the half-hemisphere radiation effect.

Khuut, 2009 detected and discriminated the target at shallow depth, the polarimetric GPR system developed by the Sato Laboratory at Tohoku University, Japan, is proposed and assessed. The fact that the biggest reflections occur when the polarization of the electric field is parallel to the item causing reflection was explained in this study, which also

demonstrated how sensitivity to subsurface reflections might be improved. These findings, on the other hand, demonstrate how to lessen susceptibility to undesired reflections from objects on or above the surface.

1.4.2 Previous studies in Iraq:

Al-Khafaji, 2010 evaluated geotechnical utilizing a seismic cross-hole technique survey, GPR survey, drilling, and sampling to evaluate soil properties beneath Al-Abbas sacred holy shrine. The antennas used in this study are 250 MHz and 500 MHz. Due to the substantial absorption of electromagnetic waves within the saturated clay layer, GPR data resolution did not reach seven meters in depth. As a result, the high-resolution antenna reaches a depth of (2.5) m. (500MHz). The GPR and cross-hole seismic measurements in the studied region correspond to depths ranging from 1 to 7 m. The GPR scan reveals the assigned buried objects, such as graves, at shallow depths.

Saeed, 2010 used GPR to locate subsurface bodies at the Jadriya location at Baghdad University. The electrical resistivity approach was compared with the GPR method (with 250MHz, 500MHz, and 800MHz antennas). This test indicates that the 800MHz antenna is the best for detecting at a depth of 1 m, whereas the 250MHz and 500MHz antennas can only detect these bodies with clear dielectric contrast and big diameters, According to this research, the 500MHz frequency is the optimum for detecting subsurface structures at depths of 4 to 5 m.

Al-dami,2011 used ground-penetrating radar (GPR), In The university of Technology-Baghdad, as a non-destructive, rapid, low-cost, and

strong tool for detecting any change in the composition of subsurface materials, which may then be applied in urban and built areas. The study's main goals are to replicate GPR data obtained by 250 and 500 MHz antennas for shallow engineering investigations by detecting various buried bodies, investigating foundations, and evaluating the quality of reinforced concrete. The study suggests that the 500 MHz antenna could be used to investigate and detect the underlying reinforced concrete in this site's foundation. It also recommends that the 250 MHz antenna might be utilized to analyze the reinforced steel bars, their design, and network, which are used in covert measurements at the Building Department's site.

Al-Shijiri, 2013 use the GPR technique and geotechnical evaluation to Investigation of subsidence phenomena in Baghdad City. Two sites in have been chosen to explore the subsurface soil characteristics that cause subsidence. A GPR survey was conducted along the 22 traverses, 14 of which are at Site-1 and the rest (8) at Site-2. The study discovered that most raw data radargrams (preprocessing) do not show the presence of weak zones. The surface images become so clear and reflect the weak zone beneath the ground surface after processing the raw data with appropriate filters and other interpretation tools, such as RAMAC and a RadExplorer software. Two adjacent weak zones are clearly visible at depths of 1.55, 1.62, 2.56, and 2.94 m at site 1 using a 100 MHz antenna, and the soil varies from loose to compact, resulting in subsidence.

1.5 Aim of the study:

1. Investigation of the possibility of applying GPR to detect weak areas and voids in shallow depths in Fallujah city.

2. Detecting the weakness areas represented by the fragility of the soil and shallow groundwater that affect the foundations of civil buildings in the city.

Chapter Tow

Theoretical Background and field work

2.1 Preface:

The GPR is a high-frequency electromagnetic technique that scans the inside of the earth by piercing the surface with pulses of electromagnetic waves (Annan, 2002, 2003; Neal, 2004). Before being reflected back to the surface and picked up by a receiver, these waves experience changes in the sub surface's dielectric characteristics.GPR uses a transmitting antenna positioned along the surface (i.e., the air-ground interface) that radiates short pulses of electromagnetic (EM) waves commonly in the frequency band between 10 MHz and 1 GHz. These propagating EM waves respond to changes in material electrical properties and are recorded with a separate receiving antenna also located on the surface (Atekwana et al., 2000; Cassidy, 2007).

Reynolds(1997) presents a thorough overview of current GPR advancements. Since GPR is a non-destructive method, it can be used in urban and delicate environments. Numerous geological uses of GPR exist, including the mapping of the water table and the high-resolution imaging of shallow soil and rock structure. Additionally, it has several non-geological applications, including in forensic investigations for the location of recently disturbed ground where burial has occurred and in archaeology for the location of buried walls or cavities.

2.2 GPR Method:

GPR uses radio waves propagate the ground, and then uses the receiver to detect the reflected signal from the subsurface features. The GPR Antenna (Transmitter) sends electromagnetic waves to the subsurface and at each subsurface feature, the waves travel With a velocity that depends on the permittivity of the material and the electrical properties. During waves propagate through the material, and some waves are reflected and detected by the receiving antenna (Daniels, 2000). Reflection occurs whenever an energy pulse enters a material that has a different dielectric permittivity (dielectric constant) from the materials around it. It is influenced by changes in the mineralogy of the soil and sediment, the amount of clay present, ground moisture, burial depth, differences in bulk density at different stratigraphic levels, surface topography, and water content changes, which are the most significant. The GPR energy pulses pass through the materials until some of them are reflected back to the antenna, some of them continue to travel through the materials until they are lost (attenuation), and the remaining pulses are scattered. Distance (or depth in the earth) can be determined if the velocity through the ground is known and the energy pulses' travel periods are accurately measured; (Olhoeft,2000., Conyers, 2004), (Figure 2.1).Even though many elements can influence the depth of inquiry in a GPR survey selecting the antenna type with the suitable operating frequency is one of the most essential variables to get the depth of examination of the features of interest with acceptable resolution.

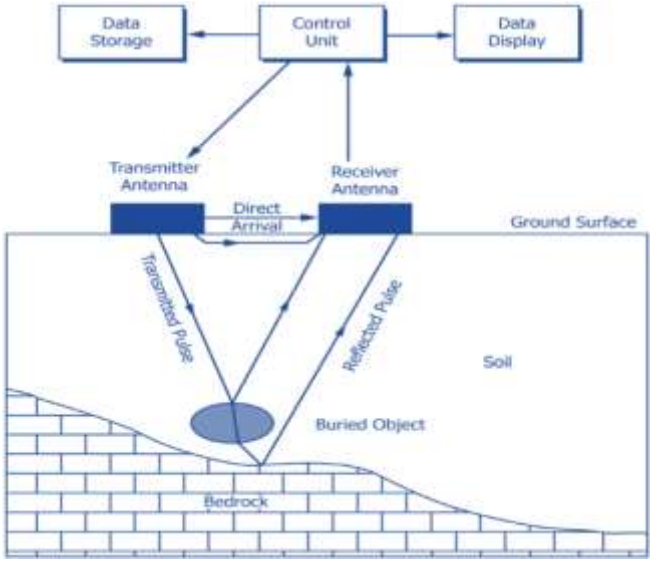

Fig. 2.1 Schematic diagram of a GPR System (Investigation, 2007)

2.3 Electromagnetic Theory:

The electromagnetic (EM) theory underlying all of the void and geologic anomaly detection methods is based upon the propagation of EM wave energy from a transmitting source of EM waves to a receiver. The traveling of EM waves is composed of transverse electric and magnetic field components, (Stolarczyk, 2003). The generation of electromagnetic waves depends on the relationship between the electric and magnetic fields. A changing magnetic field (H) will induce an electric field (E) (Ampere's Law), and a changing electric field will induce a magnetic field (Faraday's Law). Electromagnetic waves have energy, momentum, mass, and flow in the direction of propagation through space by means of wave motion. The electric (E) and magnetic (H) fields of an EM wave are at right angles to each other and to the direction of propagation, as shown in figure (2.2). The fields are vector quantities having direction as well as intensity.

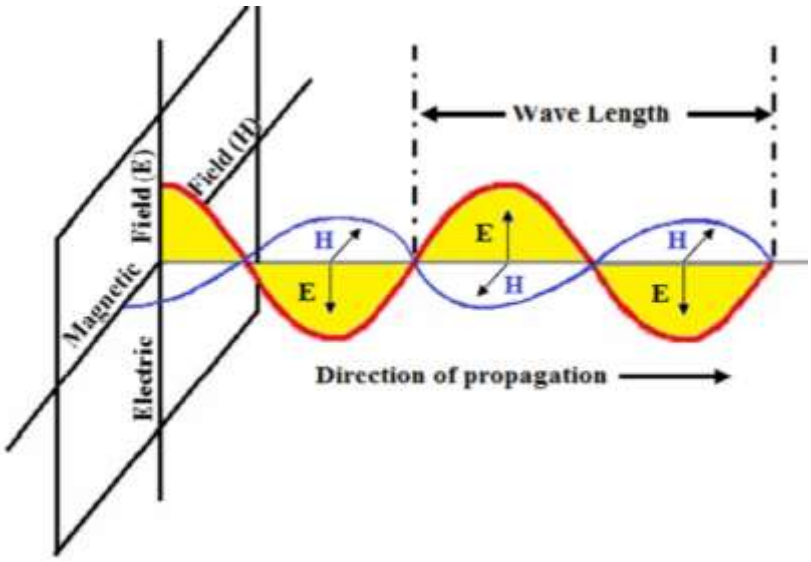

Figure 2.2 EM wave propagation (modified from WHO,1993)

Maxwell's equations described and proved mathematically the propagation of an electromagnetic field. The electric and magnetic fields propagate in the same direction but perpendicular (Smith, 1997). Any dielectric material will dissipate part of the energy from an electromagnetic wave propagating through it. The source of these losses may investigate by considering Maxwell's equations (Al-Mattarneh, 2008). The Varying electric fields with time are producing magnetic fields depending on the relative magnitude of losses, the fields may diffuse or propagate as waves. At low frequencies and high losses, the equations reduce to the diffusion equation and are called electromagnetic induction. At the high frequencies of radar, the energy storage in dielectric and magnetic polarization creates wave propagation, (Smith, 1997). The equations that control the movement of E.M. waves in any medium can be defined by the following:

2.3.1 Maxwell's Equations:

Maxwell's equations are mathematical expressions of electromagnetic field relationships. The electric field intensity, E, the magnetic flux density, B, the electric flux density, D, and the magnetic field intensity, H are the four fundamental vector field parameters in electromagnets. Maxwell's equations relate these quantities to one another, as seen below (Annan, 1999):

2.3.1.1 Faraday's Law:

From Maxwell's equations, Faraday's law is a key relationship. The negative induced electromagnetic fields (emf) in a coil are equal to the rate of change of magnetic flux multiplied by the coil's number of turns. It involves the interaction of a magnetic field with a charge.

$$\nabla \times \vec{E} = -\frac{\partial \vec{B}}{\partial t} \qquad \textbf{(2.1)}$$

Where:

∇-Curl operator (rotation)

Ē-The electric field density vector in Volt/meter.

B - The magnetic flux density vector (in units of Tesla, T), also called The magnetic induction.

t - Time (s).

2.3.1.2 Ampere's Circuital Law:

The magnetic field source is described by Ampere's circuital law.

$$\nabla \times \mathbf{H} = \mathbf{J} + \frac{\partial \mathbf{D}}{\partial t} \qquad \textbf{(2.2)}$$

Where:

H -The magnetic field density vector in Ampere/meter.

J - The electric current intensity vector in Ampere/meter^2.

D -The current displacement vector in Coulomb/ meter^2.

2.3.1.3 Magnetic Gauss Theorem:

The magnetic field divergence is always zero and hence magnetic field lines are solenoid.

$$\nabla \times B = 0 \qquad (2.3)$$

Where:

∇- Divergence operator.

2.3.1.4 Electric Gaussian Theorem (Gauss's Law in electric.)

The electric charge source is determined by Gauss's law.

$$\nabla \times D = \rho v \qquad (2.4)$$

Where:

ρ -The electric charge intensity in Coulomb/meter 3.

2.4 Propagation of radio waves:

The pulses interact with subsurface materials in a variety of ways as they propagate downwards into the earth at various velocities, including reflection, attenuation, scattering, and diffraction.

2.4.1 Velocity:

The velocity of a radio wave in a material (*V*m) depends on speed of Light in free space (c = 0.3 m/ns), the relative dielectric constant (εr), permittivity of free space (εo = 8.854 x 10-12 farads (F)/m) and the relative magnetic permeability (μr = 1 for non-magnetic materials).

Reflection/transmission losses in the substrate, signal scattering losses produced by objects equidimensional with the radar signal wavelength, absorption (EM energy converted to heat), and geometrical signal

broadening during propagation are all factors that might cause signal loss The loss factor (P), which may be stated as: $\mathbf{P = \sigma/\omega\varepsilon}$, where $\boldsymbol{\sigma}$ is the conductivity, $\boldsymbol{\omega = 2\pi f}$ where **f** is the wavelength frequency, and $\boldsymbol{\varepsilon}$ is the permittivity $=\boldsymbol{\varepsilon_r \varepsilon_o}$, accounts for these components(Reynolds, 1997):

$$V_m = C \,/\, \{(\varepsilon_r \mu_r /2)\,[(1 + P_2) + 1]\}^{1/2} \qquad \textbf{(2.5)}$$

2.4.2 Attenuation:

The attenuation factor (α), which is the primary cause of reduced signal energy, is the cumulative loss of energy due to electric conductivity (σ), magnetic permittivity (μ), the dielectric permittivity (ε) of the material through which the signal is introduced. Neal (2004) indicates that for low loss materials, α can be expressed as:

$$\alpha = \frac{\sigma}{2}\sqrt{\mu\,/\varepsilon r} \qquad \textbf{(2.6)}$$

The expression of α indicates that the conductivity of materials exerts the greatest control over α (Theimer *et al.,* 1994; Neal, 2004).

Pulse radar transmits short pulses into the ground as mentioned above. Only a short period time following the transmission of the pulse gives measurable reflections from the underlying medium, due to quick attenuation of the received signal (Parasnis, 1972). While the transmitted pulse can be of considerable power, the actual power reaching the reflecting surface decreases exponentially with distance from the antenna. This is because the power is spread over a bigger area as it reaches further away from the source. Another factor is the absorption of the pulse in the medium. The power reflected is only a factor of the

received power and the reflected signals power also decreases exponentially with distance to the receiver. Normal attenuation factor for traveling from the antenna to a reflecting surface and back are several decibels per meter. Pulses are transmitted repetitively from the antenna with a certain repetition frequency. This frequency is called pulse repetition frequency (PRF). Today's systems usually have a PRF of 100 KHz. As the pulses are transmitted, the reflected signal is recorded (Björklund and Johnsson, 2005).

2.4.3 Scattering:

When an electromagnetic wave collides with a substance having a differing permittivity, the electromagnetic energy changes direction and character. This transition at a boundary is known as scattering (Daniels et al., 2008). The amplitude of the radar signal is reduced by scattering from thin layers or point-type objects such as rocks, and these losses are frequently incorporated in the attenuation term (Davis and Annan, 1989; Annan, 2009).

2.4.3.1 Spectral reflection:

Scattering is based on the law of reflection, which states that the angle of reflection equals the angle of incidence (Figure 2.3-a). When a wave hits an interface, the energy is scattered based on the form and roughness of the interface, as well as the difference in electrical characteristics between the host material and the item. A portion of the energy is distributed back into the host material, while the rest may flow into the item. The refracted portion of the wave is the part that travels into the item (Lowrie, 2007).

2.4.3.2 Refraction:

Because the electromagnetic wave velocity tends to decrease with depth, refracted waves are unusual as a GPR propagation mode (Figure 2.3-b). This is due to the fact that the water content has the greatest impact on seismic and electromagnetic wave velocities in partially saturated and unconsolidated materials (Lowrie, 2007) .

2.4.3.3 Diffraction:

The bending of electromagnetic waves (Figure 2.3-c). When a wave is partially stopped by a sharp border, diffraction scattering occurs. Fresnel was the first to notice that when a wave scatters off of a point, it spreads out in numerous directions. The nature of the diffracted energy is determined by the sharpness of the boundaries and the object's shape in relation to the incident wave's wavelength. Diffractions are semi-coherent energy patterns that splay out in multiple directions from a point, or along a line, in GPR data (Oswin, 2009).

2.4.3.4 Resonant scattering:

When a wave impinges on a closed object (e.g., a cylinder) (Figure 2.3-d), resonant scattering occurs, and the wave bounces back and forth between different points on the object's boundary. Part of the energy is refracted back into the host material, and part is reflected back into the object every time the wave hits a boundary. This causes the electromagnetic energy within the object to resonate (also known as ringing). The trapped resonant energy inside the object quickly evaporates as some of it radiates to the outside of the object. Closed objects are said to have a resonance frequency, which is determined by the object's size, electrical qualities, and surrounding material. The ability of an object to resonate, on the other hand, is determined by the wavelength (the object's velocity divided by the wave's frequency) in relation to its dimensions. The permittivity contrast between the object

and the surrounding material determines the length of time that an object resonates (Dante, 2007).

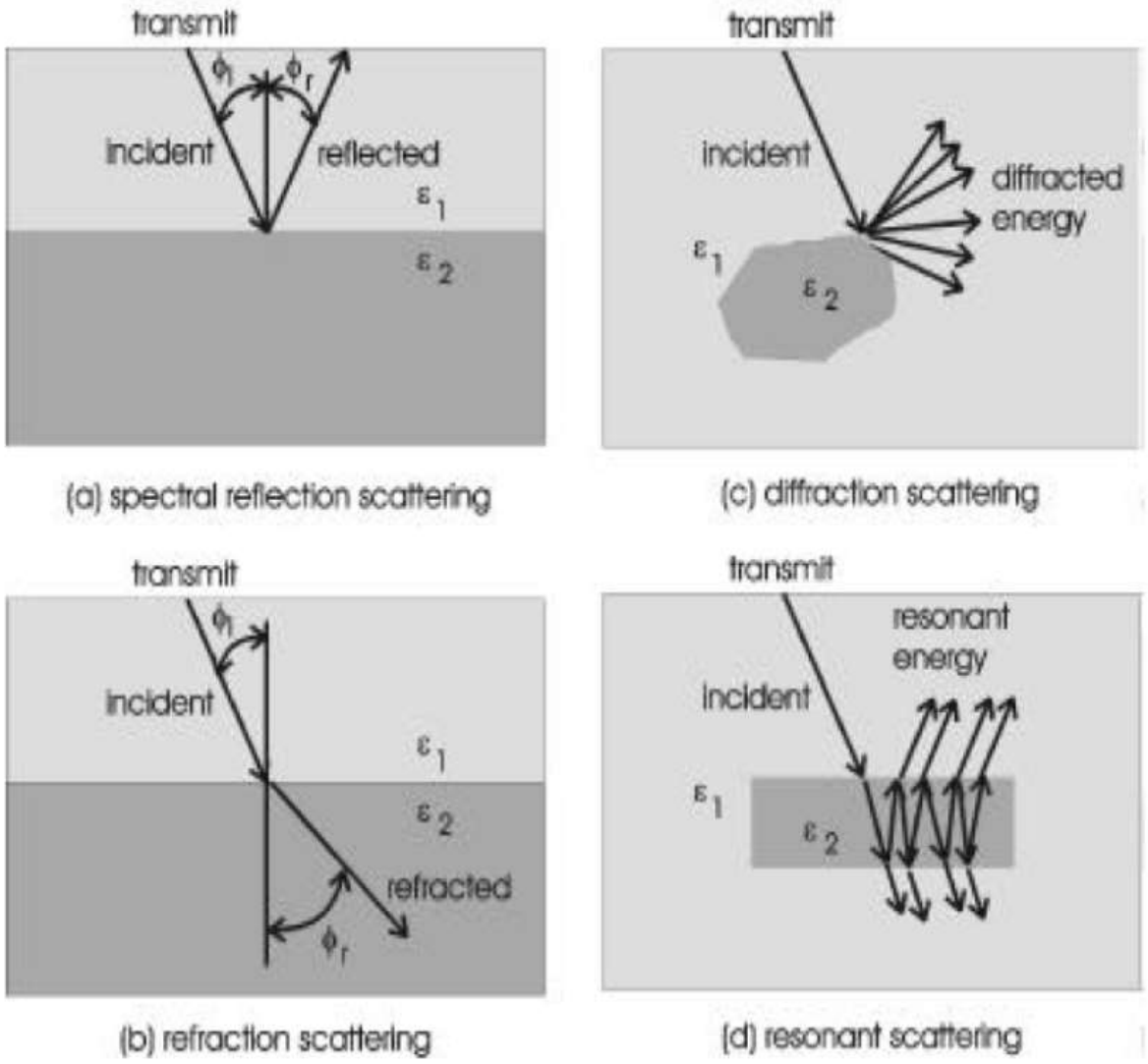

Figure 2.3: Scattering mechanisms: (a) specular reflection scattering, (b) refraction scattering, (c) diffraction scattering, and (d) resonant scattering.(Daniels, 2000)

2.4.4 polarization:

The electromagnetic waves are polarized by perpendicular electric and magnetic field (Maxwell equation) and the ability of different materials to store energy (Figure 2.4). Linearly polarized antennas are used in the majority of commercial GPR systems. The most typical antenna configuration is for the transmitter and receiving antennas to

have their electric fields aligned in parallel with each other, parallel to the earth, and towed in a traverse direction perpendicular to the electric field direction. As a result, a wave propagates perpendicular to the earth's surface and into the earth. When such an arrangement is applied to a buried metallic pipe (or wire or rebar) with electric fields aligned parallel to the pipe's length, the pipe shows as an outstanding reflector in ground penetrating radar data, with a hyperbolic shape (the shape is the result of the antenna pattern and geometry of traverse motion). When the antennas are rotated 90 degrees such that they cross the pipe with the electric field direction at right angles to the pipe's long axis, the pipe vanishes, but it is still visible (Olhoeft, 1988).

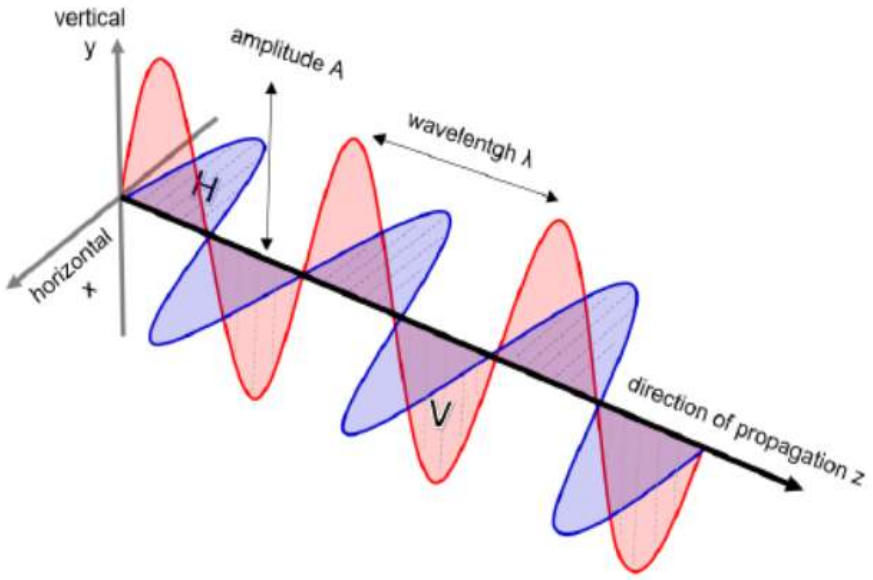

Figure 2.4: Vertical and horizontal polarization of an electromagnetic wave(Braun, 2019).

2.4.5 Penetration depth:

The length of time it takes for an electromagnetic wave to travel from the transmitting antenna, through the subsurface to an object or interface, and back to the receiving antenna determines the depth to the object or interface. As shown in (Figure 2.5), the amount of time recorded is

referred to as the two-way travel time (TWTT). The capacity and speed of electromagnetic energy propagation through a material, as well as the attenuation of electromagnetic energy after it is transmitted, are all affected by variable electromagnetic properties of earth materials (composition and water content), which affect the capacity and speed of electromagnetic energy propagation through a material (Reynolds, 1997).

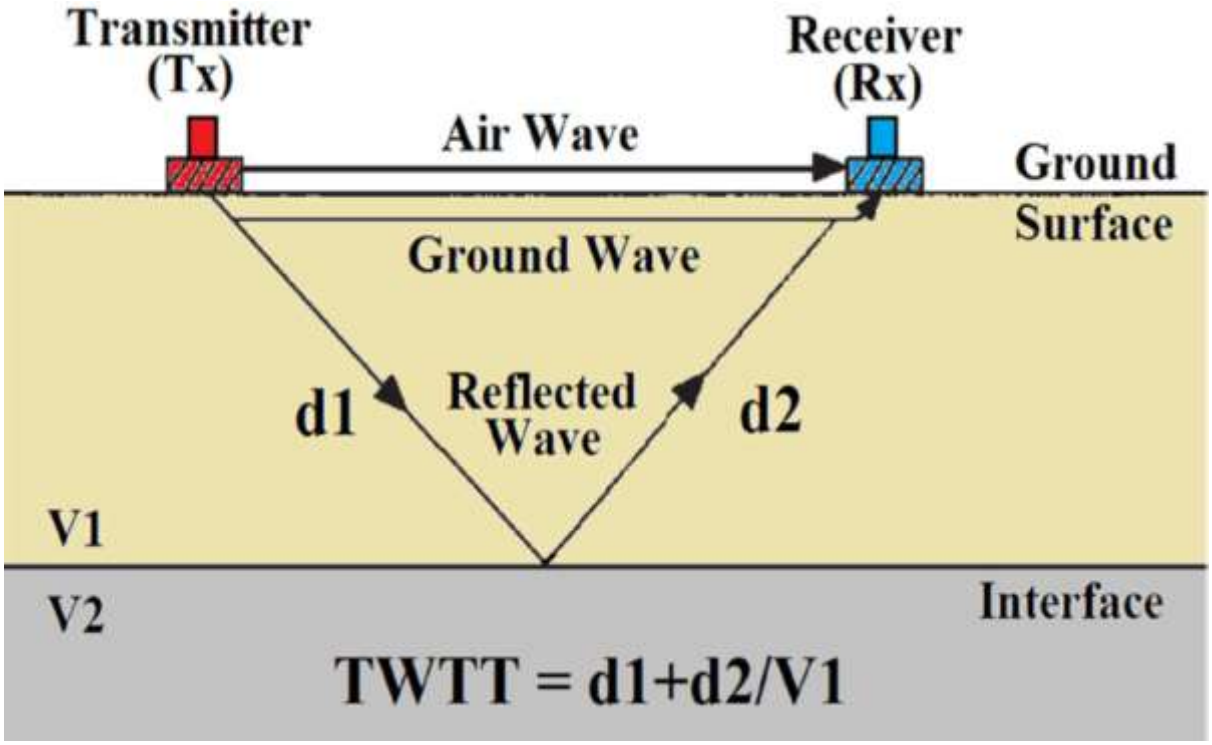

Figure 2.5: Two-way travel time of GPR signal (modified from Conyers, 2004).

The frequency of the system's transmitting antenna determines the depth of penetration of the electromagnetic wave and the GPR system. Higher-frequency radar antennas are unable to penetrate the subsurface to the same amount as lower frequency antennas. Reduced frequency units, on the other hand, have greater penetration depths but have lower spatial resolution (table 2.1), (Hanninen 1992; Annan, 2009).

Table 2.1: Antenna frequency (MHz), the lower limit of object target size (m), approximate depth range (m) and approximate penetration depth (m) (Operating manual of RAMAC, 2009).

Antenna frequency) MHz)	Lower limit of Object target size(m)	Approximate Depth range (m)	Approximate penetration depth (m)
100	0.1 – 1	2 – 15	15 – 25
250	0.05 – 0.5	1 – 10	5 – 15
500	0.04	1 – 5	3 – 10
800	0.02	0.4 – 2	1 – 6

2.4.6 Resolution:

The energy reflected from subsurface features is the signal received in a typical GPR scan. The relationship between the GPR operational features and the obtainable resolution must be recognized in order to detect individual objects within the material under inquiry. The resolution of a GPR system is the shortest distance between two objects that allows each object to be detected separately, and it is measurable in both the vertical and horizontal planes. Radar is a ranging technique that measures distances to objects in units of time (RADAR stands for Radio Detection and Ranging). In the temporal dimension, resolution is defined as the difference in time between two things that can be measured. Thus, if two objects' reflections can be distinguished in time, they may be resolved in distance. The bandwidth and pulse width of a signal

determine the relationship between it and time in radar. A reflection pulse has a defined width (W) that is measured at half-height, as shown in (Figure 2.6) (Jol,2009).

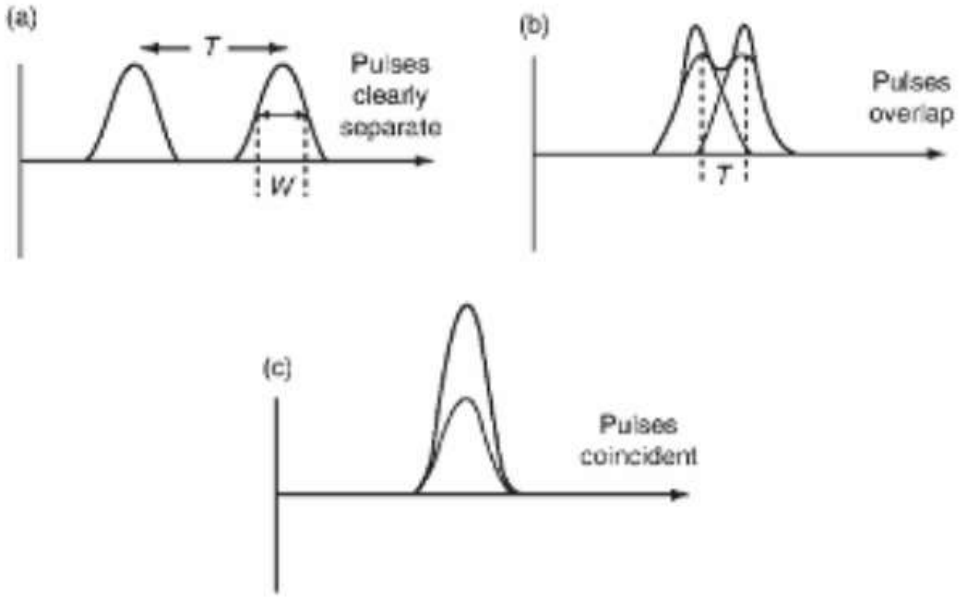

Figure 2.6: Temporal pulses with half width W. (a) Pulses are clearly separable when T >> W. (b) Two pulses are said to be distinguishable until T ≈ W. (c) When T << W then two events are not distinguishable (Jol,2009).

The sources will not be distinguishable if two reflection pulses overlap. The two pulses can be resolved as independent pulses if they are separated by more than W. The link between pulse width and signal bandwidth shows the bandwidth of the signal (Jol,2009):

$$W = \frac{1}{B} \qquad \textbf{(2.7)}$$

The greater the bandwidth (B), the shorter the pulse width (W). Hence, higher bandwidth Signals are able to resolve objects with smaller separation.

2.4.6.1 vertical Resolution:

The wavelength of the energy in the ground determines the vertical resolution of a GPR. As a result, higher center frequency antennas have better vertical resolution but less depth penetration. For the stratigraphy to be resolved, there must be enough physical difference between the layers in all circumstances (Linford, 2006).

2.4.6.2 Horizontal Resolution:

Horizontal resolution is more challenging and is dependent on the incident energy's radiation pattern in the earth, which can be represented by a cone widening with depth to illuminate a growing 'footprint' of the subsurface for most antenna (figure 2.7) (Linford, 2006).

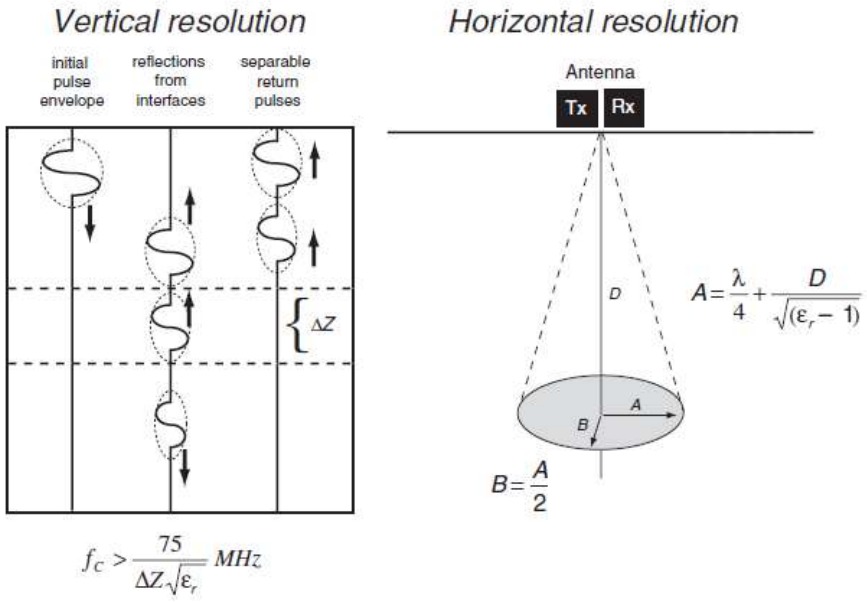

Figure 2.7: Vertical and Horizontal resolution. Where ***fc*** is centre frequency, ***ΔZ*** *is* spatial separation, **εr** relative permittivity, ***D*** *is a* given depth, ***λ*** *is a* wavelength, (Annan and Cosway 1992).

2.5 Surface-based Reflection of GPR Configuration:

Surface-based reflection GPR, borehole reflection GPR, and helicopter GPR survey designs are the most common GPR survey configurations. The most typical GPR survey setup is for a surface-based GPR survey. The surface based GPR survey is carried out with ground linked systems, in which the antennae are put directly on the ground's surface or just a few centimeters above it, and are manually or with vehicles across the studied line (Forte et al., 2019). A step size has been used to govern the movement of the transmitter-receiver antennas across the invisible line. The geographic sample interval, or step size, determines how frequently a trace is captured spatially (for example, one trace every 0.2 m), (Robinson et al., 2013). The higher the resolution of the data collected, the smaller the step size. Signal overlapping occurs as a result of the overly tiny step size, as seen in (Figure 2.8). When two signals are overlapping, one event with a bigger amplitude is produced. If two pulses are separated by half their half-width they are distinguished; otherwise, they are interpreted as one signal (Jol, 2009).

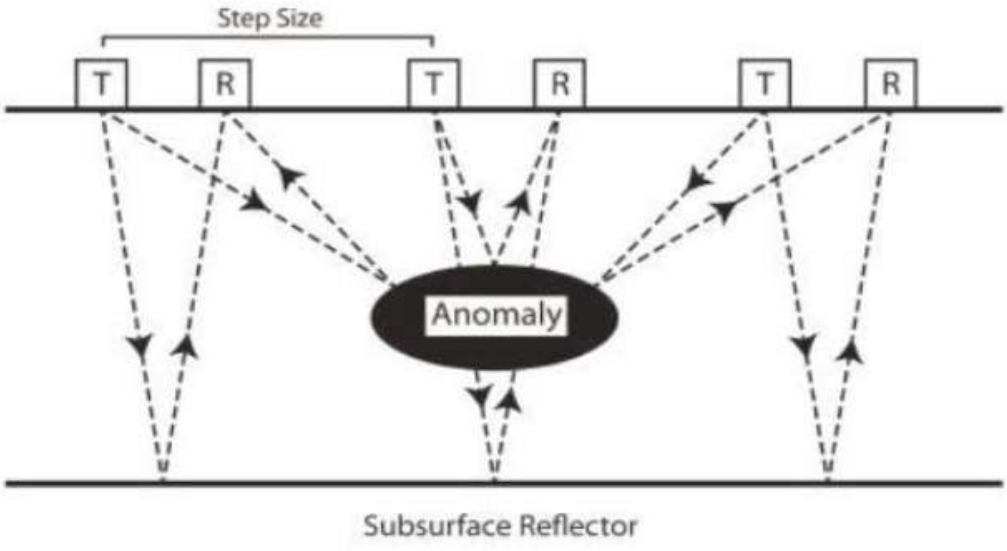

Figure 2.8: Sketch of the Step Size (modified from Robinson et al., 2013).

The direct airwave, direct ground wave, and reflected wave are the three principal waves visible in the surface-based GPR survey, as depicted in (Figure 2.8). As illustrated in (Figure 2-9), the first two waves travel directly from the transmitter to the receiving antenna: the first travels through the air, while the second travels slightly below the soil surface (Yochime et al., 2013, Neal, 2004). The reflected wave, which travels along the path transmitter-reflector-receiver, is the third wave.

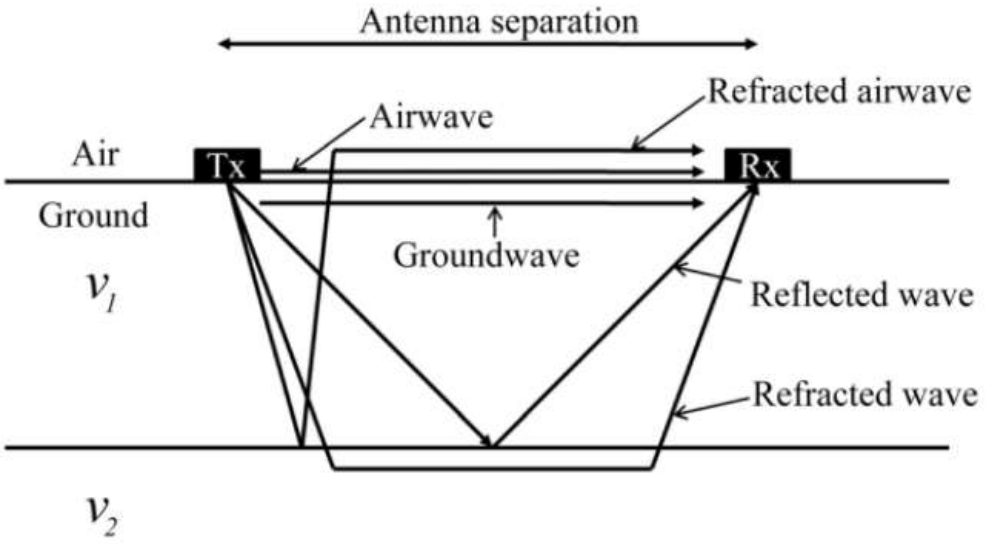

Figure 2.9: EM signals paths between transmitting and receiving antennae for the airwave (Neal, 2004).

2.5.1 Velocity analysis by direct wave travel time**:**

The time it takes for an EM wave to go directly from the transmitter to the receiver through the very shallow subsurface is referred to as the direct ground wave transit time. The GPR scan determines the direct ground wave's travel time, which can be translated to ground wave velocity. Yochim et al., 2013; Neal, 2004) calculate the ground wave velocity by dividing the length (distance between the transmitter and receiver antenna) by the direct ground wave travel time. In general, the

EM wave propagation velocity (v) through a non-magnetic, low-loss geological medium (e.g., soil) can be translated to the soil mixture's dielectric constant, as shown in Equation (2-8). (Illawathure, 2019; Yochim et al., 2013; Steelman and Endress, 2012).

$$V = \frac{co}{\sqrt{\varepsilon r}} \qquad \textbf{(2.8)}$$

v = velocity of EM propagation (m/ns)

co = velocity of light in the space (0.3 m/ns)

ε r = dielectric constant of the host material (K_{mix}), which is unit less.

2.5.2 Central Frequency:

In order to determine resolution and penetration depth, the center frequency must be established (Robinson et al., 2013). The lower penetrated depth, but the better the resolution, the higher the central frequency is used. The choice of the suitable central frequency is a compromise between the depth of investigation, the resolution required, and the portability of the system (Sensor & Software, 2019).

2.6 GPR Survey parameters:

Several criteria must be prepared and controlled to conform with the survey objectives in order to execute a successful GPR survey; these parameters are listed below.

2.6.1 Antenna frequency:

The capacity of electromagnetic waves to penetrate the ground to a specific depth is principally determined by two factors: their frequency and the properties of the ground, (Conyers, 2004). Because only the wave frequency can be modified, selecting the right antenna frequency for a GPR scan is crucial. Low-frequency antennas with long wavelengths penetrate the deepest, but high-frequency antennas with short wavelengths can only image superficial objects (Neubauer et al., 2002). As a general rule, Conyers (2004) recommends using a 400-900 MHz antenna to photograph features within 1 m of the surface, and a 250-500 MHz antenna for images 1-3 m below the surface. According to Goodman et al. (2009), you should choose a radar frequency (and time window length) that will gather data to a depth of at least 1.5-2 times the target region (Dojack, 2012). The survey parameters for the most popular antennas are listed in Table 2.2.

Table 2.2: lists the antenna survey parameters (taken from Annan, 2005; MALA, 2005; Ortyl, 2006).

Antenna Frequency (MHz)	Depth (m)	Depth range (m)	Max. penetration depth (m)	Sampling Interval (ns)	Max. Sampling Interval (ns)	Sampling frequency (MHz)	Trace interval (m)	Sample Number	Time Window (ns)
1000	**0.5**	**0.05-2**	**0.5-4**	**0.09**	**0.17**	**15000-30000**	**0.01-0.05**	**402**	**34**
800	**0.7**	**0.4-2**	**1-6**	**0.11**	**0.25**	**6500-14000**	**0.02-0.04**	**380**	**30**
500	**1**	**1-5**	**3-10**	**0.16**	**0.33**	**4000-7000**	**0.02-0.05**	**356**	**60**
250	**1.84**	**1-10**	**5-15**	**0.39**	**0.75**	**600-3500**	**0.03-0.10**	**179**	**71**
200	**2**	**1-10**	**5-15**	**0.64**	**0.83**	**1600-3500**	**0.03-0.10**	**145**	**74**
100	**5**	**2-15**	**15-25**	**1.67**	**1.67**	**800-1800**	**0.10-0.30**	**75**	**78.5**

2.6.2 Sample number:

The order in which the samples were measured, recorded, and stored is indicated by the sample number. The sequential placements of samples in the GPR signal are denoted by sample numbers (Dojack, 2012).

2.6.3 Sampling interval:

The instant digital values (amplitude) of the recorded radar signal at certain moments are referred to as samples. Every sampling interval, or the period between points for each recorded waveform, samples are taken (Harris, 2006). The following Equation (Annan, 2005) can be used to find the maximum sampling interval suitable for the survey:

$$t = \frac{1000}{6f} \qquad (2.9)$$

Where f is the center frequency of the antenna (MHz), t is the maximum sampling interval (ns).

2.6.4 Trace interval:

The trace interval is typically chosen while considering the survey's required lateral resolution. The lateral resolution is determined by the depth of the targets and the antenna's center frequency. Within the range of antenna frequency used, point interval values are inversely proportional to resolution (Johansson and Friborg, 2005).

2.6.5 Time window:

Time window refers to the period of time following the transmission of a pulse during which the received signal is recorded. As a result, the time window also controls the measurement's depth, as any reflections received after the time window are discarded (Conyers, 2013). In most circumstances, temporal periods of 60 to 100 nanoseconds are appropriate for archaeological applications. This yields a measuring depth of 3 to 2 m, but this is highly dependent on the ground

composition (Conyers, 2004). The suggested time window can be computed using the equation (Annan, 2005) for a more precise measurement:

$$W = 1.3\left(\frac{2d}{v}\right) \quad \textbf{(2.10)}$$

where W is the time window length (ns), *v* is the minimum velocity of waves through the material (m/ns), and d is the maximum depth to be resolved (m).

2.7 GPR Data Processing:

One of the great advantages of the GPR method is the fact that the raw data is acquired in a manner that allows it to be easily viewed in real-time using a computer screen (Griffin and Pippett, 2002). In digital data, post-recording processing can be used, where the advantage of it, is that processing can be done more systematically and non-causal operators to remove or enhance features can be applied (Annan, 2001).

GPR Data processing includes four fundamental steps to produce the final image of the radargram (Fig. 2.10). However, it is not necessary to use all these steps in the processing path. These steps are:

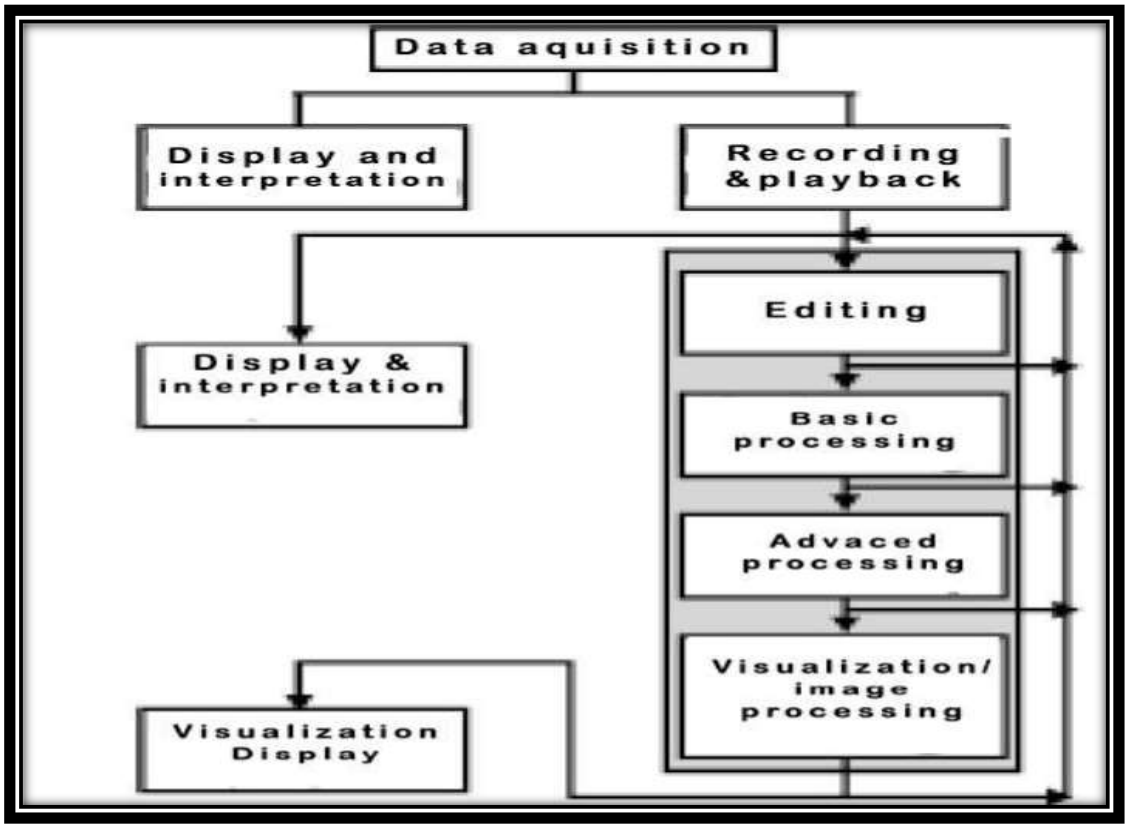

Figure 2.10: A typical overview of the GPR dataset flow (Anann, 2001).

2.7.1 Data Editing:

Field measurement is rarely so routine that there is no room for error, inattention, or an oversupply of datasets. Reorganizing data, integrating data files, updating data headers or background details, relocating, and including elevation detail with the dataset are all examples of dataset modifications (Al-Nuaimy et al., 2000).

2.7.2 Basic Processing:

To provide a more passable primary exegesis and data assessment, the basis doctrinaire is used to the dataset. In most cases, this type of processing is already being done in real time to create the real-time show (Al-Nuaimy et al., 2000). Although the detail in the raw radargram may have been appropriately implemented previously, it should be processed first to remove any undesirable system or terrain impact. Background clutter removal, path loss repairs, antenna separation correction, and low-pass filtering are all part of this process (Al-dami, 2011).

2.7.3 Advanced Data Processing:

Finding and distinguishing true target reflections from misleading reflections is essential for properly distinguishing subsurface items from the surrounding chaos (ASCE Publications, 1993). This procedure necessitates a certain amount of user bias, which results in datasets that are significantly different from the raw data that was supplied to the processing (Al-Nuaimy et al., 2000).

2.7.4 Visualization Processing:

In this category, processing almost always results in a dataset that is completely different from the original data. Processing in this category includes topics such as migration, the implementation of various algorithms, event selection, subjective gain enhancement, and capacity analysis. All of these need the completion of the preceding processing steps as well as the availability of corollary control details (Al-Nuaimy et al., 2000).

2.8 Filtering Tools:

To reduce the impacts of distortion and erroneous GPR signals, filtering techniques are applied . Filters are used to process GPR data in a variety of ways. Dewow, time-zero correction, band-pass filtering, and gain control are the basic filters (Cassidy, 2009). The following are the descriptions of these filters:

2.8.1 Subtract mean (Dewow):

Due to the close position of transmitter and receiver antennas, the fields near The transmitter contain low-frequency energy associated with electrostatic and inductive fields, which decay rapidly with distance. This low-frequency energy caused the base level of the received signal to bow up or down, and This effect is known as baseline 'wow' in the GPR technology (Jol,2009). Dewow filtering is used to remove the low-frequency components present in the data by applying a running average filter to each trace and eliminating a long waved part of the signal that is caused by the EM induction (Dojack.,2012. , Group, BW.,2006. , Sheriff, S., 2010). It is a vital step as it reduces the data to a mean zero level and therefore, allows the positive-negative color filling to be used in the recorded traces (Figure 2.11) (Jol,2009).

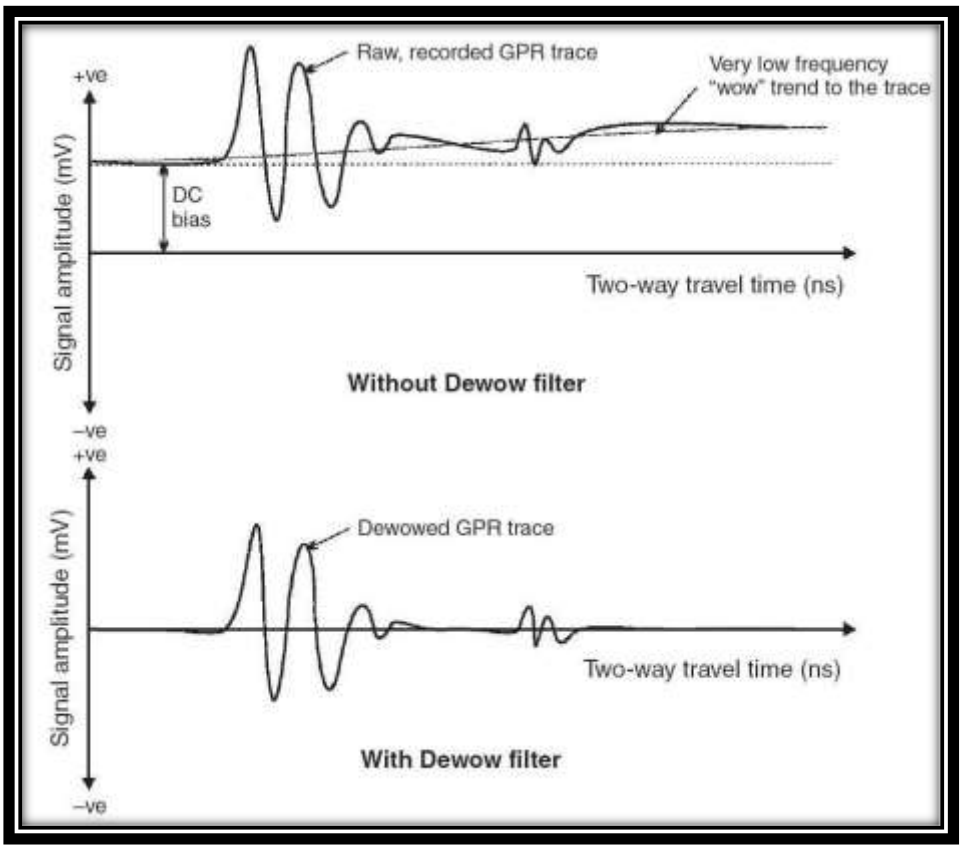

Figure 2.11: Dewow filter correction on a raw GPR trace (Jol,2009).

2.8.2 Time zero correction:

Time zero (T0) can be defined as the first break (or the first arrival) of the air ground wave or the first reflection of the GPR trace (Cassidy, 2009; Conyers, 2013). It occurs mainly due to several factors such as various system hardware components, the fiber optic cable length, the transmitter and receiver separation, and the total time window (Sensors and software, 2001). The T0 must apply to the GPR traces before any other processes because if T0 remains without correction, the depth of the successive reflections will be inaccurate. Finally, some instruments and software are done this correction automatically, while others do not (Utsi, 2017; Cassidy, 2009).

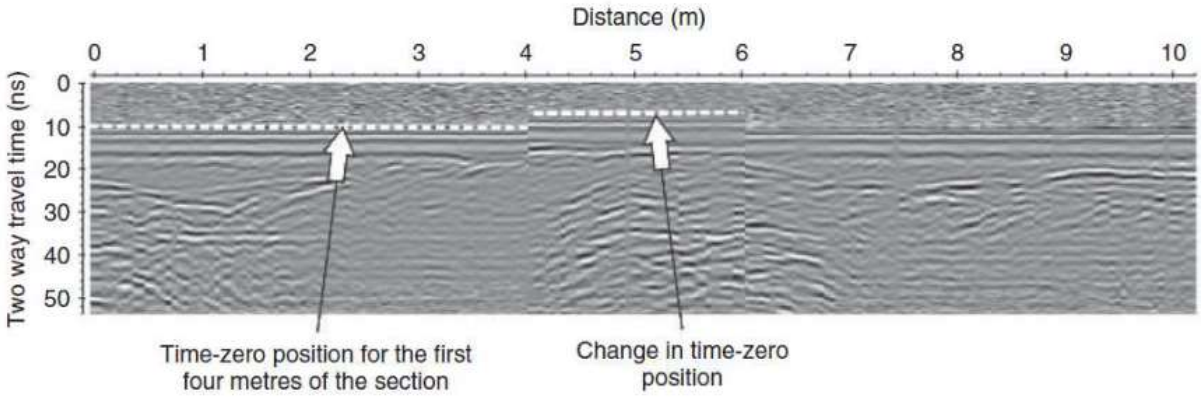

Figure 2.12: Changing in a time-zero position is an example (Cassidy, 2009).

2.8.3 Background Removal:

The use of background removal is one of the most prevalent techniques especially performed to GPR data. Background elimination is a type of spatial filtering that usually takes the form of a high pass filter or one that subtracts the mean of all traces in a region from each trace (Akinpelu, O. C. (2010). Background removal used to remove horizontal or almost horizontal features from GPR data by applying a horizontal

spatial high pass filter to allow subtle weaker signals to become visible in the processed section (Parkin *et al.*, 2000).

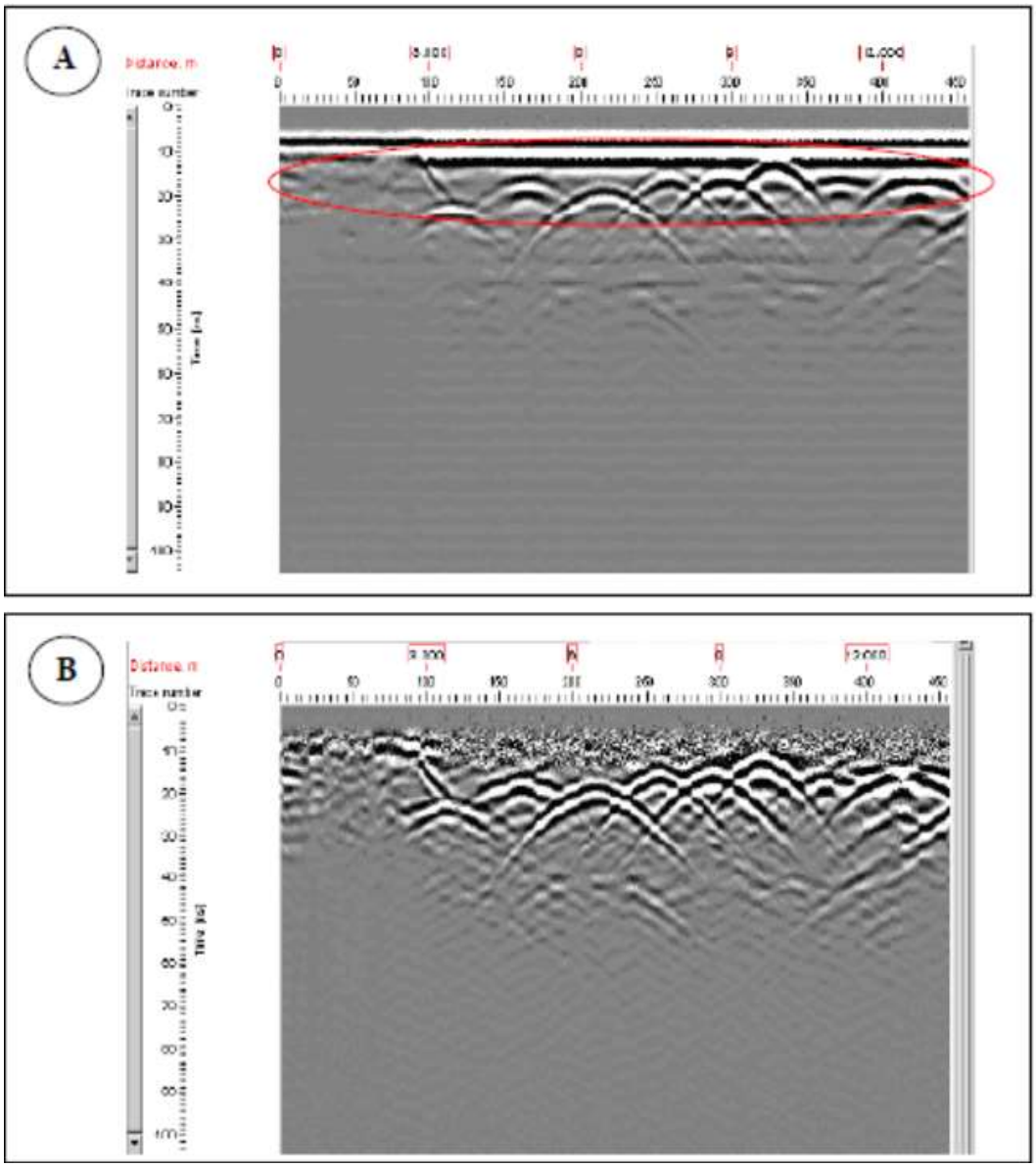

Figure 2.13: (A) GPR profile before background removal (B) GPR profile after background removal (Akinpelu, O. C. 2010).

2.8.4 Bandpass filter:

Bandpass filtering is a technique used to remove undesirable frequencies or spurious noise caused by human-induced and system noise like high-frequency radio transmissions (Cassidy, 2009; Goodman and Piro, 2013; Utsi, 2017). Bandpass filtering is effective at eliminating the low/high unwanted frequencies, but it should be applied judicially. It

may remove significant features from the GPR profile if it is contaminated strongly by noise (Cassidy, 2009). As GPR systems emit the EM waves in a frequency range, which are mainly between half to two times the center frequency (Conyers, 2013), this filter is very useful to remove all frequencies that occur outside of the GPR systems range (Utsi, 2017).The bandpass filtering is based on the fast Fourier transform (FFT), where the GPR traces will be converted from the time domain to the spectral (frequency) domain. All GPR waves can be decomposed into superposition individual frequencies that have different amplitudes and phases. To apply this filter successfully, one should define its lower and higher cut-off frequencies. Once the filter removes the unwanted frequencies, the inverse FFT will be applied to return the filtered frequency components to time-domain radar signals (Goodman and Piro, 2013; Sensor and Software, 2018). Finally, it is preferable to do filtering before the gain process because the data is in its truest form. If the filtering is applied post-gain, great attention should be paid to understanding the effect of the gain on the amplitude and spectral content before starting the filtering process

2.8.5 Time Gain:

As the radar waves propagate deeper into the ground, some of their parts are rapidly attenuated and the others are reflected back to the antenna making the deeper features hard to be distinguished as weak reflections (amplitudes) on the GPR profile (Annan, 2005; Utsi, 2017). Therefore, it is useful to increase the strength of these weak reflections at greater depths (Neal, 2004), which is normally done by applying the Gain. Gain can improve the visual form of GPR profiles (Cassidy, 2009), by compensating the loss of amplitude of the weak reflections to make all reflections visible as much as possible (Utsi, 2017). However, there are different ways of Gain to apply to the GPR data such as Automatic Gain Control (AGC),

Spreading & Exponential Calibrated Compensate (SEC), and Constant Gain. The AGC applies for each trace individually and tries to equalize the amplitude of all GPR signals. It is based on the variance between the mean amplitude on the specific time window to the maximum amplitude of the trace (Cassidy, 2009; Sensors and Software, 2018). This type of Gain is suitable for stratigraphic horizon continuity and low frequency investigations (Jol and Bristow, 2003; Annan, 2005; Utsi, 2017). The SEC attempts to increase the Gain amount with depth increasing to mimic the waves' amplitude variations as they propagate in the ground (Annan, 2005; Cassidy, 2009).

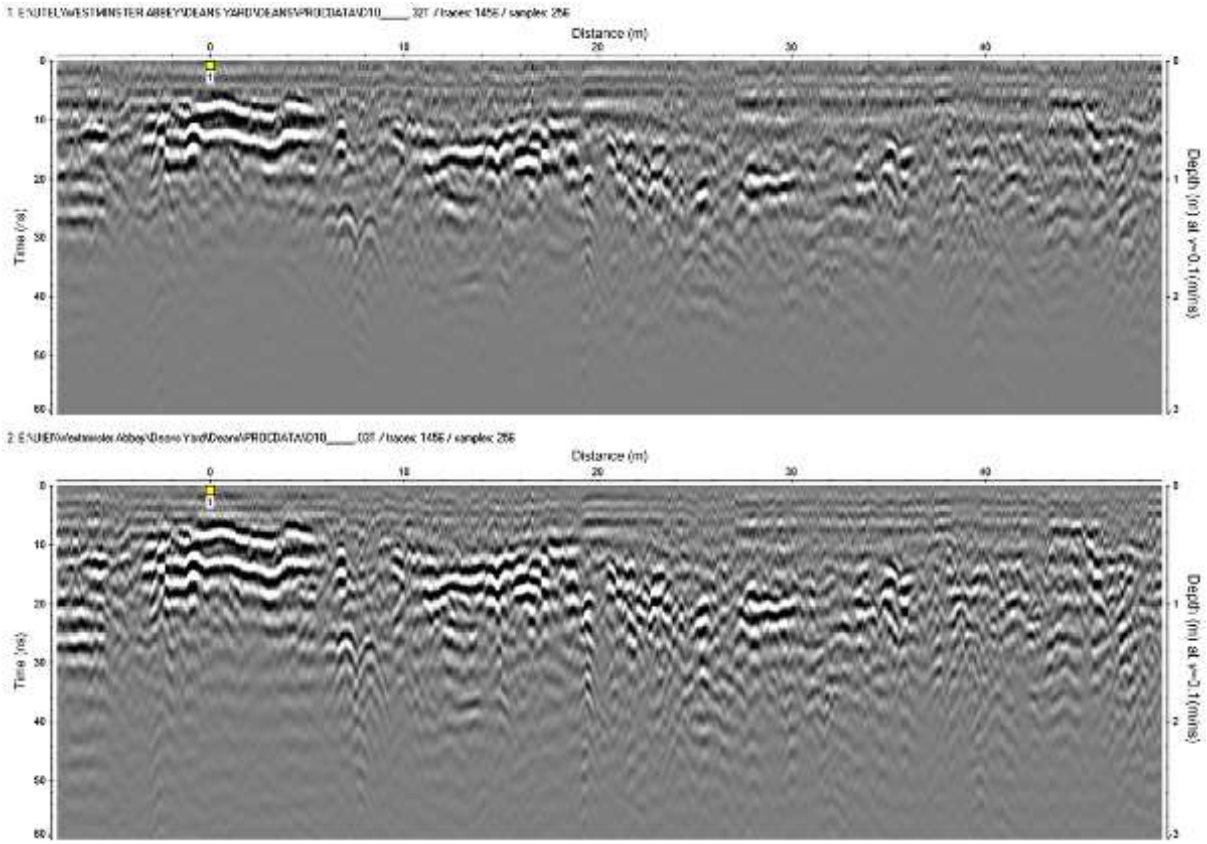

figure 2.14: Radargram without the addition of gain (above) and with an appropriate amount of gain added (below) (Carrick Utsi, E. 2017).

2.9 Data Display and Interpretation:

The presentation of data is crucial to data interpretation. In fact, putting up a good show is an important aspect of interpretation. Surface data can be displayed in three ways: 1) as a one-dimensional trace, 2) as a two-dimensional cross section, and 3) as a three-dimensional display. A one-dimensional trace isn't very useful until it's combined with others to form a two-dimensional cross section or a three-dimensional block view, as shown in (figure 2.15). All displays are built around the wiggle trace (or scan). A single trace can be used to detect items beneath the surface (and determine their depth). GPR traces are recorded at various points on the surface, and three-dimensional representations are essentially block views of those traces (Daniels et al., 2008).

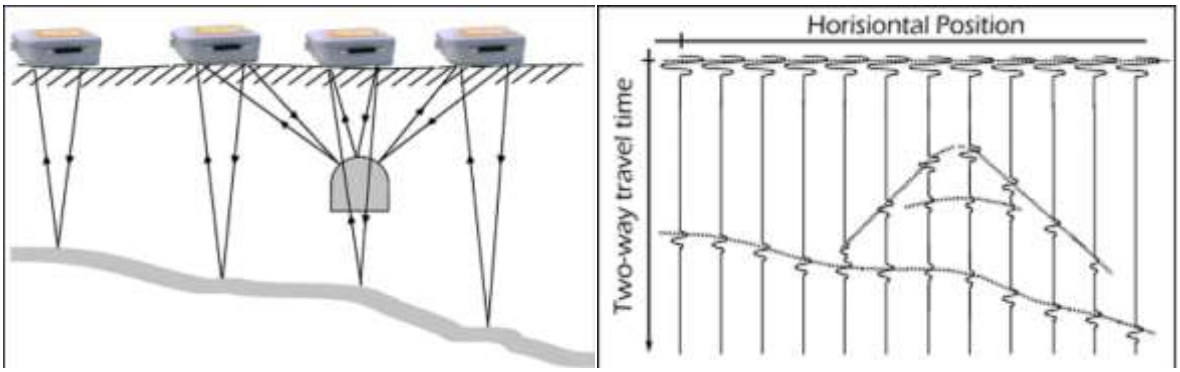

Figure 2.15: Explain how a one-dimensional trace changes when an antenna is relocated and many traces are stacked side-by-side to form a two-dimensional cross section. (Nissen and colleagues, 2001).

The process of recognizing anomalies in GPR data and establishing the nature (size, form, and physical attributes) of the object in the subsurface that is producing each anomaly is referred to as interpretation. The interpreter's talent (or the sophistication of the pattern recognition algorithms), the quality of the data gathered in the field, and the clarity

of the processed display used for interpretation all contribute to a good interpretation. The interpretation process starts with a clear display that makes it simple to spot anomalies, with interpretation and processing eventually overlapping (Daniels et al., 2008).

The following are the most important factors to consider while interpreting data. Anann et al., 2001).

1. Make sure you know what the survey's goal is.
2. Create a geological setting or application structure model.
3. Sort the information into logical groups that can be easily linked to site maps.
4. Establish a velocity and attenuation estimate (or depth of exploration achieved).
5. Create a scenario for the predicted radar response (i.e. a slowly varying continuous event for a major geologic horizon, a spatially limited diffraction hyperbola for a pipe). Process data to improve the type of reaction predicted if at all possible.
6. Use geologic control and ground truth, such as drilling, to correlate radar data.
7. Use a plan map to plot the locations of radar anomalies so that line-to-line correlation may be done.
8. Drilling or follow-up control work should be planned.
9. Examine the data once more control is available.

2.10 Instrumentation:

Ground-penetrating radar (GPR) is a geophysical and short-range remote sensing technique that uses radar pulses to produce cross-section photographs of underground structures. Field exploration activities should be meticulously planned and laid out in order to acquire sufficient data for project design (Perez, 2009, and Frost, 2004 in Nehaba 2019). To acquire the GPR data, MALA/Sweden type devices were used in the fieldwork (RAMAC). Two types of antennas were used separately, operating at 500 MHz and 250 MHz. The higher frequency allows for better resolution at shallow depths, whereas the lower frequency allows for a greater investigation depth.

2.10.1 RAMAC/GPR system:

An external PC, the radar control unit (CUII), the transmitter, and the receiver antenna make up the RAMAC/GPR system. Optical fibers connect the radar control unit to the transmitter and receiver antennas, and a parallel communication cable connects it to the computer. Mala Geosciences Company in Sweden purchased a RAMAC/GPR system (operating manual of RAMAC).

It is made up of numerous components or devices, such as flow:

2.10.1.1 Control Unit CU II:

The RAMAC/ GPR system's major component is the Control Unit CU II. All current RAMAC/GPR antennas are compatible with the CU II. The calibration and setup default parameters are saved in the internal memory for quick and easy operation (Mines & Report, 2010).

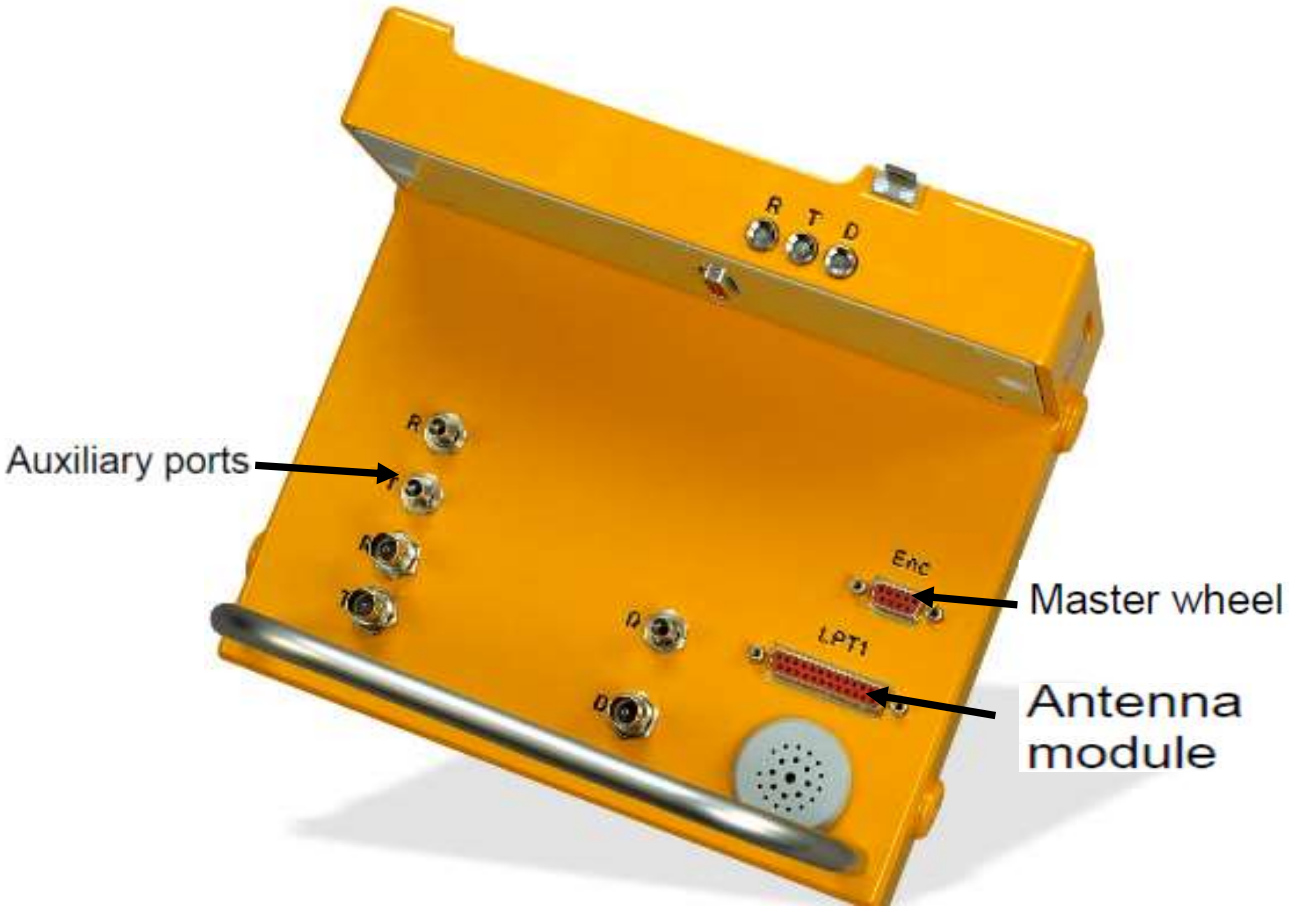

Figure 2.16: control unit CU II (Mines & Report, 2010).

The control unit CU II is powered by a 12V Li-Ion battery (Fig. 2.17). It can also be powered externally, with the power connection is located on the battery slot. Although the equipment is safeguarded against power surges and reverse polarity, all users are advised to use only MALÅ cabling (MALÅ Geoscience AB, 2011).

Figure 2.17: control unit CU II battery (MALÅ Geoscience AB, 2011).

2.10.1.2 Shielded antennas:

Shielded antennas from RAMAC/GPR are generally utilized for medium to high resolution surveys. The antennas' insulated structure makes them suitable for urban investigations or locations with a lot of background noise. The shielded antennas, like the other parts of the RAMAC/GPR system, are modular by design. This indicates that antenna electronics, pulling devices, and measuring wheels are mostly interchangeable and compatible. Utility, void, and Underground Storage Tank (UST) detection, as well as road surveys, quality assurance, and concrete investigations, are all common applications for the RAMAC/GPR shielded antennas. These shielded antennas are extremely versatile and effective tools for subsurface mapping(MALÅ Geoscience AB, 2011).

Figure 2.18 : RAMAC/GPR antenna (250MHz), (Mines & Report, 2010).

2.10.1.3 The MALÅ (RAMAC) XV Monitor:

The MALÅ XV Monitor is a specific data acquisition platform for MALÅ GPR devices with a unique user interface (figure 2.19). The XV Monitor is essentially a PC, but as a dedicated instrument, it lacks the extras and non-essential functionality found on normal commercial notebook computers; the XV Monitor is optimized for the task at hand, namely the gathering, management, processing, and presentation of GPR data. The MALÅ XV Monitor is built on a Linux platform, which means it starts up quickly, consumes little power, and runs a robust and reliable operating system. The MALÅ XV series monitor features a revolutionary user interface that is simple to learn and operate even in extreme conditions. (Platform & Interface, n.d.). A XV Monitor with a data cable connected to the control unit on one side and a 12V/13,2 Ah battery on the other side.

Figure 2.19: The MALÅ(RAMAC) XV Monitor, (Mines & Report, 2010).

The MALÅ(RAMAC) XV Monitor units are powered externally, with 12V AC/DC or any 12 V battery or with MALÅ standard Li-Ion Batteries, see Fig. 2.20.

Figure 2.20: Battery pack and battery bag of the XV Monitor from MALÅ. (A) The battery bag's internal, and (B) the connections on the outside (MALÅ Geoscience AB, 2011).

2.10.1.4 ROUGH TERRAIN CART:

MALÅ Mini is a hand-pushed cart for rough terrain suitable for many MALÅ antennas, when conducting GPR surveys on unpaved surfaces and in rougher terrain. The cart is Available in more than one size, to accommodate the choice of antenna (MALÅ Geoscience AB, 2011).

Figure 2.21: Rough Terrain Cart (RTC) (www.malags.com).

In the field work uses the rough terrain cart with whole system (The Instrument) shown in (figure 2.22).

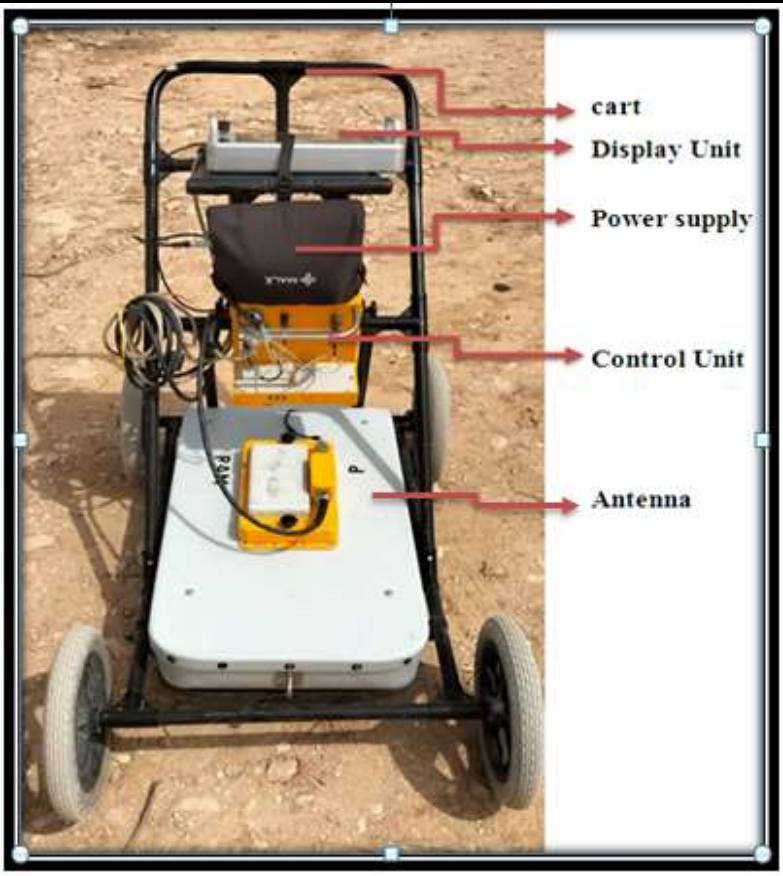

Fig. 2.22: RAMAC/GPR Instrument

2.11 Instrument calibration:

Fixed instrument calibration was selected with all radar surveys in the five sites. With antenna 250 MHz surveys the time window is 4.5ns and choose velocity of the electromagnetic subsurface wave 100 m/ns in all profiles. the sampling frequency of the GPR survey in all sites is 2600MHz. The survey was using the cart, so the wheel was chosen as the scanning mode. All the profiles are conducted with a point interval of 0.1m and number of stacks is 2.

In addition, with antenna 500 MHz where survey with time window is 3ns and choose velocity of the electromagnetic subsurface wave 100 m/ns in all profiles. The sampling frequency of the GPR survey in all sites is 2600MHz. the survey was using the cart, so the wheel was chosen as the scanning mode. All the profiles are conducted with a point interval of 0.05m and the number of stacks is 2.

2.12 The modes of GPR:

In this study we used Reflection Profiling Mode**:** (Common off Set Single Fold Reflection Profiling)

In this mode, data are acquired by moving the antenna over the earth's surface (profile direction) along the survey line. The shielded and un-shielded antenna can be used in this mode. The properties of this mode can be mentioned in the points below:

- In CO acquisition, reflection points are images by one ray path only.
- easily interpretable data.
- signal-to-noise ratio can be poor.

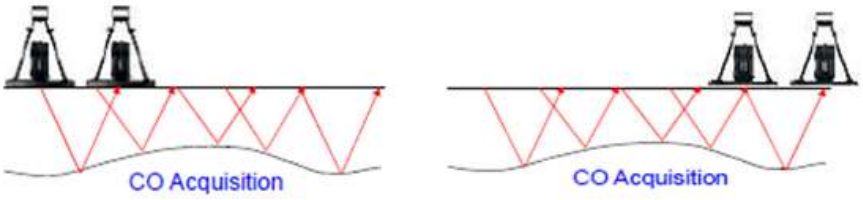

Fig.2.23: Common off Set mode (modified after Davis and Annan, 1989).

2.13 GPS Instrument:

The GPS system is mainly used to determine the geographical locations in the world of any point on the surface of the earth. The GPS cannot be used inside buildings and closed areas, and if it is used, it will not be accurate in its results, and it does not need an Internet connection, but a device that supports the system. In the current study, the GPS device (etrex) in (Figure 2.24) was used to find out the study sites with respect to longitude and latitude.

Fig.2.24: GPS Instrument

2.14 Field work:

GPR survey was carried out by using RAMAC/GPR in the study area, and five survey sites were selected and arranged in a manner that covers the study area (fig 2.25). At each site, 5 path were selected, the paths length and directions are different from one site to another, and a distance between the paths is 5m however, two transverse path were measured at each site. The initial test was carried out at each site using a 250 MHz antenna and its notes were taken. Then the same paths were scanned using a 500 MHz antenna. The first antenna, 250 MHz, was used to investigate the best possible depth to reach through this area, and the second antenna was used at 500 MHz, in an attempt to get the best possible investigation with high resolution.

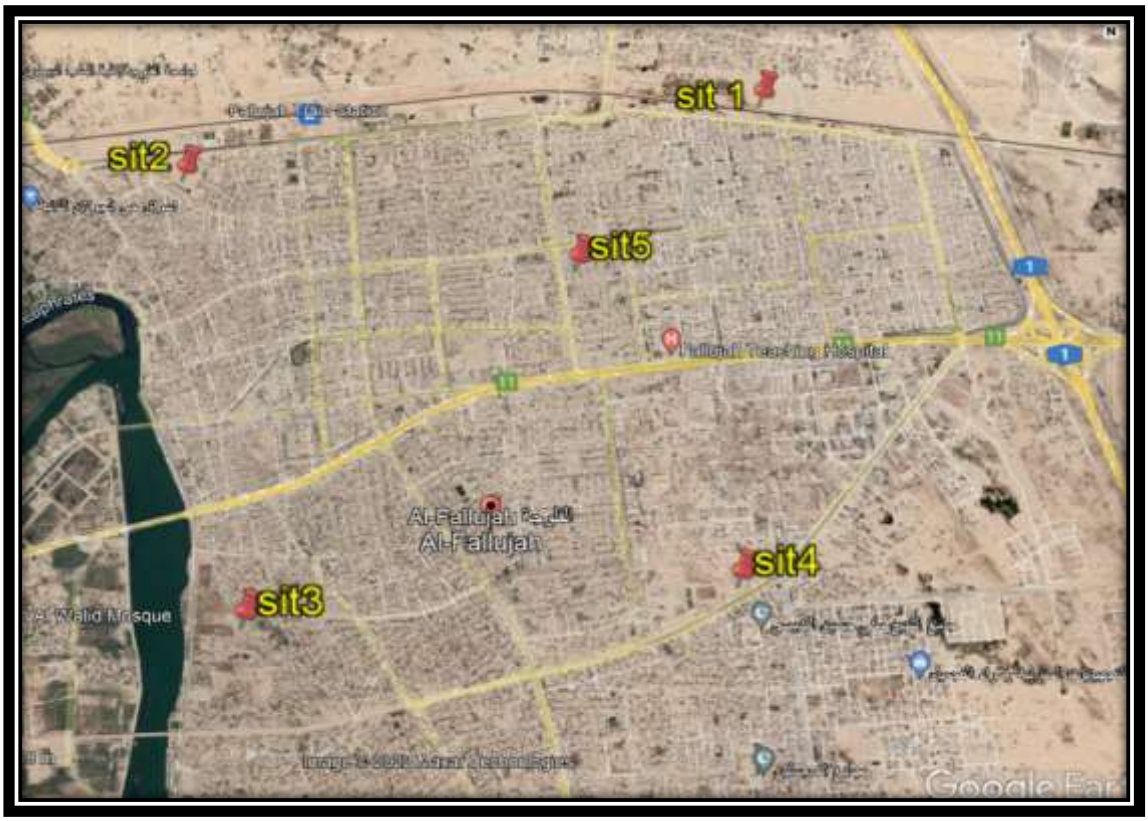

Fig. 2.25: Aerial photograph show five sites are chosen within the study area.

- **Site 1:** It is located within the north-eastern part of Fallujah city and within the geographical coordinates (33°, 22, 149 N, 43°, 47, 182 E). In the method of work, 5 equal paths of length 50 m, the distance between one path and another was 5 m, and direction E-W were chosen, and two transverse paths with N-S direction were measured and this was expressed in a 2D way, where the survey was conducted using an antenna 250 MHz for these paths, and then used antenna 500 MHz for the same paths (fig. 2.26).

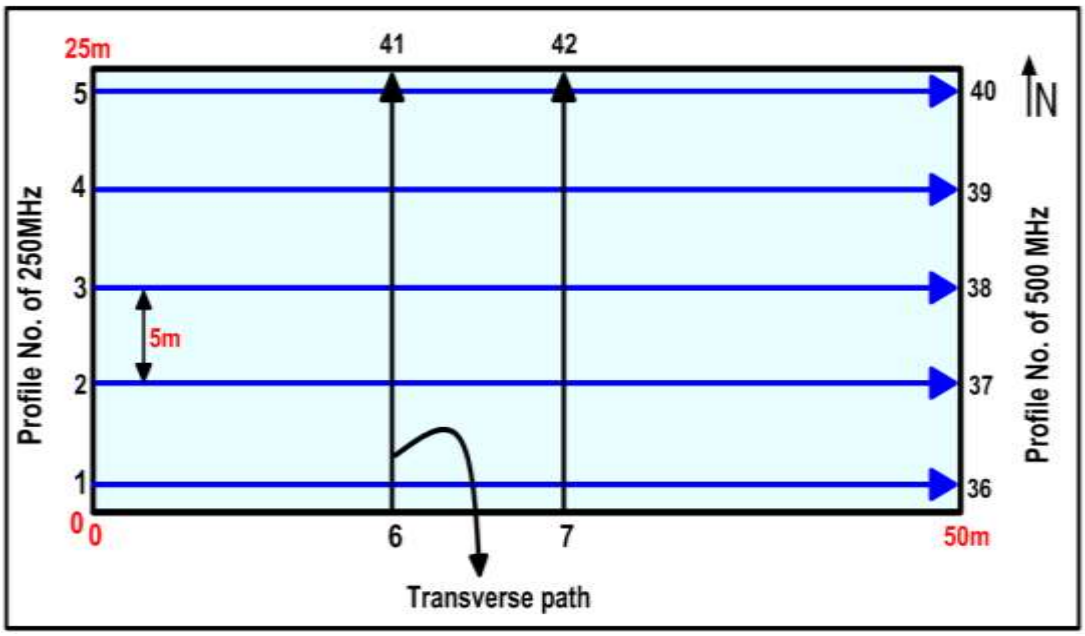

Fig. 2.26: Schematic diagram of fieldwork procedure in site one.

We also use on this site the grid survey, where I scanned an area of $(60m)^2$, (6 * 10m) The distance between one path and another was 1 m , this represents a 3D survey and also it was using the 500 MHz antennas, in an attempt to get the best resolution within this area.

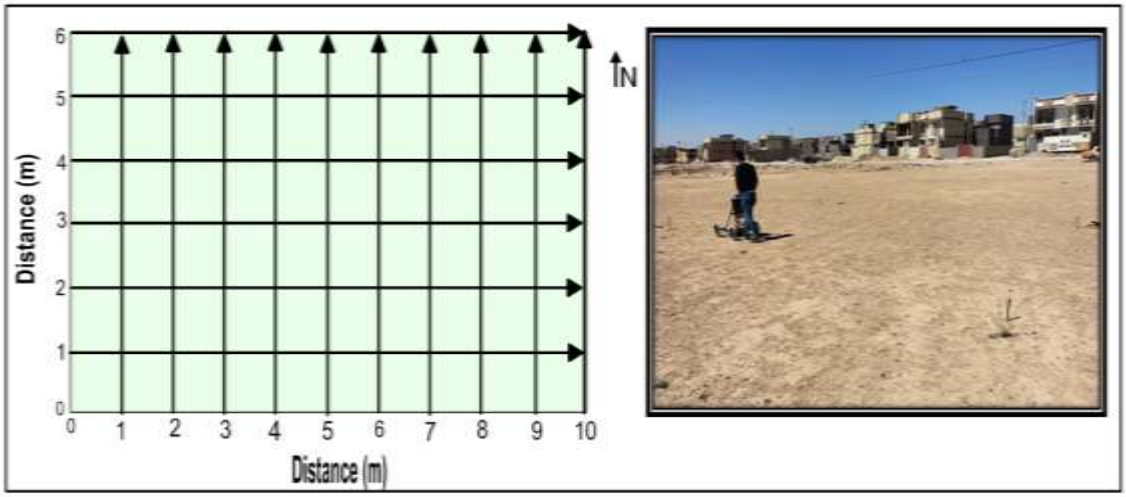

Fig. 2.27: grid survey within the site 1.

- **Site 2:** This site is located within the northwest part of Fallujah city and within the geographical coordinates (33°, 21, 857 N, 43°, 45, 696 E). The method of work here was similar to the first site, where five parallel paths of length 40 m, the distance between one path and another was 5 m, and in the direction of E-W were selected (fig.2.28). Two transverse paths with N-S direction that scanning using the same antennas was 250 MHz once and 500 MHz in another time and this is like the 2D scanning.

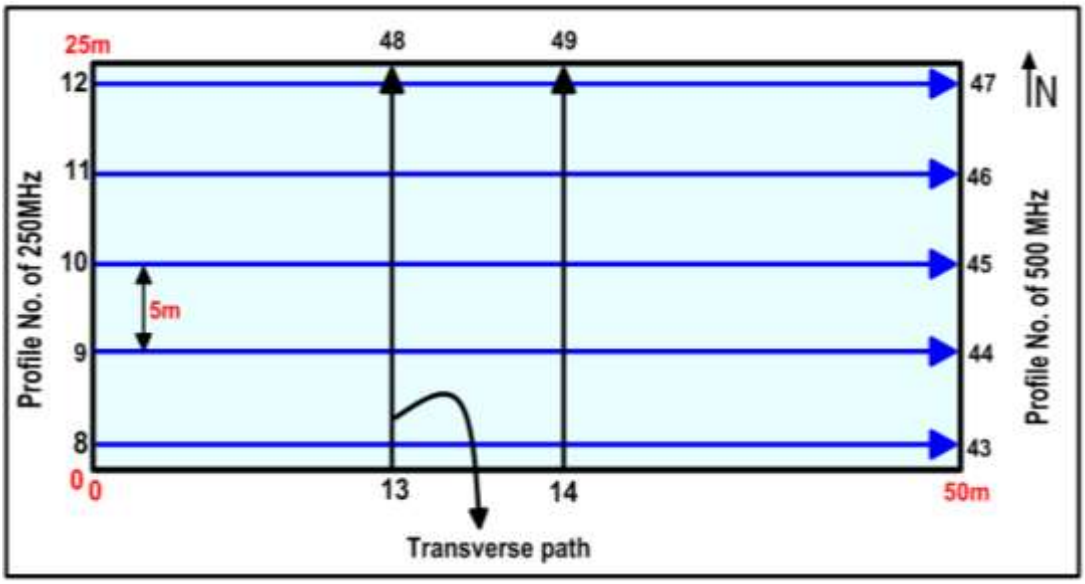

Fig.2.28: Schematic diagram of fieldwork procedure in site two.

- **Site 3:** This site is located within the south-western part of Fallujah city and within the geographical coordinates (33°, 20, 298N, 43°, 45, 955 E). The method of work was also similar to the two previous sites for parallel paths, where five parallel paths were selected, 50 m long, in an N-S direction, and two transverse paths in the E-W direction, and the survey were conducted in them using 250 and 500 MHz antennas, this is like a 2D survey.

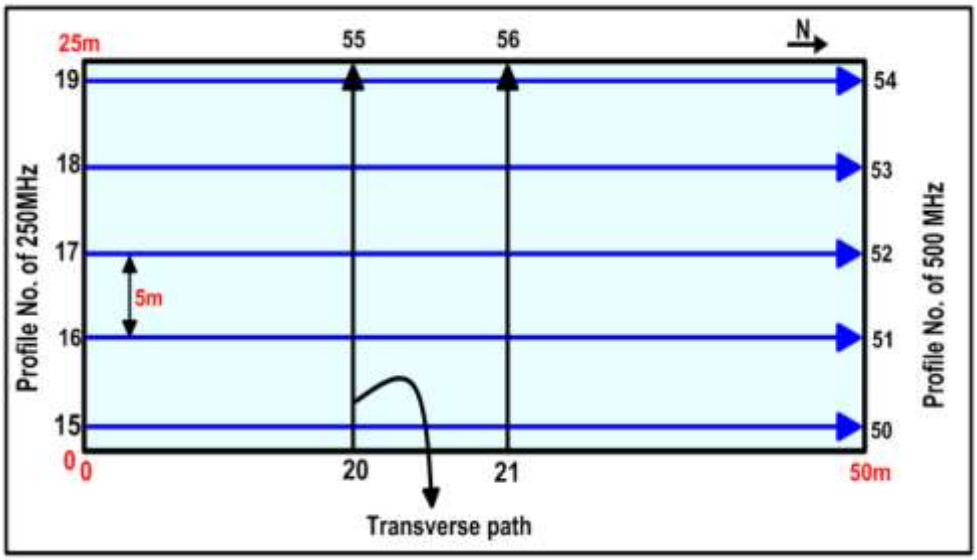

Fig. 2.29: Schematic diagram of fieldwork procedure in site three.

- **Site 4:** This site is located within the south-eastern part of Fallujah city and within the geographical coordinates (33°, 20, 429N, 43°, 47, 788 E). The method of work here was limited to equal paths, where 5 equal paths of 40 m length were selected, and they were in an E-W direction, and the distance between each path and another was 5 meters. The work also included identifying two transverse paths, which were in the direction of N-S, and the survey was conducted in all these paths with antennas 250 MHz once and 500 MHz again.

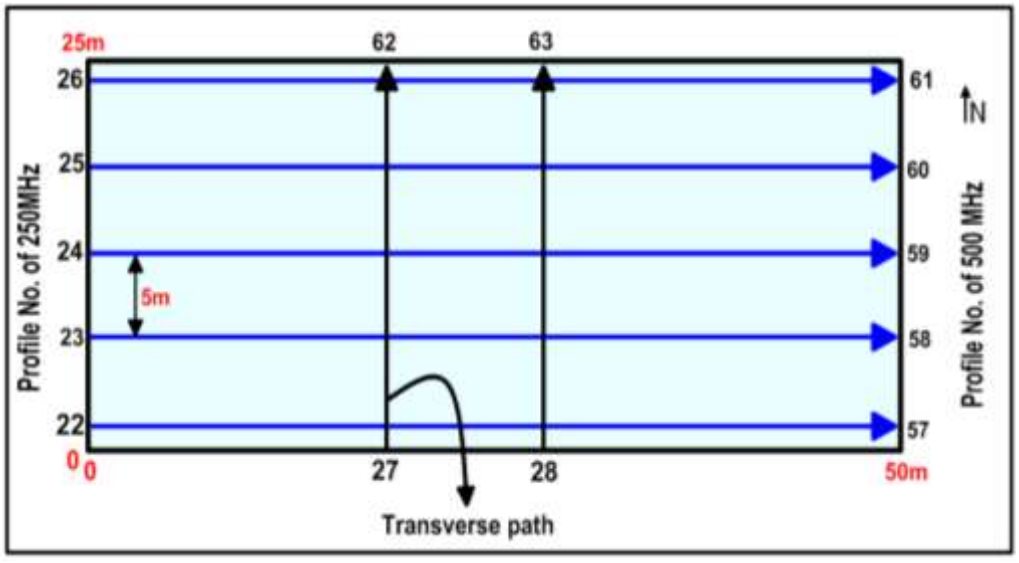

Fig.2.30: Schematic diagram of fieldwork procedure in site four.

- **Site 5:** This site is located in the centre of Fallujah city and within the geographical coordinates (33°, 20, 528 N, 43°, 47, 216 E). The work here was in the same way as the work in Site 4 where the method of work here was limited to equal paths, where 5 equal paths of 40 m length were selected, and they were in an N-S direction, and the distance between each path and another was 5m.

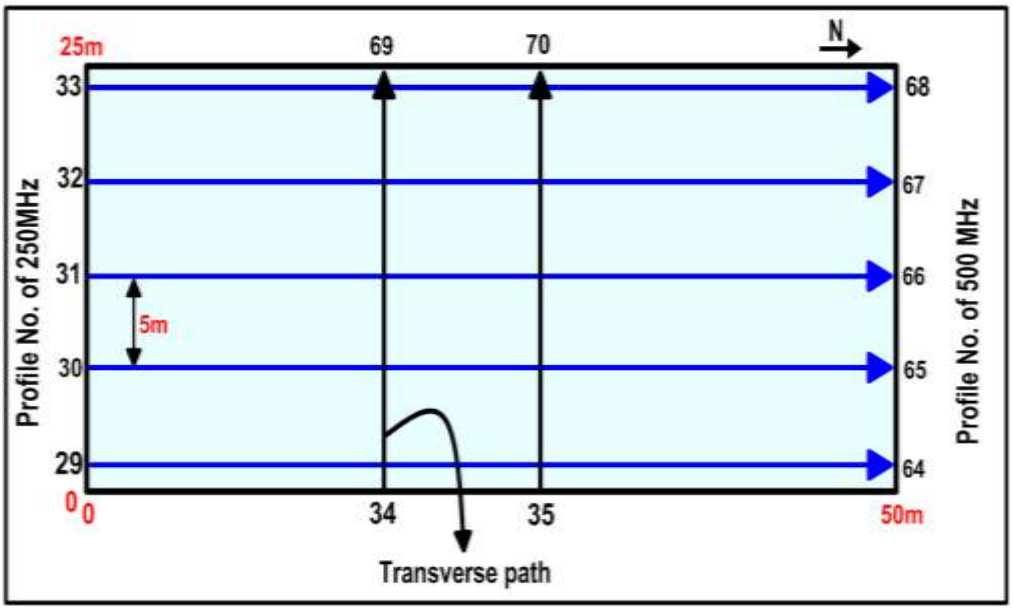

Fig.2.31: Schematic diagram of fieldwork procedure in site five.

The work also included identifying two transverse paths, which were in the direction of E-W, and the survey was conducted in all these paths with antennas 250 MHz once and 500 MHz again.

Chapter Three

GPR Data Processing and Interpretation

3.1 preface:

This chapter describes the details of the dedicated GPR software package ReflexW^{TM}, used to pre-process GPR data analyzed in this project. It gives details of the processing steps available in the software to improve the raw data quality before further processing and techniques developed in this work are applied. This chapter it also presents description and presentation of the processed GPR data, and clarification of the reflections and anomalies found in these profiles (the objective of the study).

3.2 GPR data processing:

Processing GPR data using computers are commonly used now a days, due to the inexpensive access to computer facilities. The processing procedure consists of a sum of operations applied to the raw data to enhance the signal-to-noise ratio (SNR) and produce a more realistic image of the ground. GPR provides a quick and easy way to image the first few meters of the subsurface with a relatively good resolution in determining shallow void characteristics where individual anomalies are not distinguishable by the other non-destructive geophysical methods, (Haramy et al.,2006). The raw data, acquired in this, study are represented in, 2D sections (radar grams). The GPR raw data shows, the quality of the profiles which come directly. from the field without, any processing. (Figure 3 .1) shows raw data of GPR profile (1).

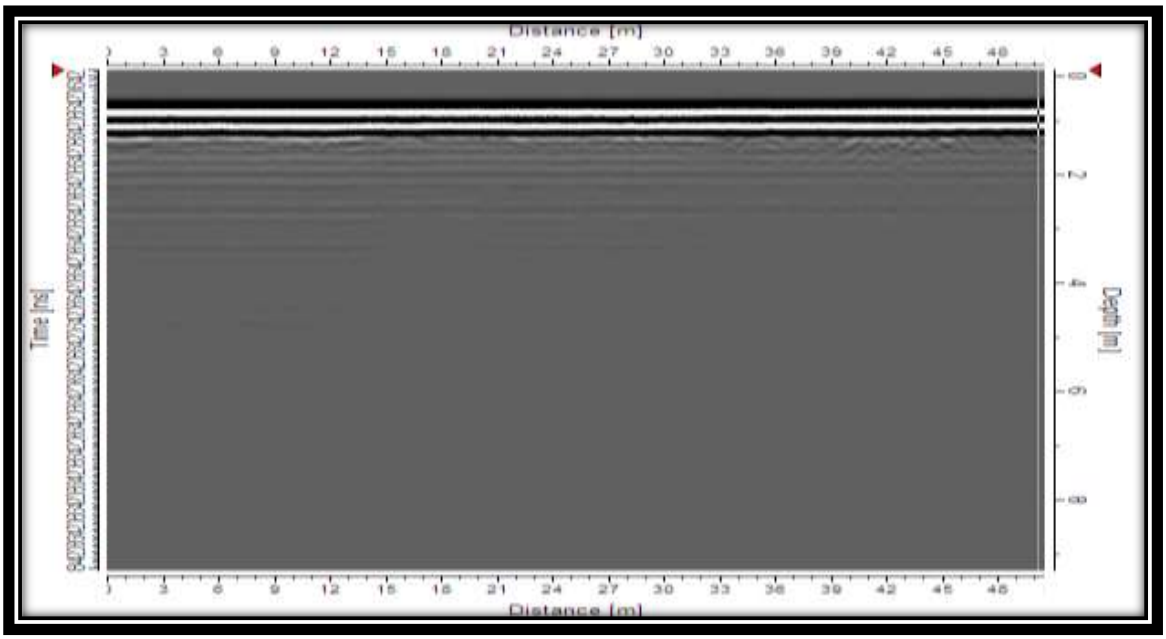

Figure 3.1: Raw data of GPR profile (1), before processing.

3.2.1 Data Editing:

In any processing sequence data editing is often the most time consuming since the files usually need sorting and rearranging as the first step in the post-collection. Effective maintenance of the data from the start is vital for good-quality interpretation, particularly with the large volumes of data (Group, 2006). Data editing is the first procedure applied to, the measured raw data. The editing includes re-organization and saving, the data. The survey information is registered. The results of data editing are essential before further, the processing is made.

3.2.2 ReflexW software program:

In this work, the collected GPR data was imported and processed using ReflexW^{TM} which is an independent package software that can import a range of different data types. It has been developed by K. J. Sandmeier for the processing and interpretation of reflection and transmission data specifically in GPR application, and reflection, and refraction of seismic and ultrasound data (Sandmeier, 2009).

3.2.3 Basic Processing:

The basic processing, steps are usually applied, to the raw data, (often automatically) and, introduce minimal operator bias, into the data without, the need for additional, subsurface information typically in the form of trace editing; filtering, or data correction, (Harry, 2009). These steps can be used with the majority of collection modes.

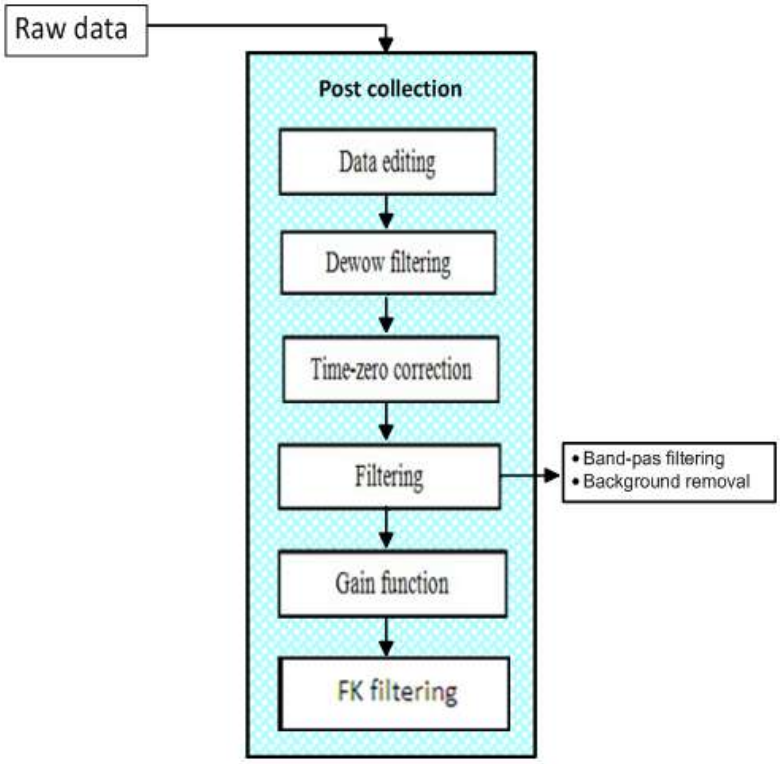

Fig. 3.2: GPR data processing flow using ReflexW.

Figure 3.2 describes the processing flow used for analyzing GPR data using ReflexW. The basic descriptions of each step are: After collecting the raw data basic processing is applied within the first stage data editing to remove, and correction of bad/poor data, and sorting of data files. Then the second stage is applying the de wow filtering to correction of low frequency and DC bias in data. The third stage of basic processing is applying the time zero-correction to correct of start time to match with surface position. The fourth stage is applying the 1D and 2D filtering to improve the signal-to-noise ratio and visual quality. The five

stages are applying the gain function to the improvement of data display and interpretation. Unwanted reflections from the borders of the investigation medium are often characterized by a distinct slope that corresponds to medium or air velocity. Those structures can be easily removed using a multichannel filter. The most popular filter is the so-called frequency, wavenumber (F-K) filter which works within the frequency wavenumber range, This is the last stage of basic processing.

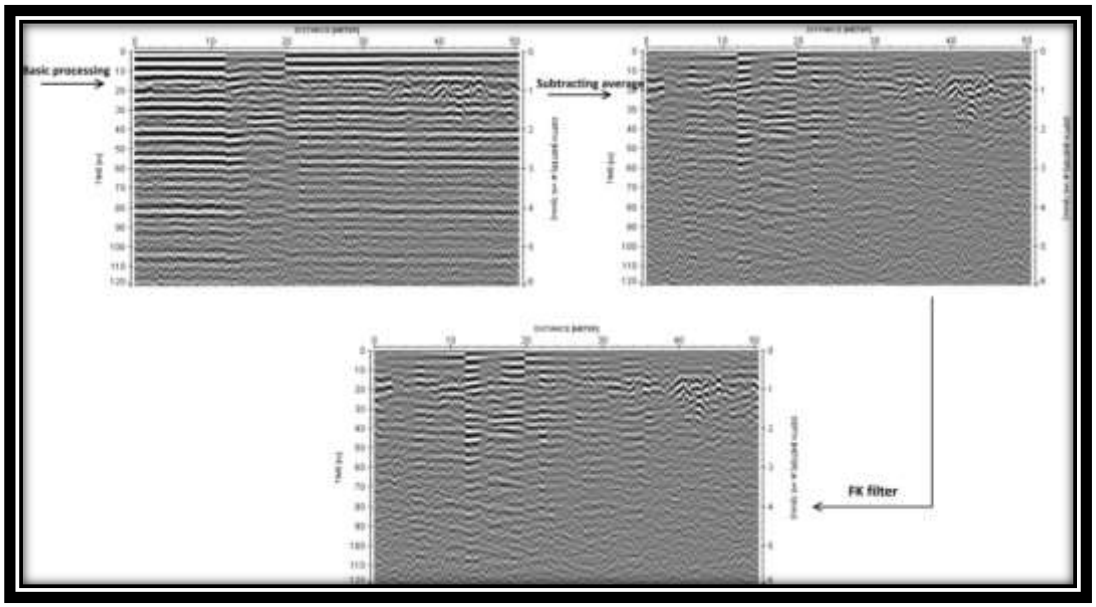

Fig.3.3: show the applying of the basic processing stage for the raw data of antenna 250 MHz.

3.3 Result and Interpretation of GPR profiles:

GPR data interpretation is a difficult process that occasionally involves subjectivity and other times is rather clear-cut. Depending on the type of antenna, the penetration depth ranges from 3 to 6 m. After processing the radargram data, it was discovered that an anomalous feature was present throughout each survey site. Because of the shallower contact and greater contrast between the loose and compacted soil layers, the first interface becomes significantly more visible in all antenna profiles at 250 and 500 MHz.

3.3.1 Antenna 250 MHz:

In the raw data of radargrams, the areas of weakness and anomalies do not appear, but after processing by filters they appear as shown in (figure 3.4). This antenna was scanned at all five aforementioned survey sites.

Site one:

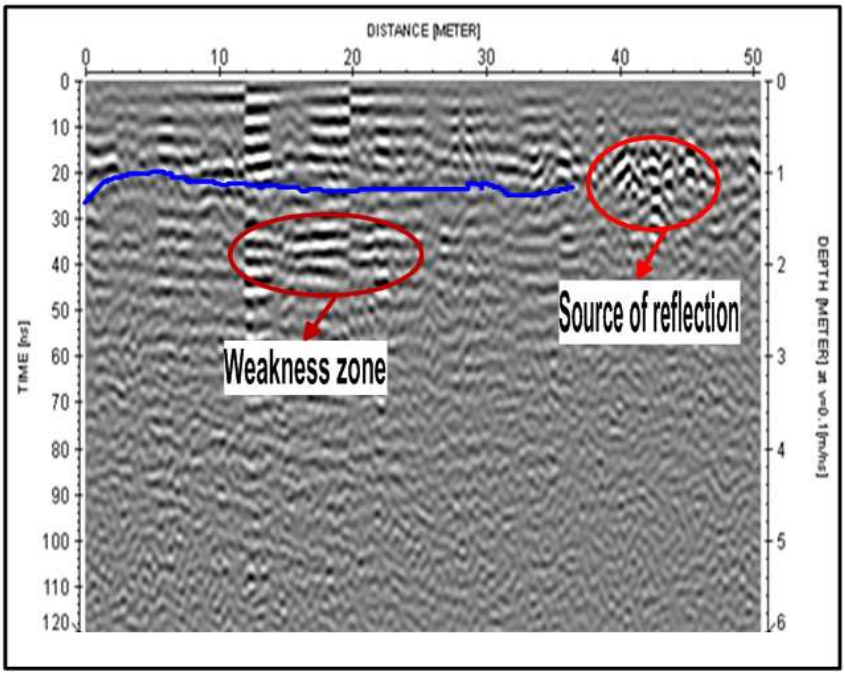

Fig. 3.4: show radargram profile (1) of antenna 250 MHz for site one.

This profile shows many reflections As a result of the contrast between the components of the soil. The profiles show topsoil strata, which indicate fill materials, at a depth range of 0 to 2 m .along the profile, so containing a reflection may be an object at a ranging depth of 1-1.5m. and show the weakness zone at a depth of 2m, It is believed that this is a gap.

Also, we can notice, that distinct hyperbolic reflections may be noise resulting from the impact of objects above the surface, such as profile 2 (fig. 3.5).

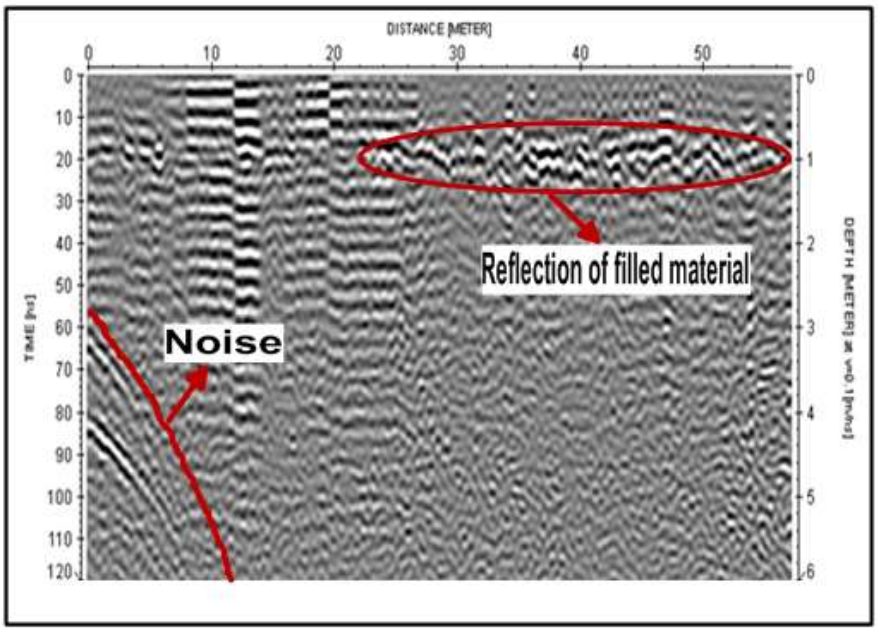

Fig. 3.5: show profile (2) of antenna 250MHz for site one.

It is also believed that there were metal objects buried in shallow depths that led to the doubling of electromagnetic waves and formed a state known as a ringing starting from a depth of (0.5 to 6 m) as shown in profile 3 (fig. 3.6).

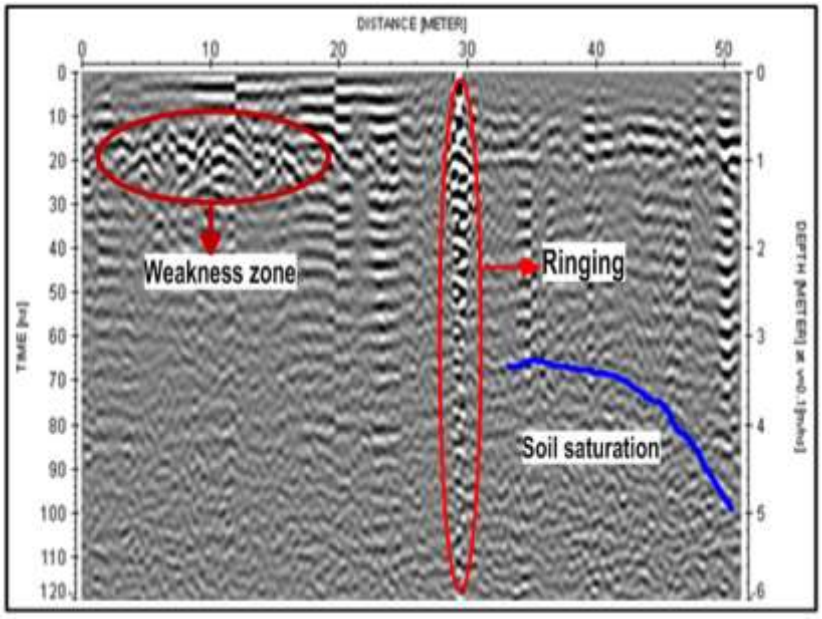

Fig. 3.6: show profile (5) of antenna 250MHz for site one.

The grid survey in this site showed the density of weak areas or gaps within this site (figure 3.7), which are due to the shallowness of the groundwater and the burial operations during non-continuous periods.

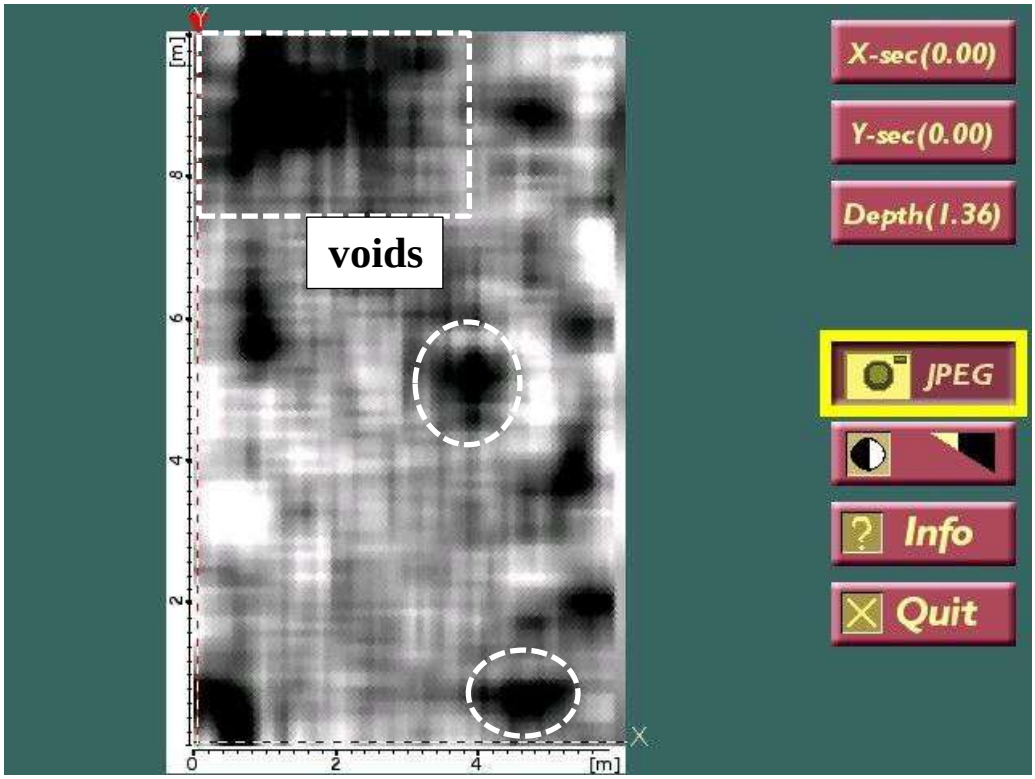

Fig. 3.7: Grid survey within site one.

On this site, there is a pool of water flowing through a well 10 meters deep, which was dug for agricultural purposes more than ten years ago. This is evidence of the abundance of shallow groundwater which has caused the creation of weak areas (figure, 3.8).

Fig. 3.8: A pool of water flowing through a well 10 meters deep.

- **Site two**: The profiles of this site were processed using the aforementioned filters and processing methods. This chapter will explain part of them and the other part will be in the appendix.

  (Fig. 3.9) shows the Weaknesses zone at shallow depths at two profiles which are expected to form gaps and indicate the presence of loosening in the soil to a depth of two meters.

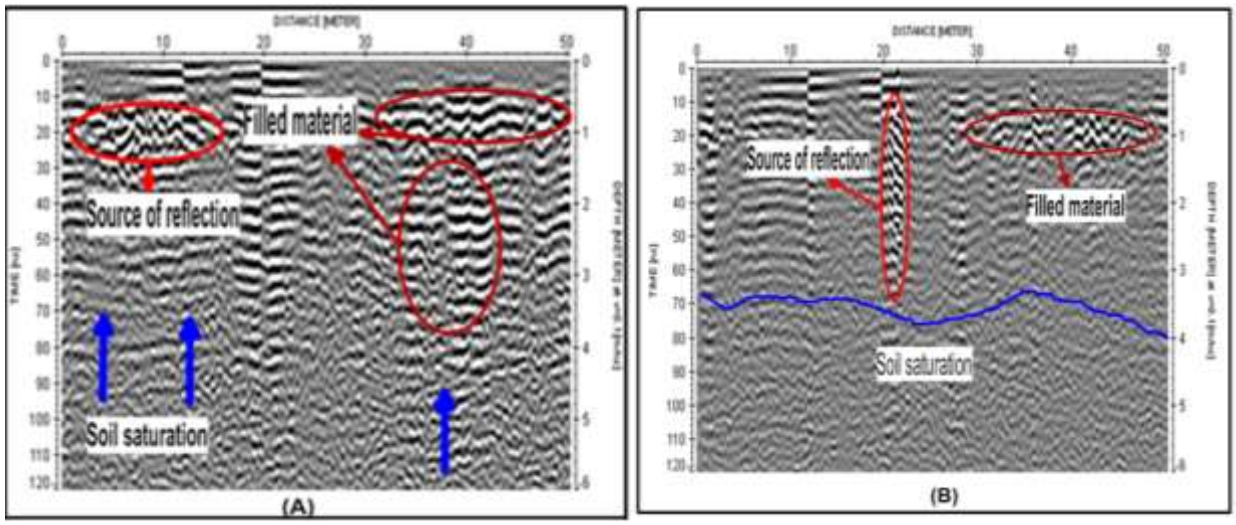

Fig. 3.9: (A) show profile (8) and (B) show profile (9) of antenna 250 for site two.

(Fig. 3.10) is noted in this profile as a group of clear reflections resulting from filling the materials in the upper part of it and clearly shows the high saturation range of the soil.

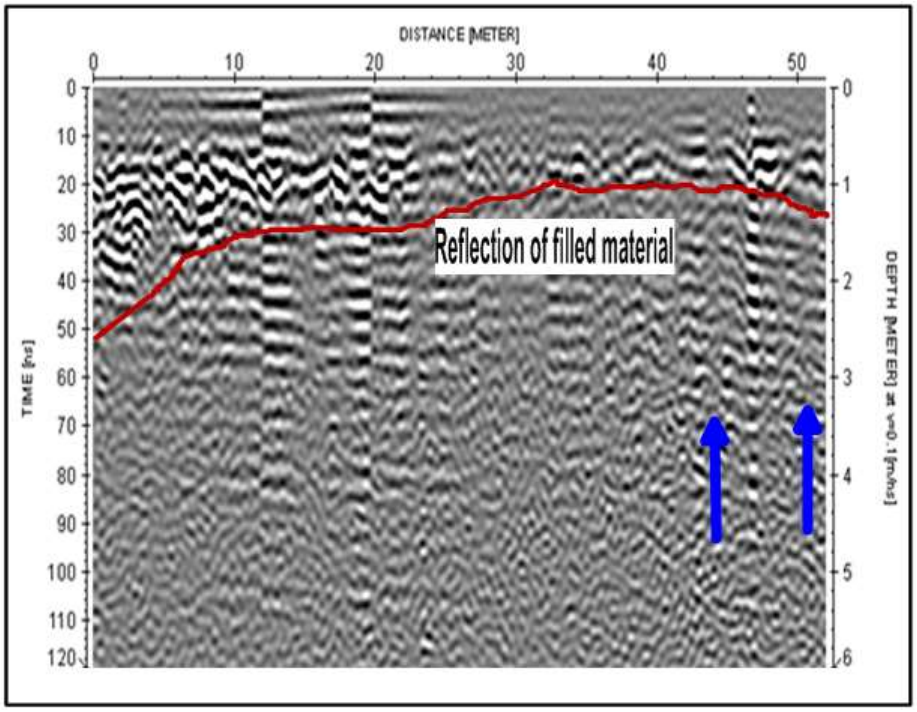

Fig. 3.10: profile (12) of antenna 250 MHz for site two.

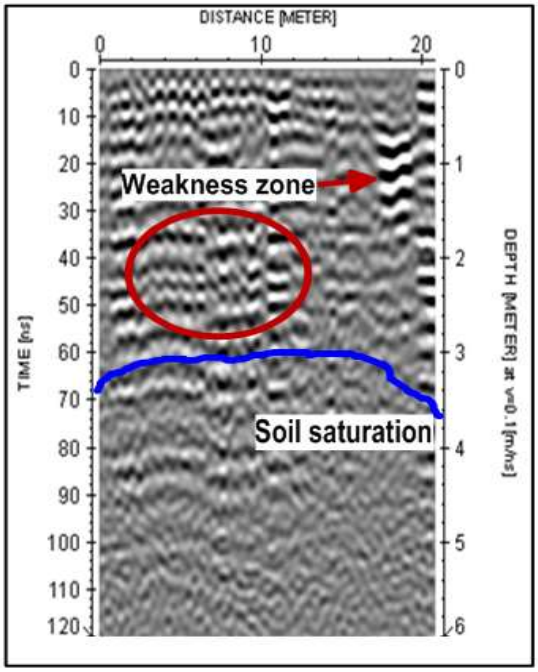

Fig. 3.11: profile (14) transverse path of antenna 250MHz for site two.

Site three: A number of the profiles of this site have been processed as follows:

(Fig. 3.12) shows that many distinctive reflections in the yellow circle indicate the presence of anomaly that may be the result of buried body, and other reflections show the areas of weakness in this soil.

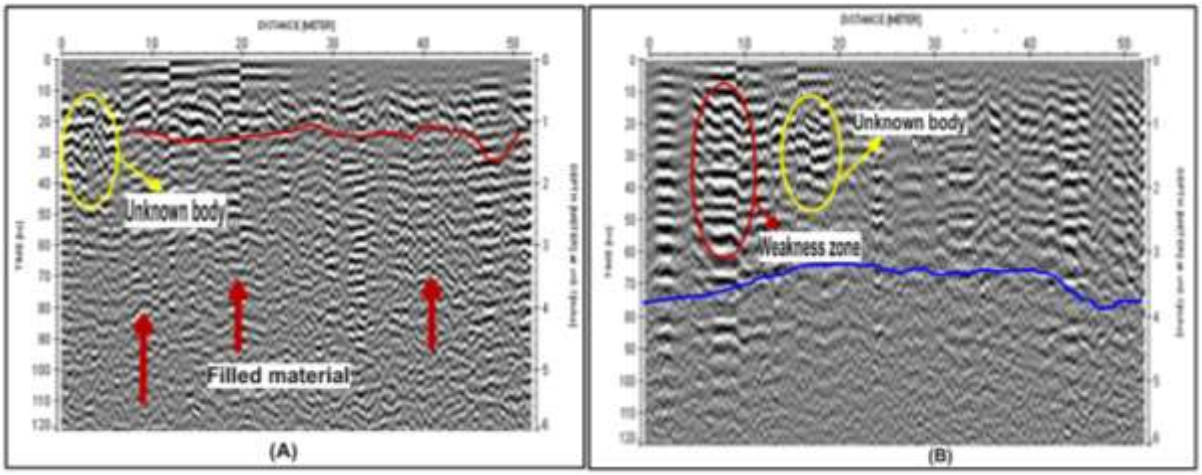

Fig. 3.12: (A)show profile (15) and (B) profile (16) of antenna 250MHz for site Three.

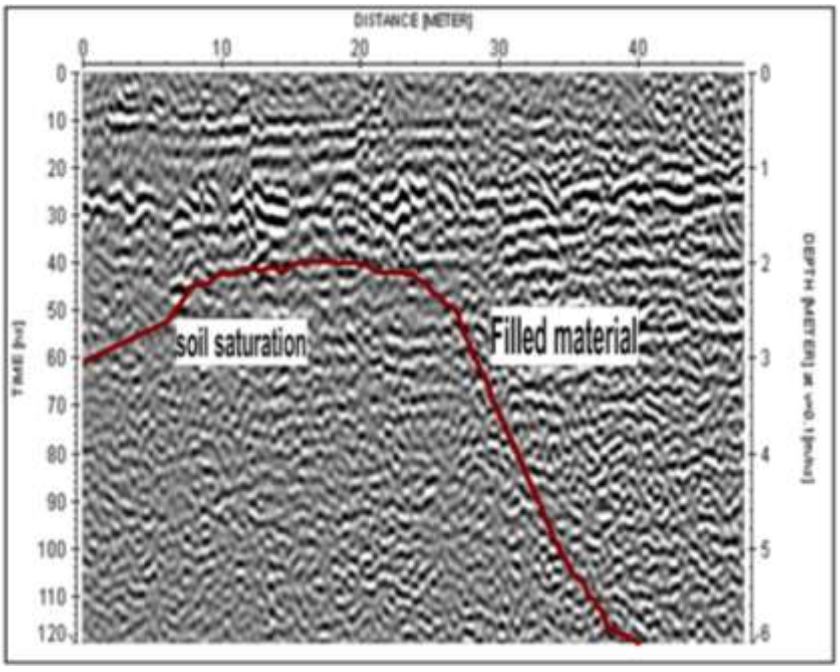

fig. 3.13: profile (17) of antenna 250MHz for site Three.

- **Site four:** The figures (3.14; 3.15; 3.16) show the locations of soil saturated zones, which represent areas of weakness that may have an impact on the foundations of construction in the city.

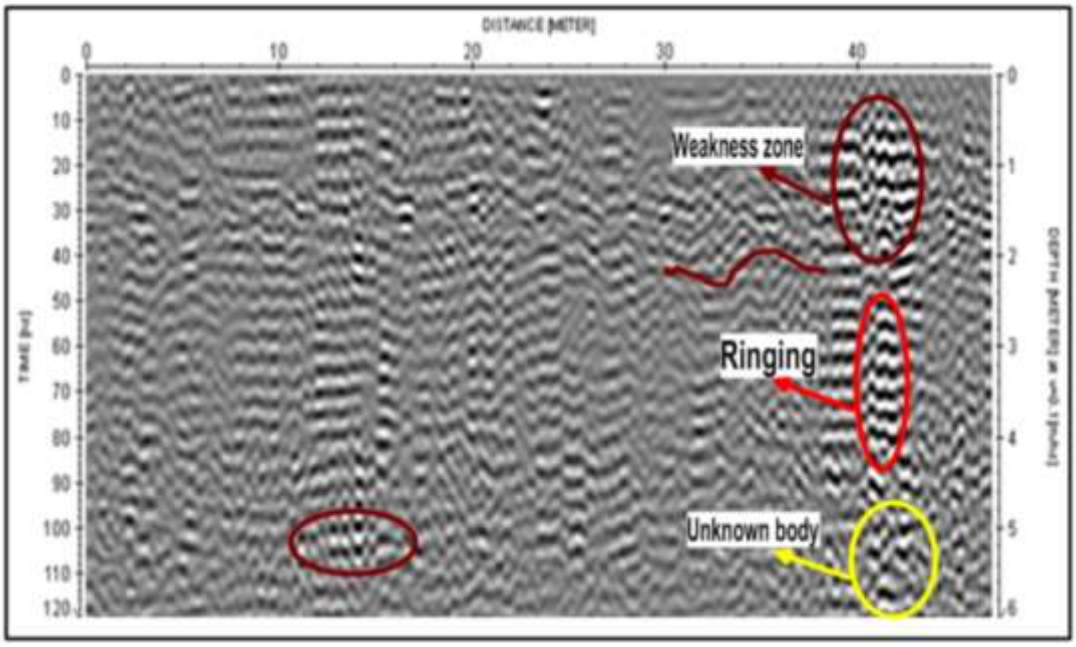

Fig.3.14: profile (23) of antenna 250MHz for site four.

In this figure, a lot of distinctive reflections appear, marked against each of them in a circle. The first, marked in dark red, represents a weak area in the soil, which is formed as a result of loosening in the soil, and the second marked in red is a ringing (type of noise), in addition to the area marked in yellow color, which It may be caused by the presence of an object buried at this depth.

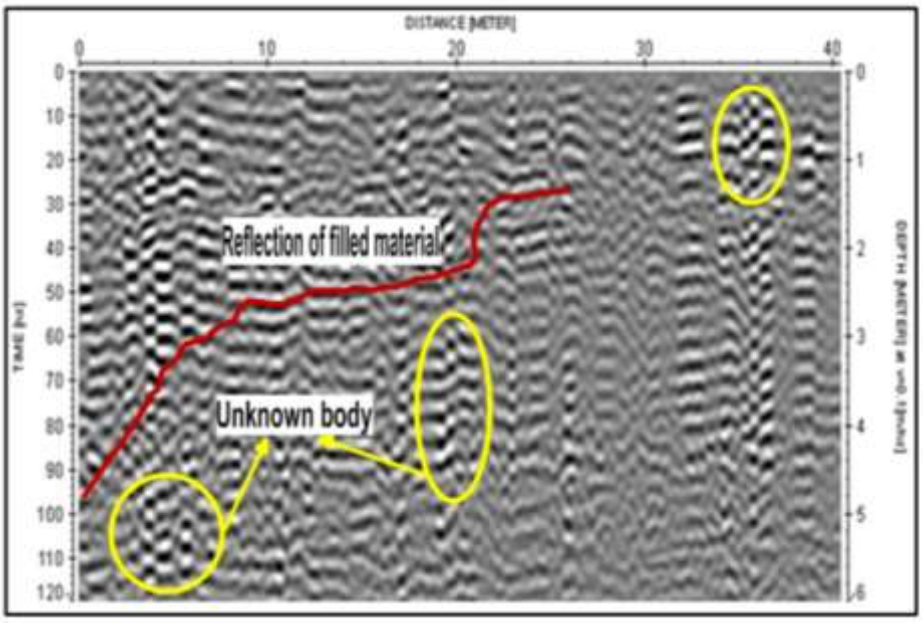

Fig. 3.15: profile (25) of antenna 250MHz for site four.

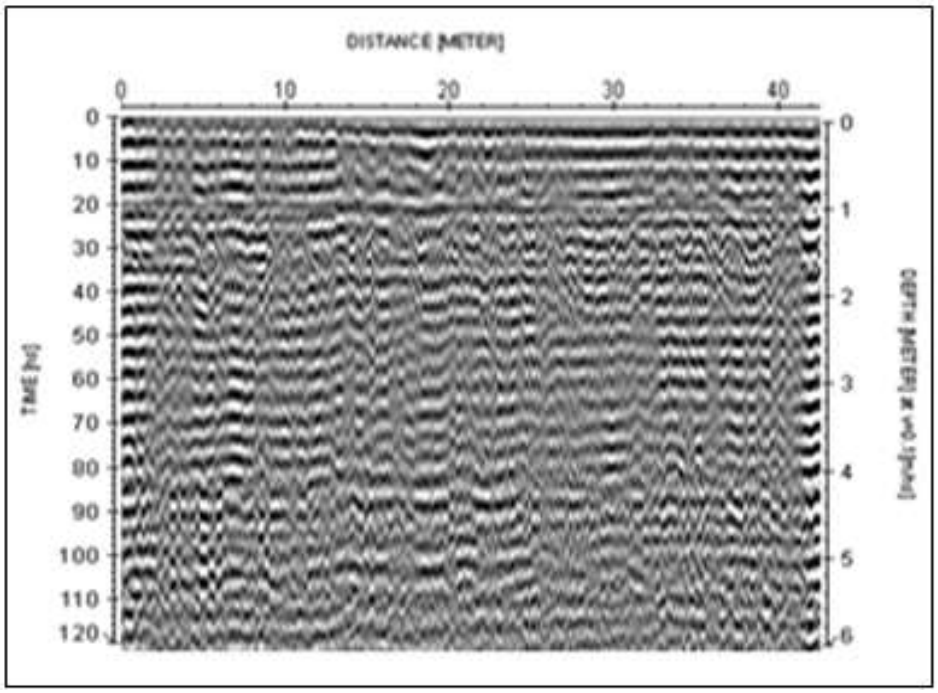

Fig. 3.16: profile (26) of antenna 250MHz for site four.

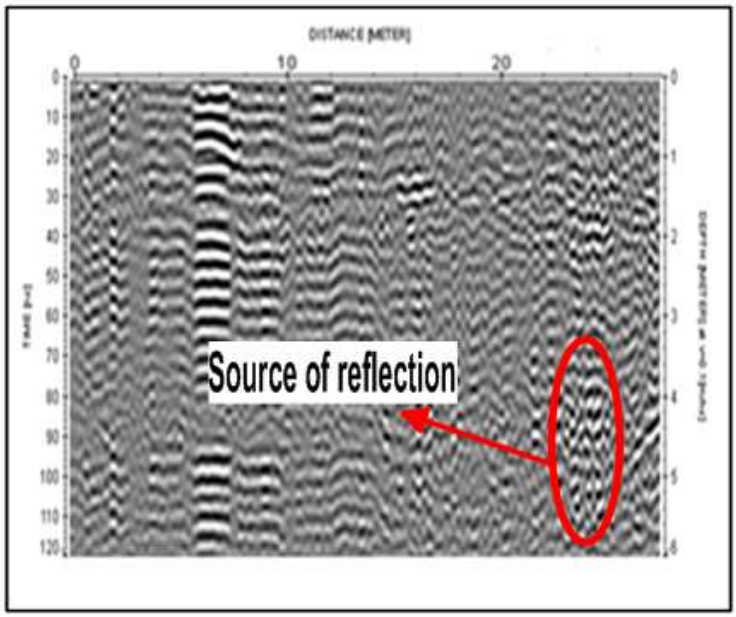

Fig. 3.17: profile (28) transverse path of antenna 250MHz for site four.

- **Site five:** The figures (3.18; 3.19; 3.20) show the locations of the areas of fill material zones, which represent areas of weakness that may have an impact on the foundation. In addition to the presence of buried objects in this location that had a strong reflection of electromagnetic waves.

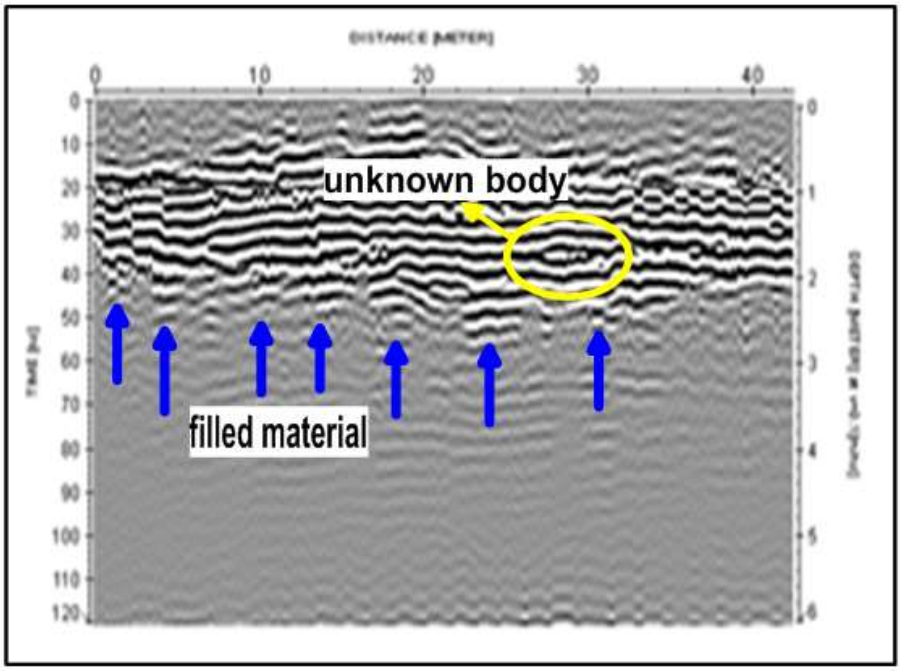

Fig. 3.18: profile (29) of antenna 250MHz for site five.

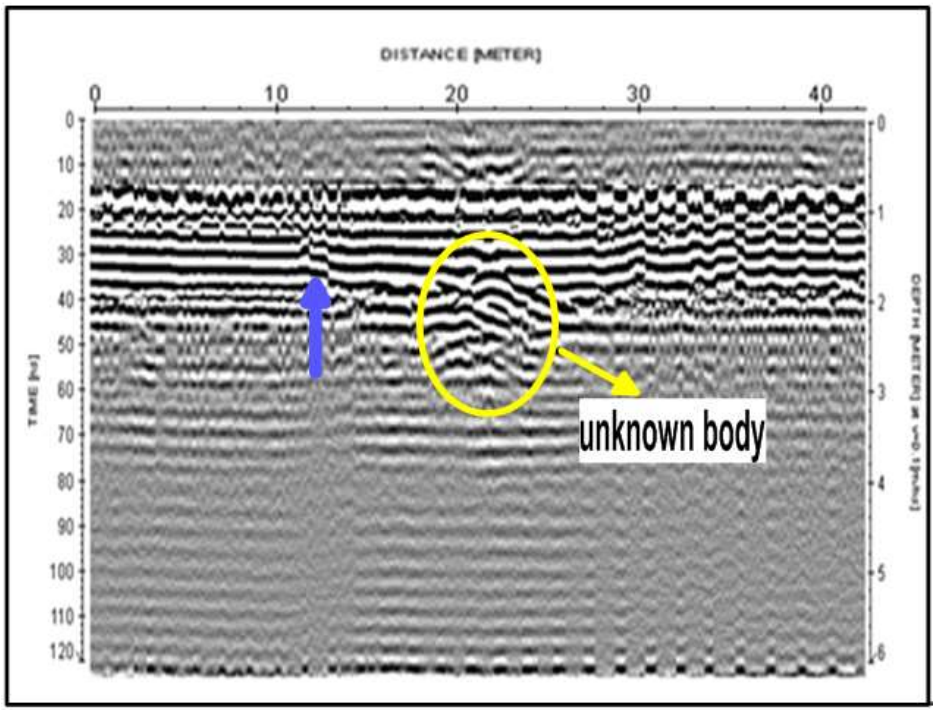

Fig. 3.19: profile (31) of antenna 250MHz for site five.

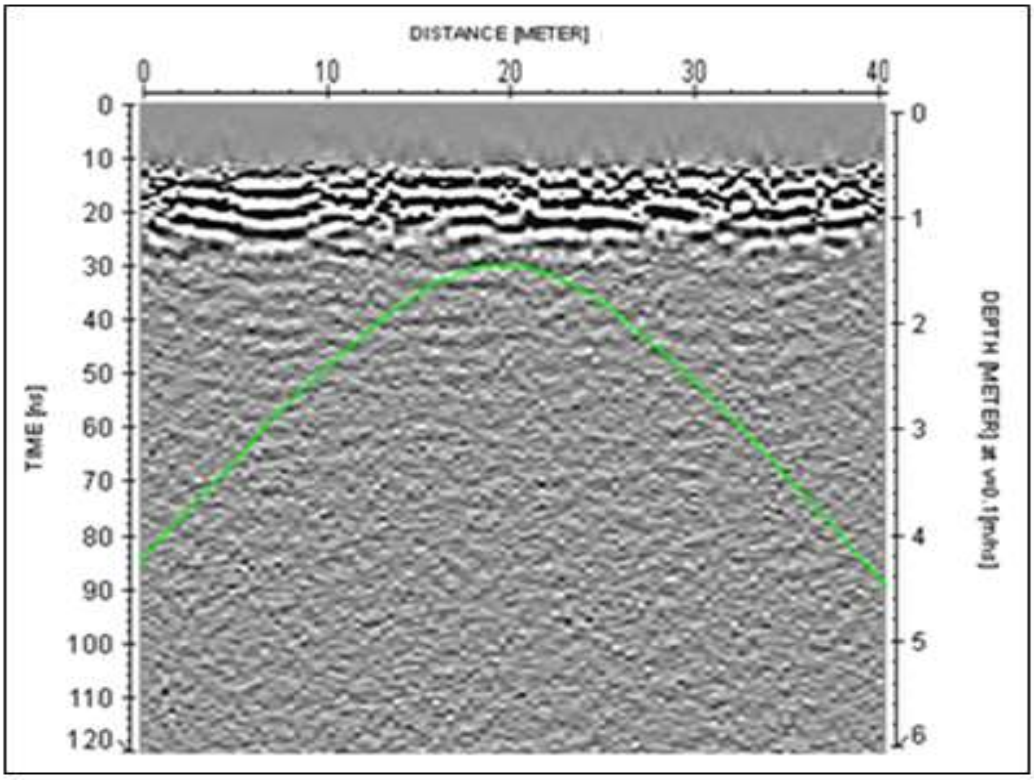

Fig.3.20 : profile (32) of antenna 250MHz for site five.

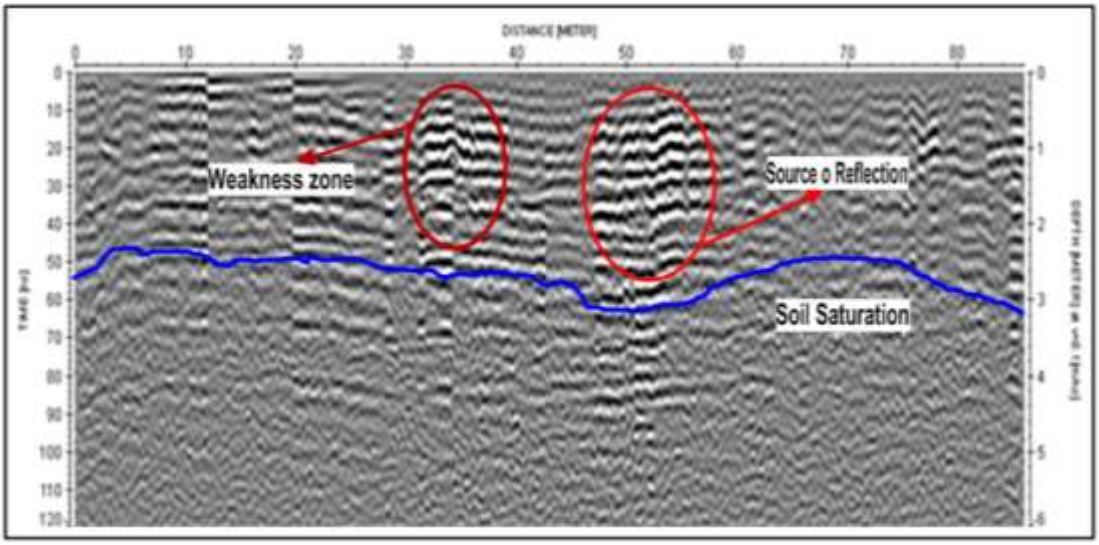

Fig.3.21: profile (35) transverse path of antenna 250MHz for site five.

3.3.2 Antenna 500 MHz:

Use this antenna to get a high reflection accuracy of buried objects and areas of weakness that were pre-diagnosed with the 250MHz antenna. The penetration rate of this shield was from 1 to 3 m, and it showed the presence of many anomalies close to the surface, which will be clarified through the following profiles of the five survey sites distributed over the study area, the profiles number of this survey start from profile 36.

- **Site one:** The image appears below the surface more clearly, but at shallow depths. Figures (3.22; 3.23) highlight the range of areas filled with transported materials and deposited by groundwater or burial during the reconstruction of the city by a man during the time since the establishment of the city. In addition to saturated soil.

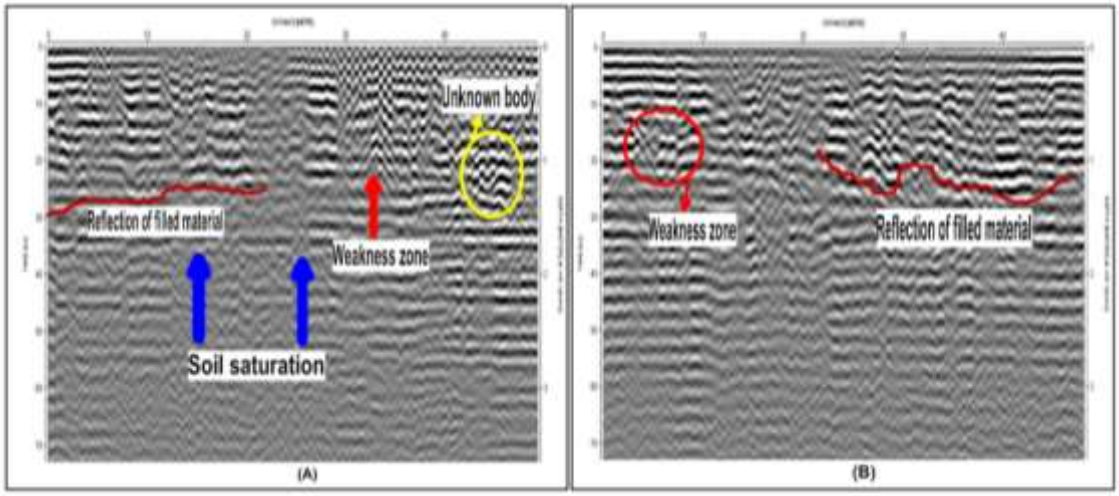

Fig.3.22: (A) show profile (36) and (B) show profile (37) of antenna 500 MHz for site one.

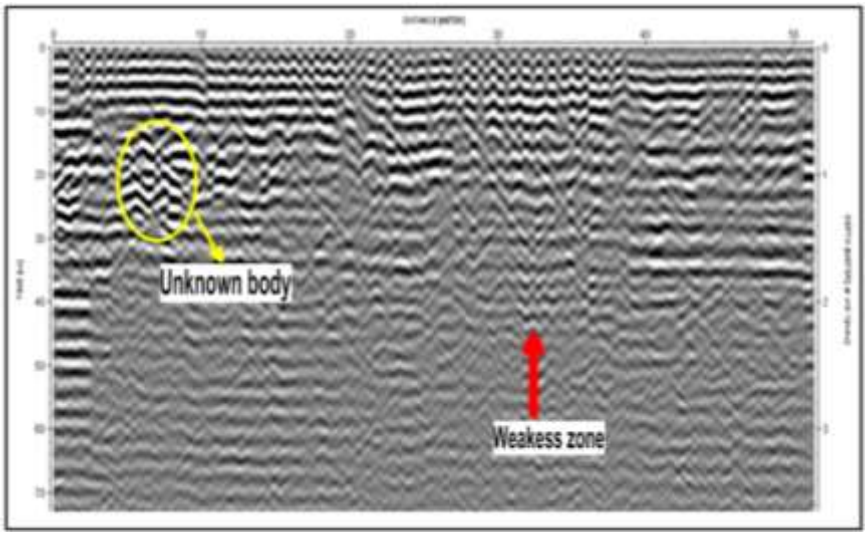

Fig.3.23: profile (38) of antenna 500 MHz for site one.

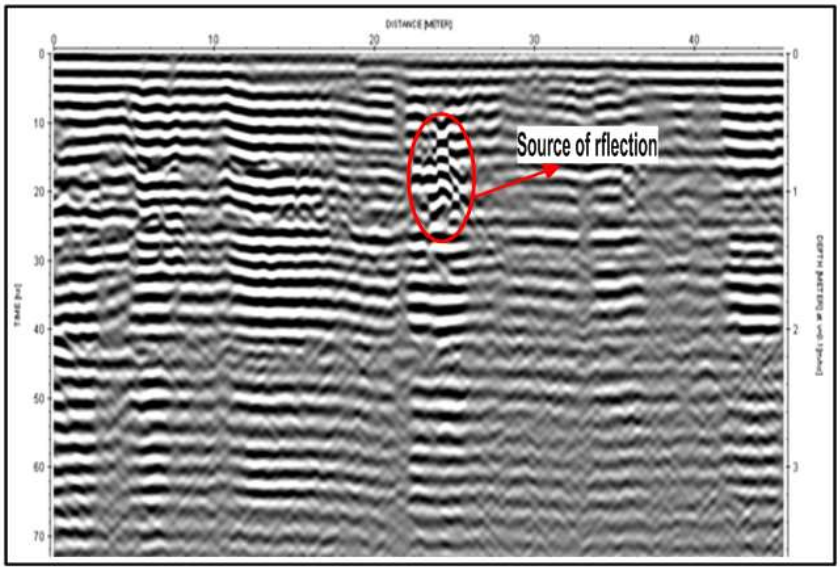

Fig.3.24: profile (41) transverse path of antenna 500 MHz for site one.

- **Site two:** figures (3.25, and 3.26) show many distinct weak areas in the upper part of the profiles marked in yellow, which may be caused by the presence of gaps or confusion of bodies buried in the soil. In addition to the presence of a clear anomaly that may be caused by a buried metal object that multiplied the electromagnetic waves forming the condition, which is known as the ringing and is visible in both profiles. As well as the presence of zones of soil saturation in which the reflections are almost non-existent.

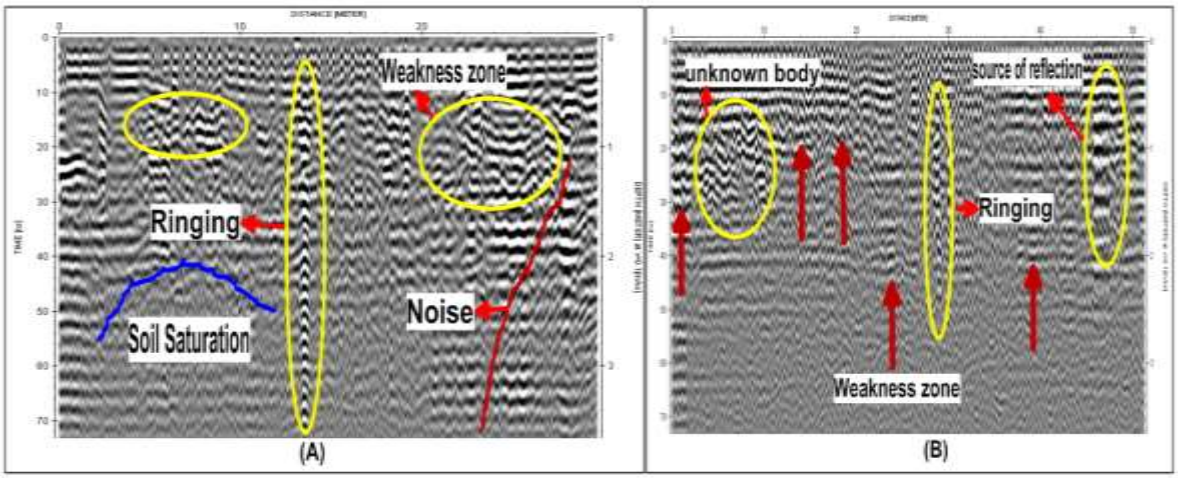

Fig. 3.25: (A) profile (43) and (B) profile (44) of antenna 500MHz for site two .

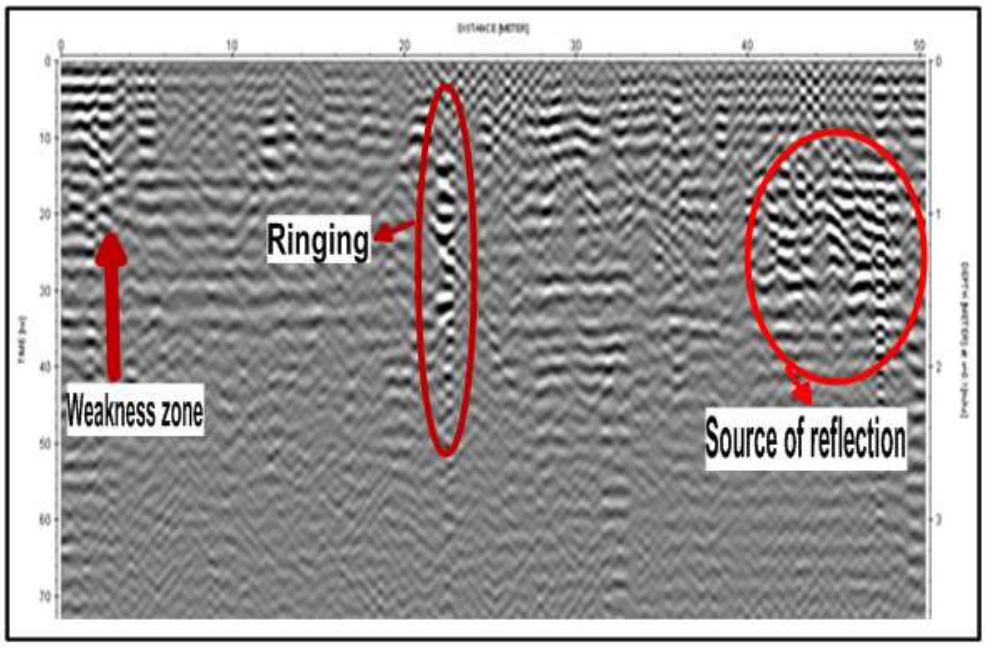

Fig. 3.26: profile (47) of antenna 500 MHz for site two.

- **Site three:** We notice in (figures 3.27, and 3.28) that the anomalies appear more clearly than they were in the 250MHz antenna, due to the high accuracy of this 500MHz antenna resulting from the short wavelength. Where it appears in profile 50 there are two objects (unknown body) indicated by yellow circles, they may be caused by the presence of bodies buried at these depths of 1m, in addition to many areas of weakness shown in this profile and indicated by red arrows. The bottom part of this profile shows saturated soil in which the reflections are not clear or non-existent. Profile 51 shows objects similar to the previous profile 50, and it is expected that they are caused by objects that were buried in the soil and at these depths, as well as the obvious weaknesses in this profile, which may be caused by the presence of gaps and areas of loosening in the soil.

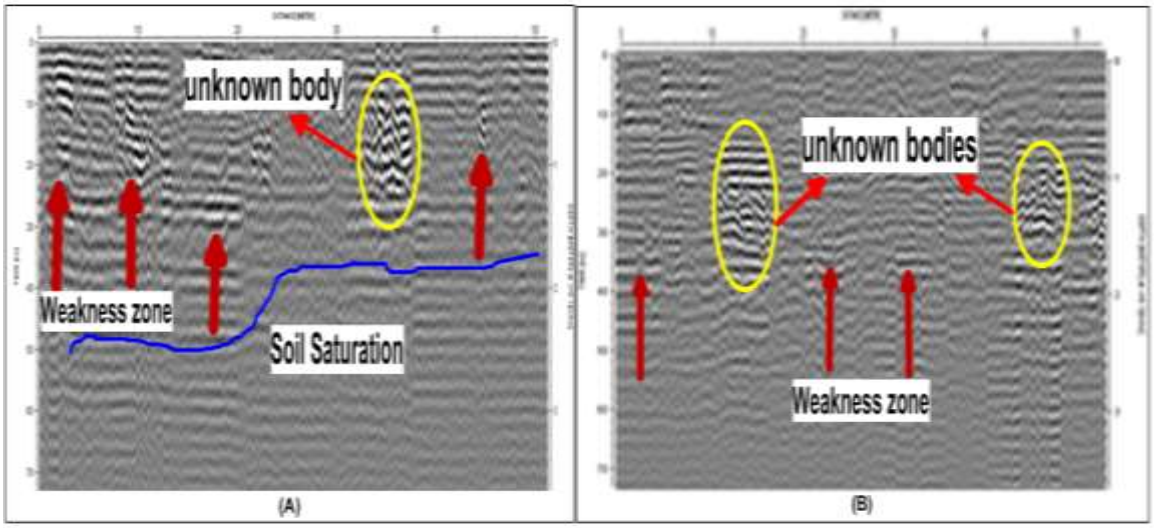

Fig. 3.27: (A) profile (50) and (B) profile (51) of antenna 500Mhz for site three .

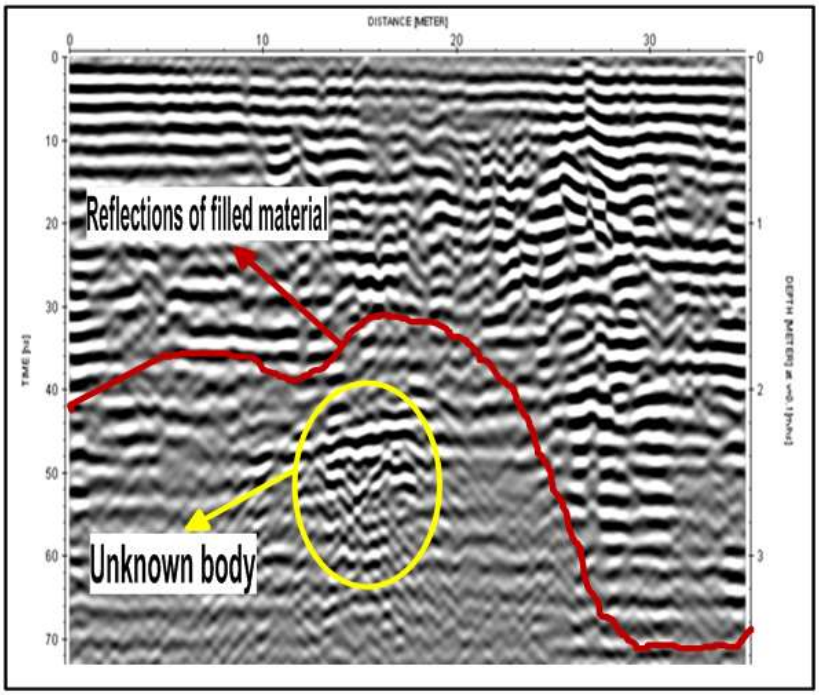

Fig. 3.28: Profile (52) of antenna 500 MHz for site three.

- **Site four:** Figures (3.29; 3.30) show a different group of anomalies represented by areas of saturated soil and areas filled with materials in addition to buried bodies. It is possible to refer here to the clarity in the picture compared to the 250 Hz antenna.

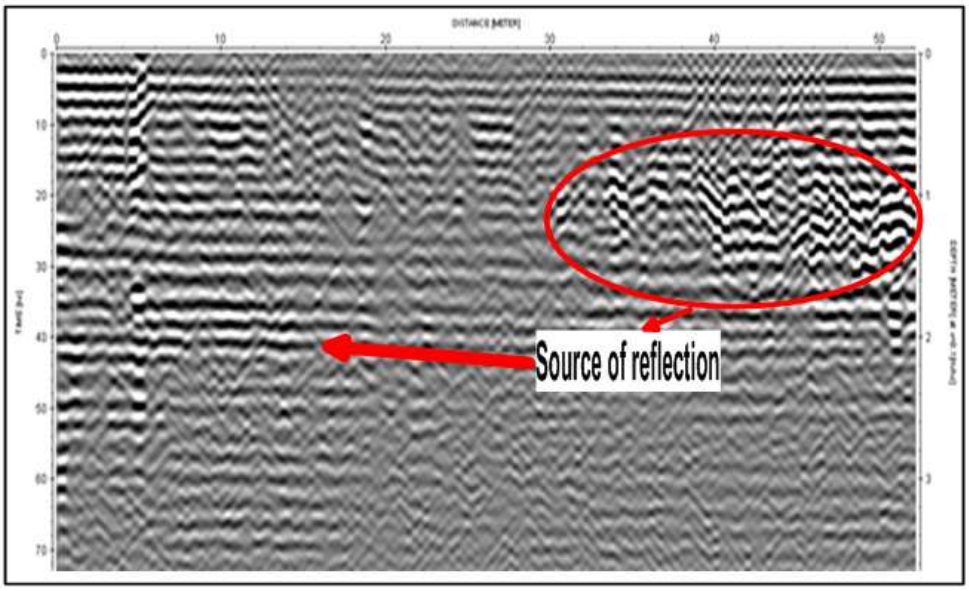

Fig. 3.29: Profile (57) of antenna 500 MHz for site four.

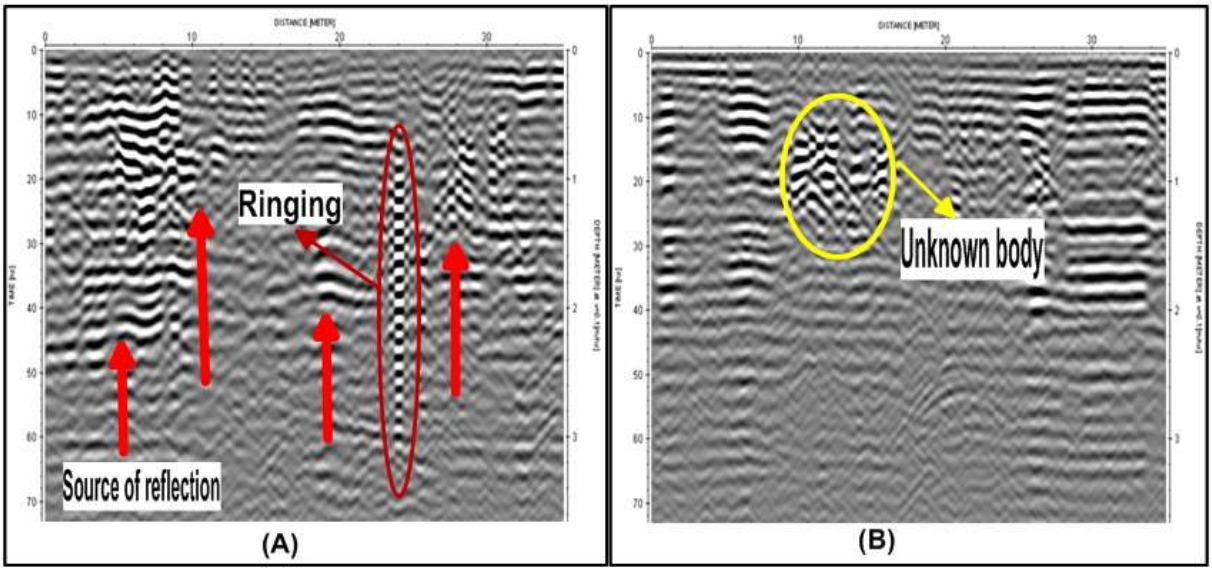

Fig. 3.30: (A) profile (58) and (B) profile (60) of antenna 500 MHz for site four.

- **Site five:** In the two sites from the figures (3.31 – 3.32), the GPR profiles show distinctive high amplitude reflections that may represent weak zone, ringing (type of noise), and clear reflections that represent the filled materials. These reflections are concentrated in the upper part of the profiles. There are no reflections in the lower part of the profiles, the reason for this is due to the shallowness of the groundwater, which leads to saturation of the soil and thus attenuates the radar waves.

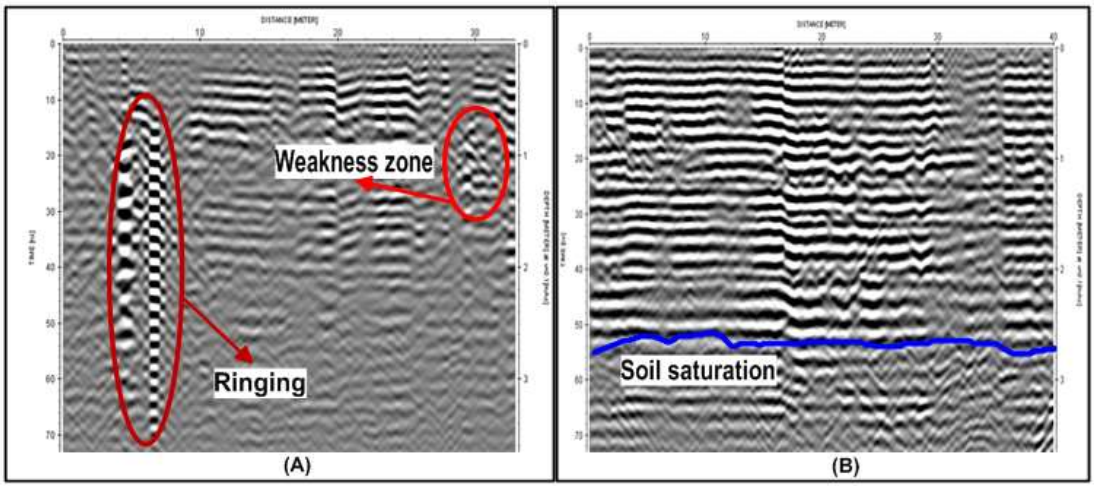

Fig. 3.31: (A) profile (64) and (B) profile (65) of antenna 500 MHz for site five.

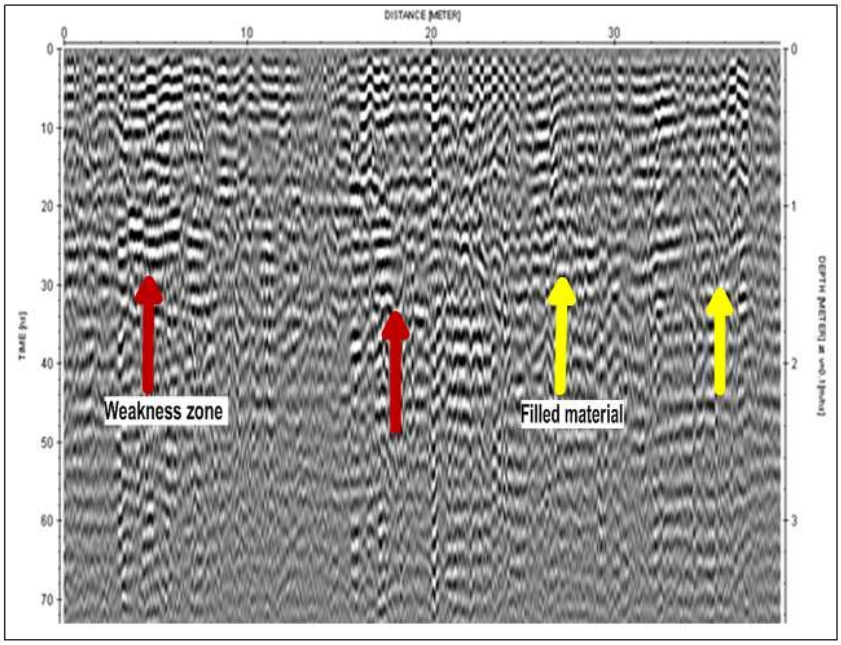

Fig.3.32: Profile (67) of antenna 500 MHz for site five.

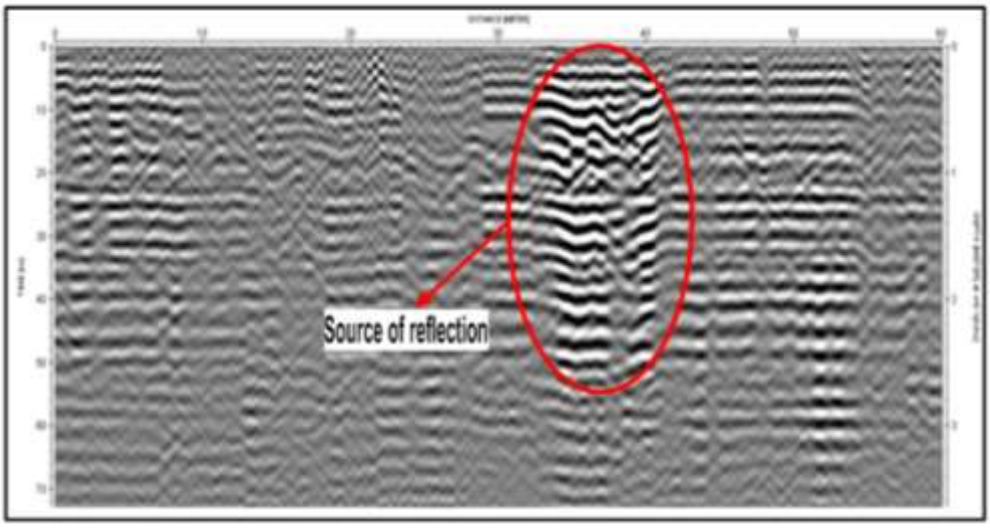

Fig.3.33: profile (70) transverse path of antenna 500MHz for site five.

The reflection appears in this transverse profile of this 500 MHz antenna more clearly than in the opposite profile 35 in the 250 MHz antenna, where the reflection source appears here surrounded by the red circle that it may be the result of an object buried at this depth.

3. 4 Discussion:

By interpreting the radar data, it becomes clear that the weakness zone is at a depth of 1 to 3 m (Fig. 3.4, Fig. 3.12, Fig 3.21). This corresponds to the excavated section near the first site (Fig. 3.34).

The geological section in the study area near site three consisted of the following layers of different nature and various thicknesses described below:

- Medium strengthen too stiff with depth, having brownish visions in colors, (Sandy)_ lean to fat Silty Clay with shiny crystals of soluble salts and black spots of organic matter/plants roots close to surface together with rusty (yellowish) traces of iron oxide compounds, overlying;
- Loose to medium dense strengthens with depth to dense and very dense, having grayish, greenish, and brownish appearances in colors, fine to medium-grained (Clayey) Silty Sand with rusty (yellowish) traces of iron oxide compounds and shiny crystals of silica minerals together with some fine-grained Gravel, intervened by a layer of very stiff (Sandy) fat Silty Clay having brownish visions in colors. In Figure (1.3), one of the well drilling records was taken to a depth of 20 m, which is the closest described to the first site in the study area.

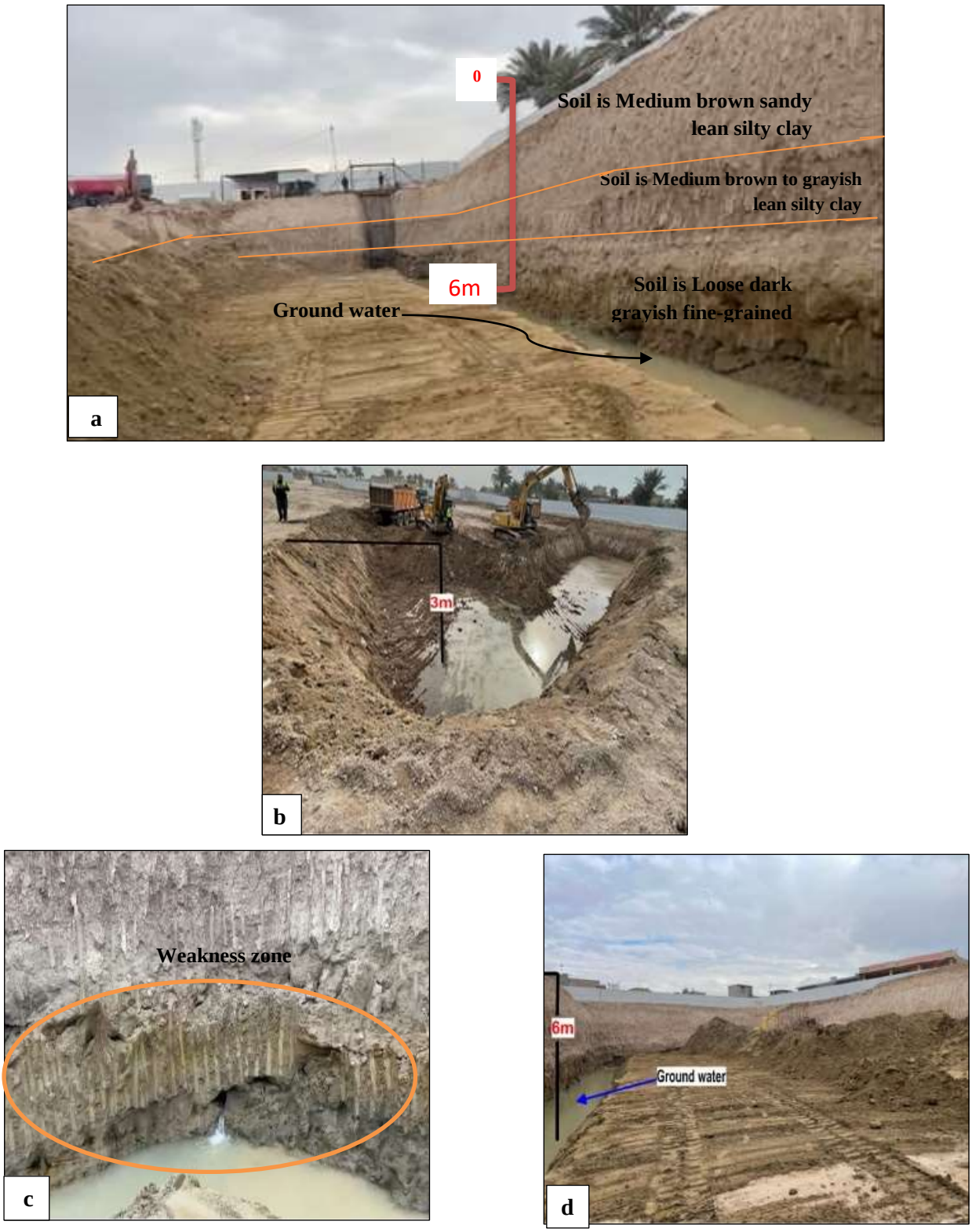

Fig. 3.34: Soil sections of site three.

Chapter four

Conclusion and Recommendations

4.1 Conclusion:

The conclusions of this study can be briefed as follows:

1. It has been demonstrated that GPR is a very easy-to-use technique for identifying buried bodies, weak zones, and soil subsidence.
2. Some obstacles related to the ground conditions can be overcome by utilizing some filters resulting in high resolutions after such processing.
3. The majority of radar grams' raw data does not initially show the presence of subsurface substances or structures. However, once the data had been processed and the proper filter and other interpretation tool parameters had been applied, many of the analysed subsurface structures became visible, demonstrating the excellent resolving power of the method.
4. In the wet condition, the depth of penetration, by GPR decreases reflecting the more clear appearance of the buried bodies near the surface than the deeper bodies.
5. The degree of clarity of subsurface bodies is dependent less on the higher dielectric constant of the bodies themselves and more on the dielectric contrast between the bodies and the host medium as well as the size of the body in relation to the buried object bodies that were visible in the same radar gram.
6. Through the present study, it was found that the effect of groundwater close to the surface leads to the formation of weak zones.
7. Radar technology has been effective in detecting and identifying clear collapse areas that are a reference to the weakness zone due to multiple stages of construction and at different time stages and a depth of about 6 m, in addition to the burial stages at interval times.
8. The results of this investigation show that the best detecting depths for 250 MHz and 500 MHz antennas are, respectively, 2 m and 4 m. In addition, the shallow groundwater is the main reason for the rapid attenuation of radar pulses.

4.2 Recommendations:

We recommend conducting a direct engineering geological study of the weak areas affecting the foundations of buildings in the city of Fallujah using the results of this study.

Using another geophysical method such as resistivity imaging survey and magnetic method to get more depth, support and comparison the results which is obtained within our study.

References

References

- Akinpelu, O. C. (2010). Ground Penetrating Radar Imaging of Ancient Clastic Deposits : A Tool for Three-Dimensional Outcrop Studies. Ph. D. thesis submitted to Geology Department University of Toronto.
- Al-Khafaji, A. J. M., 2010, "Geophysical and Geotechnical Investigations of Soil Underneath the Foundation of Al-Abbas Holy Shrine Site in Kerbala`a Governorate", Ph. D. thesis submitted to the College of Science in University of Baghdad.
- Al-Mattarneh H., 2008, Determination of Petroleum Contamination Level of Sandy Soil using Electromagnetic Measurement Techniques, Malaysia.
- Al-Nuaimy, W., Huang, Y., Nakhkash, M., Fang, M. T. C., Guyen, V.T.N. and Eriksen, A., 2000, "Automatic detection of buried utilities and solid objects with GPR using neural networks and pattern recognition", Journal of Applied Geophysics 43. P.p157–165.
- Al-Shijiri, Sabah Jasim Dahbush. (2013). Investigation of subsidence phenomena by GPR technique and geotechnical evaluation in Baghdad City. (Doctoral dissertations Theses and Dissertations Master). University of Baghdad, Iraq, https://search.emarefa.net/detail/BIM-609707
- American Society of Civil Engineers, Design and Construction of Urban Stormwater Management Systems, ASCE Publications, 1993.
- Annan, A.P. and Cosway, S.W., 1992. Ground penetrating radar survey design. Proceedings of the Symposium on the Application of Geophysics to Engineering and Environmental Problems, SAGEEP'92, Oakbrook, IL, April 26–29, pp. 329–351.
- Annan, A.P. (1999) Practical Processing of GPR Data. Sensors & Software Inc., 16 p.
- Annan, A.P. (2001) Ground Penetrating Radar Workshop Notes. Sensors & Software Inc., 192 p.

References

- Annan, A.P., 2002. The history of ground penetrating radar. Subsurface Sensing Technologies and Applications, Vol. 3, No. 4, October 2002, pp. 303–320.
- Annan, A.P., 2003. Ground penetrating radar: Principles, procedures & applications. Sensors and Software Inc. Technical Paper.
- Annan, A.P. (2005) Ground-Penetrating Radar. In: Butler, D.K. (ed) Nearsurface geophysics. Society of Exploration Geophysicists, Tulsa, Oklahoma, USA, pp. 357- 438.
- Annan, A.P. (2009) Electromagnetic Principles of Ground Penetrating Radar. In: Jol, H.M. (ed) Ground Penetrating Radar Theory and Applications. Elsevier B.V., Amsterdam, pp. 1-40.
- Atekwana E. A., W. A. Sauck, and D. D. Werkema, 2000. Investigations of geoelectrical signatures at a hydrocarbon contaminated site. Journal of Applied Geophysics, 44 (2-3), 167–180.
- Björklund, N. and Johnsson, T. (2005) Real-time Sampling of Ground Penetrating Radar and Related Processing. M.Sc. Thesis, Department of Computer Science and Electrical Engineering, Luleå University of Technology, 29 p.
- Braun, A. (2019). Radar satellite imagery for humanitarian response: Bridging the gap between technology and application. 225. https://publikationen.uni tuebingen.de/xmlui/bitstream/handle/10900/91317/Braun 2019 Radar satellite imagery for humanitarian response UB.pdf?sequence=1.
- Buday, T. and Jassim, S. Z., 1987. The Regional Geology of Iraq. Volume 2, Tectonism, Magmatism, and Metamorphism. Printed by Geological Survey and Mineral Investigation, Baghdad, Iraq, 352 p.
- Carrick Utsi, E. (2017). Data Processing. In Ground Penetrating Radar (pp. 83–92). Elsevier. https://doi.org/10.1016/B978-0-08-102216-0.00008-4Carrick Utsi, E. (2017).

References

- Cassidy, N. J., 2007. Evaluating LNAPL contamination using gpr signal attenuation analysis and dielectric property measurements: Practical implications for hydrological studies. Journal of Contaminant Hydrology, 94, 49–75.
- Cassidy, N.J. (2009) Ground Penetrating Radar Data Processing, Modelling and Analysis. In: Jol, H.M. (ed) Ground Penetrating Radar Theory and Applications. Elsevier B.V., Amsterdam, pp. 141-172.
- Chen, Tai-Lin G., 2006, "GPR Propagation Simulation and Fat Dipole Antenna Design", M.sc. dissertation submitted to the Department of Electrical Engineering, University of Cape Town.
- Conyers, L.B. (2004) Ground-penetrating radar for archaeology. AltaMira Press, Walnut Creek, California, 205 p.
- Conyers, L.B. (2013) Ground-Penetrating Radar for Archaeology. AltaMira Press, Walnut Creek, California, 220 p.
- Daniels, J. J. (2000). Ground Penetrating Radar Fundamentals. USEPA Publication, Appendix, 1–21. papers2://publication/uuid/B797387B-354B-4A17-98D7-FBEB34EF590B
- Daniels, J.J., Ehsani, M.R., and Allred, B.I., (2008) Ground-Penetrating Radar Methods (GPR). In: Allred, B.I., Daniels, J.J. and Ehsani, M.R. (eds) Handbook of Agricultural Geophysics. First edition, CRC Press, pp.129-145
- Dante, F., 2007, Electromagnetic and electrical resistivity methods.
- Davis, J.L. and Annan A.P. (1989) Ground-penetrating radar for high resolution mapping of soil and rock stratigraphy. Geophysical Prospecting, 37, 531-551.
- Dojack, L. (2012) Ground Penetrating Radar Theory, Data Collection, Processing, and Interpretation: A Guide for Archaeologists. Vancouver, University of British Colombia, 94 p.

References

- Forte, E., Bondini, M. B., Bortoletto, A., Dossi, M., & Colucci, R. R. (2019). Pros and Cons in Helicopter-Borne GPR Data Acquisition on Rugged Mountainous Areas: Critical Analysis and Practical Guidelines. Pure and Applied Geophysics, 1-22.
- Fouad, S. F. 2015. Tectonic map of Iraq, scale 1: 1000 000, 2012. Iraqi Bulletin of Geology and Mining, 11(1), 1-7.
- Goodman, D., Piro, P., Nishimura, Y., Schneider, K., Hongo, H., Higashi, N., Steinberg, J. and Damiata, B. (2009) GPR Archaeometry. In: Jol, H.M. (ed) Ground Penetrating Radar Theory and Applications. Elsevier B.V., Amsterdam, pp. 479-508.
- Goodman, D. and Piro, S. (2013) GPR Remote Sensing in Archaeology. Springer-Verlag, New York, 233 p.
- Group, B.W., Groundwater Resources in Burried Valleys: A Challenge for Geosciences, R. Kirsch, et al., Editors. 2006, Leibniz Institute for Applied Geosciences (GGA-Institut): Hannover. p. 296.
- Griffin, S. and Pippett, T., 2002, “Ground Penetrating Radar”, Geophysical and Remote Sensing Methods for Regolith Exploration, 144, pp 80-89.
- Haidar Abbas Neam Al-dami, "GPR data simulation for engineering investigations in shallow regions" M.sc. thesis University of Technology in Baghdad, 2011.
- Hanninen, P. (1992) Application of ground penetrating radar techniques to peatland investigations. In Proceedings: Fourth International Conference on Ground-Penetrating Radar, Geological Survey of Finland, Special Paper 16, Rovaniemi, Finland. pp. 217–221.
- Haramy, K., et al. (2009) A Comparison of Non-Invasive Geophysical Methods for Mapping Near-Surface Voids.

References

- Harris, D. (2006) Pavement Thickness Evaluation Using Ground Penetrating Radar (GPR). Ph.D. Dissertation, Faculty of Engineering and technology, Purdue University, 327 p.
- Harry, M.J., 2009. Ground Penetrating Radar, Theory and Applications. London: Elsevier Science. 524.
- Illawathure, C. (2019). Improving the GPR reflection method for estimating soil moisture and detection of capillary fringe and water table in a boreal agricultural field. (Doctoral dissertation, Memorial University of Newfoundland).
- Investigation, S. (2007). Standard Guide for Using the Surface Ground Penetrating Radar Method for. 99(Reapproved 2005), 1–18. https://doi.org/10.1520/D6432-11.2
- Johansson, B. and Friborg, J. (2005) Applied GPR technology, theory and practice. First Edition, Malå Geosciences, 150 p.
- Jol, H. M., and Bristow, C. S. (2003). GPR in sediments: advice on data collection, basic processing and interpretation, a good practice guide. Geological Society, London, Special Publications, 211(1), 9-27.
- Jol, H. M. (Ed.). (2009). "Ground penetrating radar theory and applications". London: Elsevier Science. 524.
- Kearey, P., Brooks, Michael and Hill, I., 2002, "An Introduction to Geophysical Exploration", Third Edition, Blackwell Science Ltd.
- Khuut, T., 2009, "Application of Polarimetric GPR to detection of subsurface objects", Ph. D. thesis for Graduate School of Environmental Studies Of Tohoku University.
- Linford, N. (2006). The application of geophysical methods to archaeological prospection. Reports on Progress in Physics, 69(7), 2205–2257. https://doi.org/10.1088/0034-4885/69/7/R04.

References

- Loulizi, A. , 2001, "Development of Ground Penetrating Radar Signal Modeling and Implementation for Transportation Infrastructure Assessment", Thesis for the Degree of Doctor, the Faculty of theVirginia Polytechnic Institute and State University.
- Lowrie, W., 2007, Fundamental's geophysics, Cambridge University, Second Edition, 375p.
- MALÅ (2005) XV Monitor for ProEx and X3M with Ethernet Communication: Operating manual v. 1.5, 56 p.
- MALÅ (2008) ProEx-Professional Explorer Control Unit: Operating Manual v. 2.0, 60 p.
- MALÅ Geoscience AB. (2011). MALÅ ProEx Professional Explorer Control Unit. Operating Manual v. 2.0. 61.
- MALA Geoscience. (2016). MALÅ Shielded Antennas. Antenna, 2. https://www.malagpr.com.au/uploads/3/7/9/4/37942849/mala_gpr_-_shielded_antennas.pdf.
- Matzner, R. A., 2001, "Geophysics, Astrophysic, and Astronomy, Comprehensive dictionary of physics", CRC Press LLC, Library of Congress Card Number 2001025764.
- Mines, V. A. N. D., & Report, A. (2010). Geophysical Services for the Environmental , Engineering and Ordnance Industries STRATAGEM SYSTEM. March.
- Neal, A. (2004) Ground-penetrating radar and its use in sedimentology: principles, problems and progress. Earth-Science Reviews, 66 (3–4), 261–330.
- Nehaba, M.S. (2019) Investigation of subsurface archaeological features using Ground Penetrating Radar (GPR) in ancient Babylon (South Baghdad/Iraq). M.Sc. Thesis, College of Science, University of Baghdad, 107 p.

References

- Neubauer, W., Eder-Hinterleitner, A., Seren, S. and Melichar, P. (2002) Georadar in the Roman Civil Town Carnuntum, Austria: An Approach for Archaeological Interpretation of GPR Data. Archaeological Prospection, 9, 135-156.
- Nissen, J., Johansson, B., Wolf , M. J., Skoog, L., 2001, "Ground Penetrating Radar a ground investigation method applied to utility locating in no-dig technologies", Malå Geoscience Raycon Stockholm. Pp. 1-6.
- Olhoeft, G. R. (2000). Maximizing the information return from ground penetrating radar. Journal of Applied Geophysics, 43(2–4), 175–187. https://doi.org/10.1016/S0926-9851(99)00057-9
- Olhoeft, Gary R. Geophysics Advisor Expert System. [Denver, CO]: U.S. Geological Survey, 1988.
- Ortyl, Ł. (2006) Examination of Influence of A GPR-GPS Measuring Set External Elements on Results of Georadar Sensing. In Proceedings: The Geodesy and Environmental Engineering Commission, Geodesy 42, Polish Academy of Sciences - Cracow Branch, pp. 45–60.
- Oswin ,J. ,(2009),A Field guide to geophysics in archaeology, Praxis Publishing, No 2009925774 , Chic Ester, UK, 243p.
- Parasnis, D.S. (1972) Principles of Applied Geophysics. Chapman and Hall, 214 pp.
- Parkin, G., Redman, D., von Bertoldi, P. and Zhang, Z. (2000) Measurement of soil water content below a wastewater trench using ground-penetrating radar. Water Resources Research, 36(8), 2147–2154.
- Platform, D. A., & Interface, U. (n.d.). MALÅ XV Monitor ™. 11–12. https://www.malagpr.com.au/uploads/3/7/9/4/37942849/mala_gpr_-_xv_monitor.pdf

References

- Reynolds, J.M. (1997) An introduction to applied and environmental geophysics. John Wiley and Sons Ltd, New York, 796 p.
- Robinson, M., Bristow, C., McKinley, J., & Ruffell, A. 1.5. 5. (2013) Ground Penetrating Radar.
- Saeed, H. F. M., 2010, "GPR Method and its Engineering Application in Baghdad University Site", M.sc. thesis Submitted to the College of Science in Baghdad University.
- Sandmeier, K.J., ReflexW Version 5.0 Manual. 2009, Sandmeier Scientific Software: Karlsruhe, Germany.
- Sensors and Software. (2001). EKKO-for-DVL pulseEKKO 100: User's Guide Version 1.0, Technical Manual 30. Sensors and Software Inc. pp. 66.
- Sensors and Software Inc. (2018). EKKO Project Processing Module User's Guide. Sensors and Software Inc., Ontario. pp. 102.
- Sensors & Software (2019) Sensors & Software Inc., http://www.sensoft.ca/, accessed June 2, 2019.
- Sheriff, S. (2010) *Processing Ramac GPR Data with Reflex*. 1-7.
- Smith G. S., 1997, an Introduction to Classical Electromagnetic,Radiation. http://www.amazon.com/exec/obidos/ASIN/0521580935/groradar).
- Steelman, C. M., & Endres, A. L. (2012). "Assessing vertical soil moisture dynamics using multi-frequency GPR common-midpoint soundings". Journal of Hydrology, 436, 51-66.
- Stolarczyk L. G., Peng S. S., 2003, Advanced Electromagnetic Wave Technologies for the Detection of Abandoned Mine Entries and Delineation of Barrier Pillars, a Research Presented to Mine Safety and

References

Healthy Administration (MSHA) and Office of Surface Mining Reclamation and Enforcement (OSMRE).

- Theimer, B.D., Nobes, D.C. and Warner, B.G. (1994) A study of the geoelectrical properties of peatlands and their influence on groundpenetrating radar surveying, Geophysical Prospecting, 42, 179-209.
- Utsi, E. C. (2017). Ground penetrating radar: theory and practice: Butterworth- Heinemann. Pp 209.
- WHO (1993) Electromagnetic Fields (300 Hz to 300 GHz). World Health Organization, Environmental Health Criteria 137, United Nations Environment Programme, Geneva, Switzerland, 293 p.
- Yochim, April, Zytner, Richard G. Zytner, McBean, Edward A. & Endres, Anthony L. (2013), "Estimating water content in an active landfill with the aid of GPR". Waste Management, 33(10):2015-2028.

Appendices

Appendices

Appendix 1: profiles of antenna 250 MHz.

- **Site 1:**

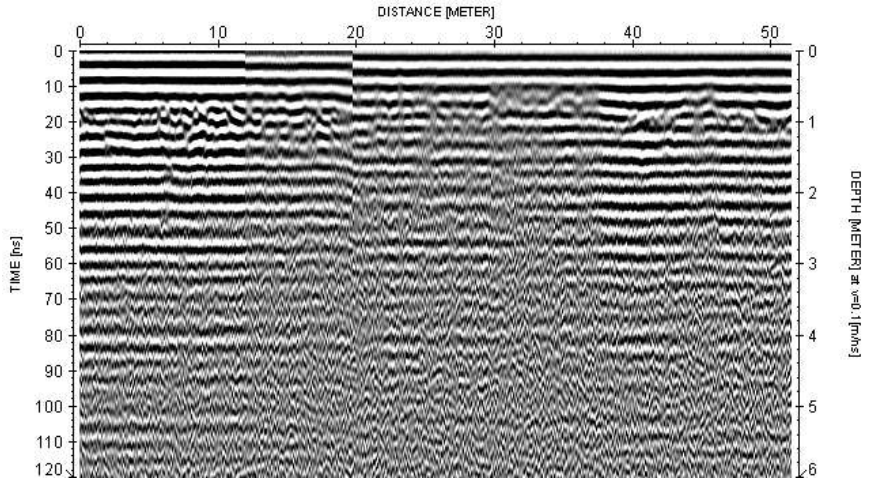

Profile 3

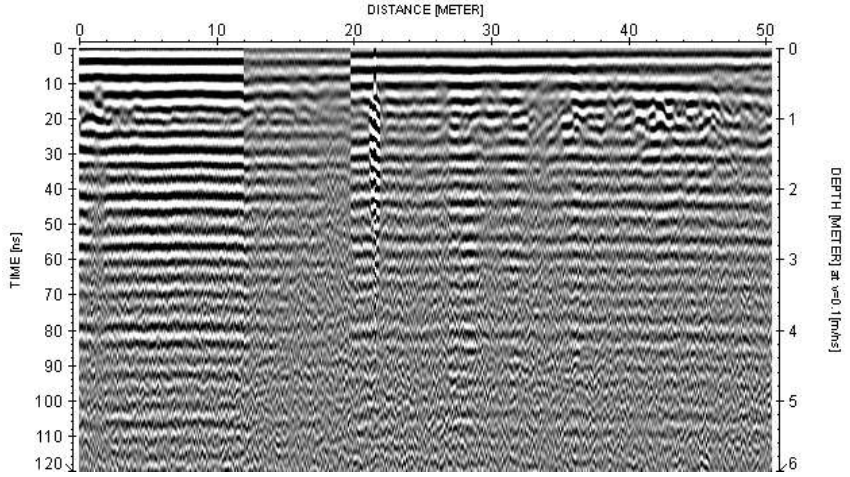

Profile 4

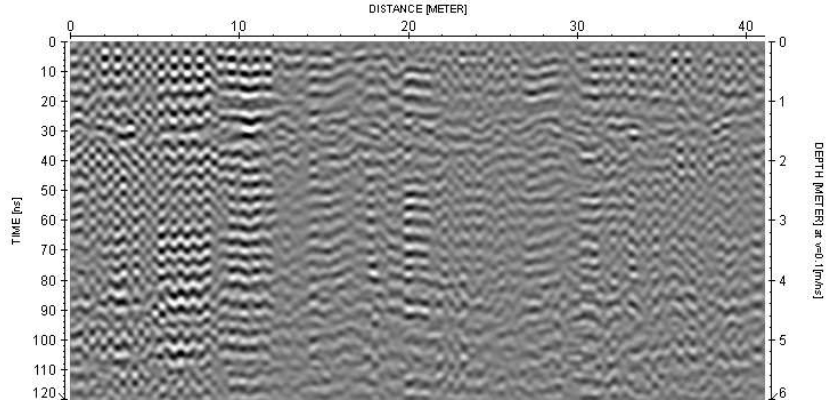

Profile 6

Appendices

- **Site 2:**

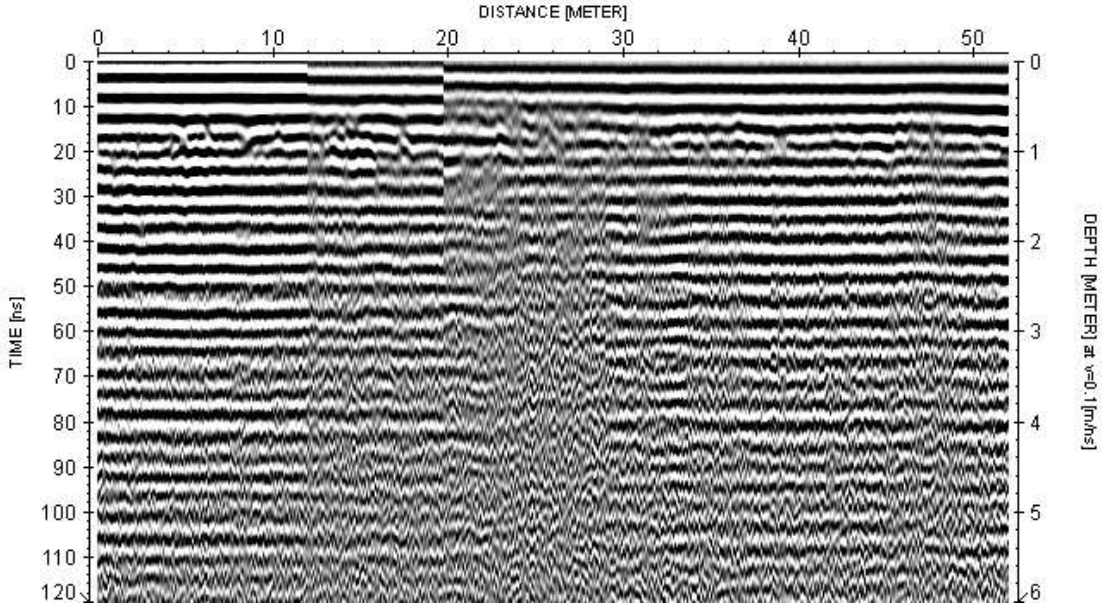

Profile 10

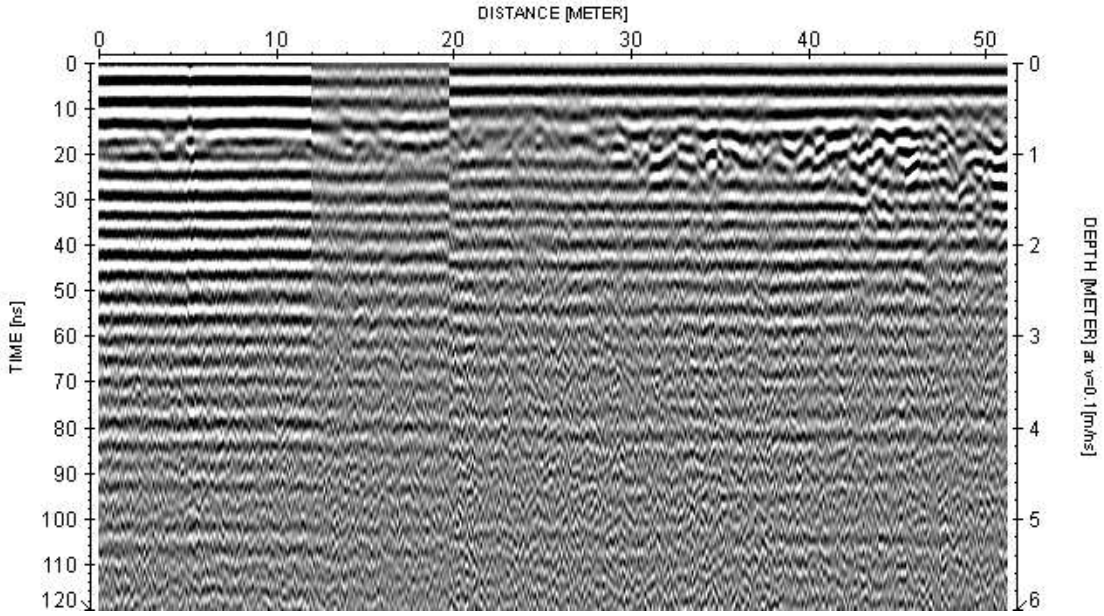

Profile 11

Appendices

- **Site 3:**

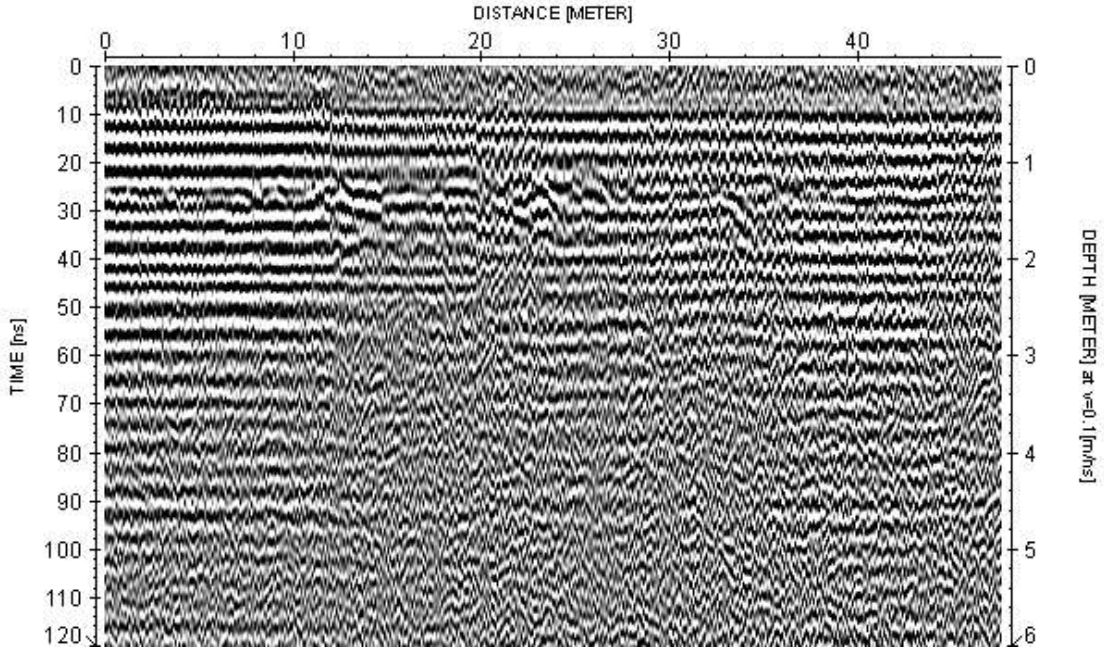

Profile 18

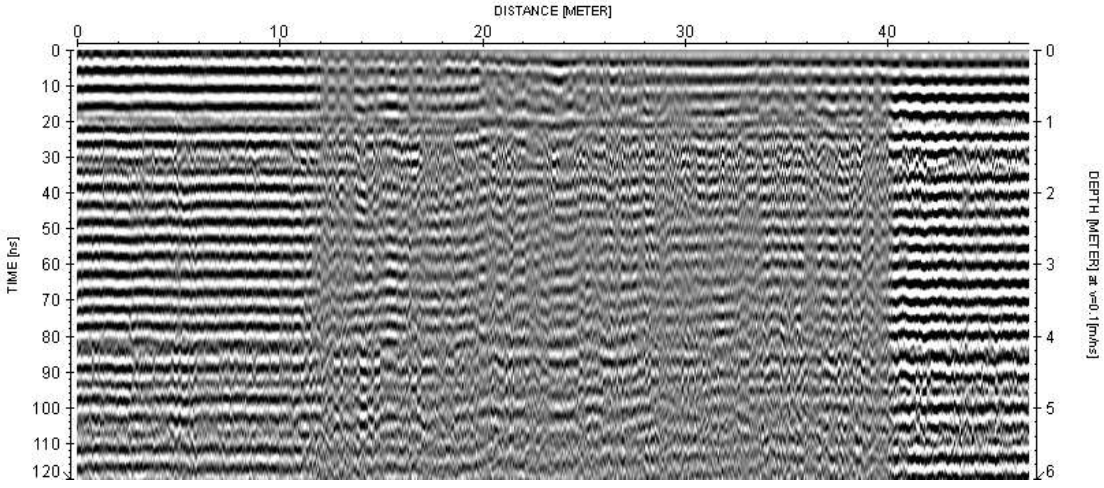

Profile 19

- **Site 4:**

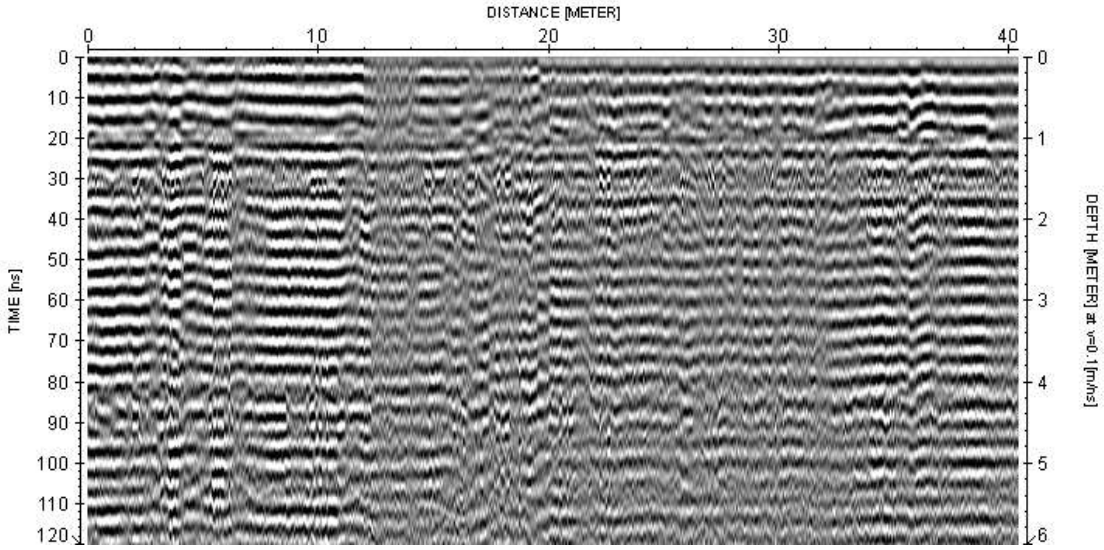

Profile 22

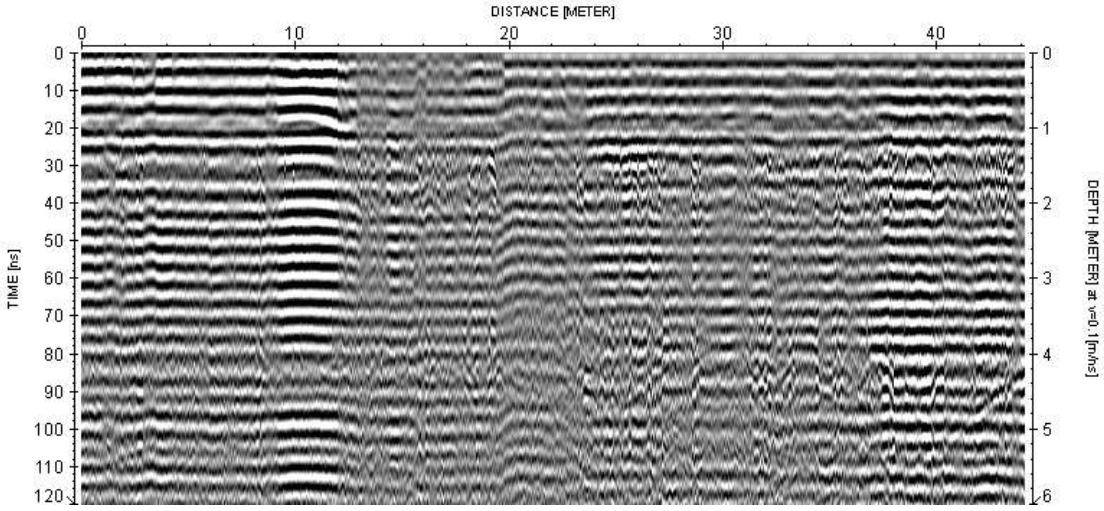

profile 24

Appendices

- **Site 5:**

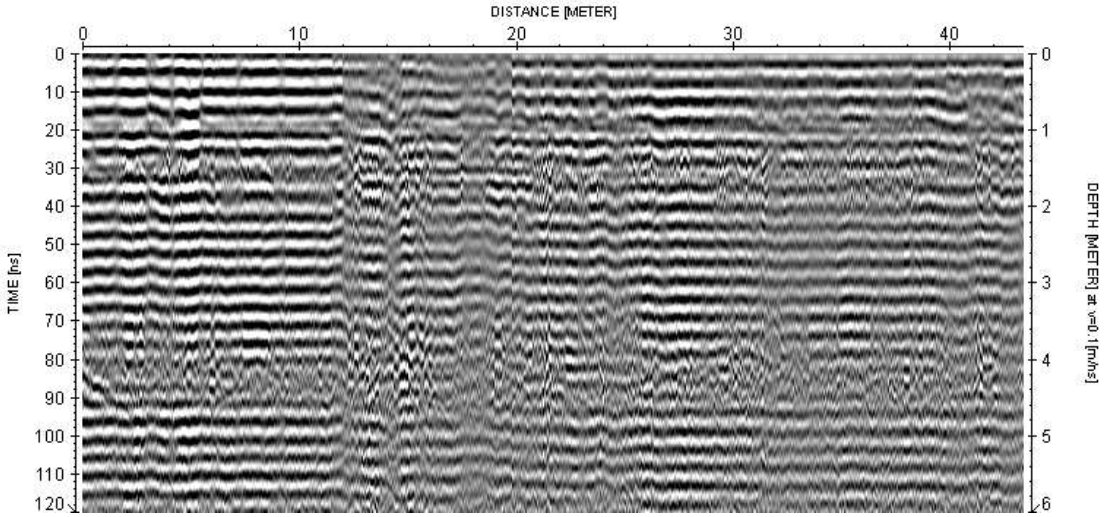

Profile 30

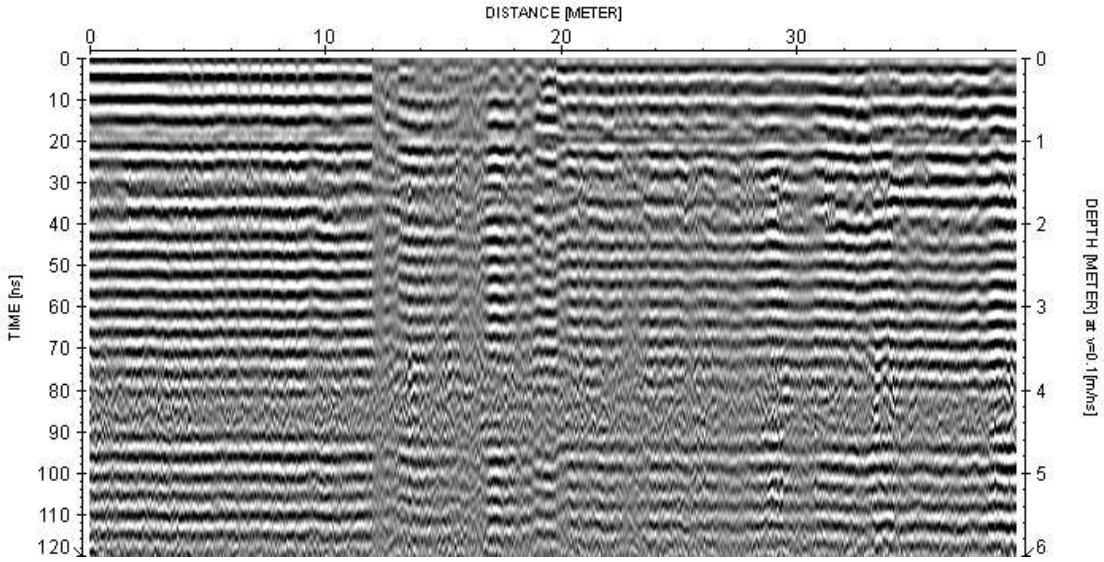

Profile 33

Appendix 2: profiles of antenna 500 MHz.

- **Site 1:**

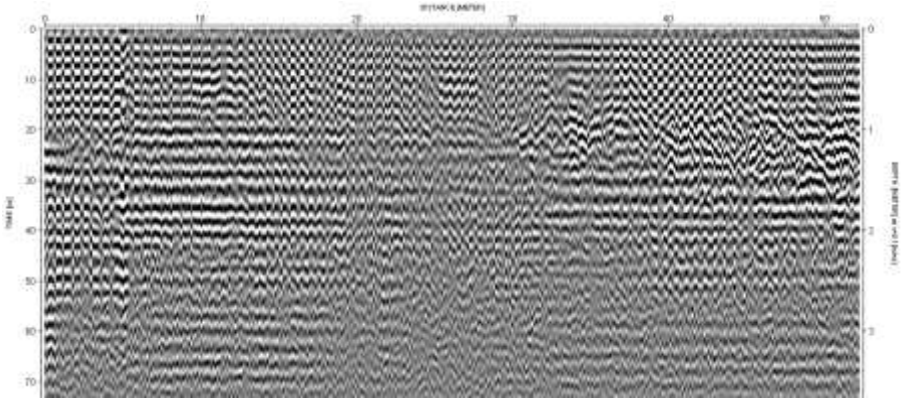

Profile 39

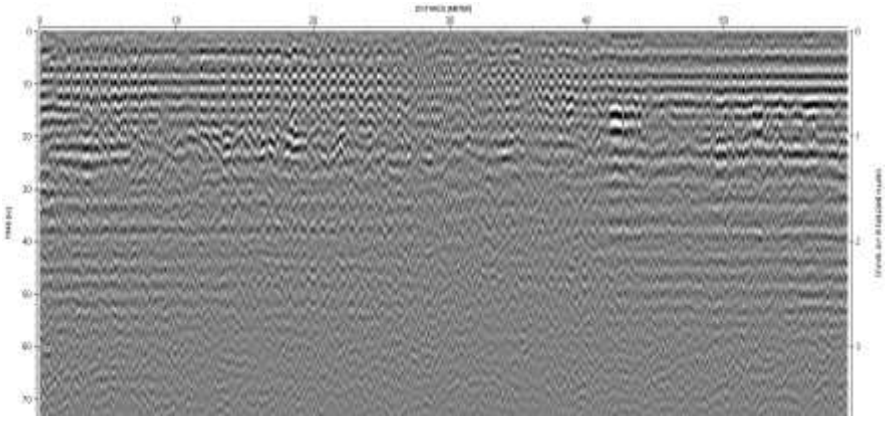

profile 40

- **site 2:**

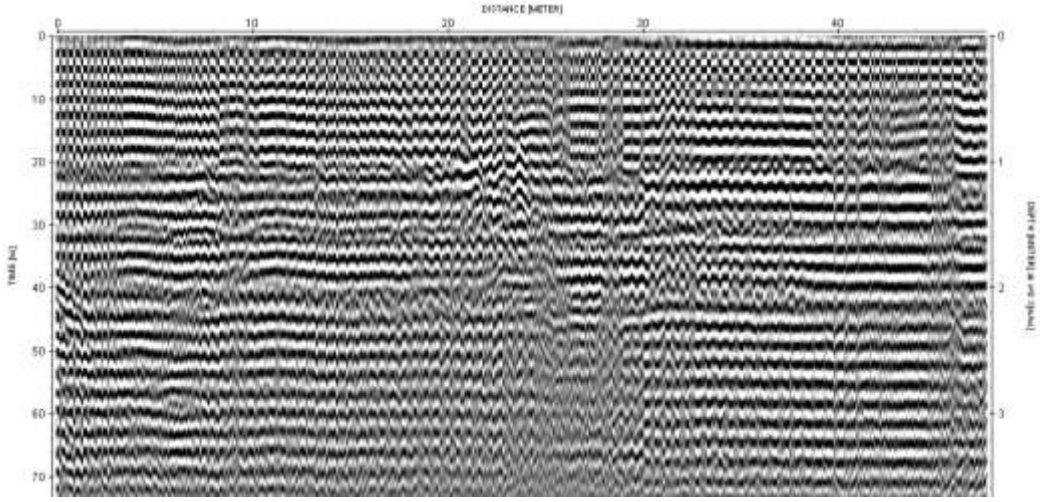

Profile 45

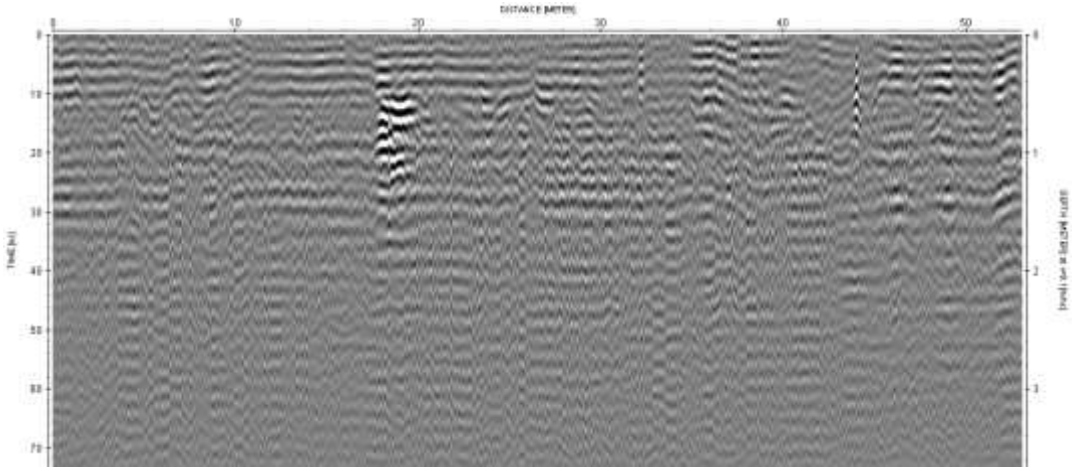

Profile 46

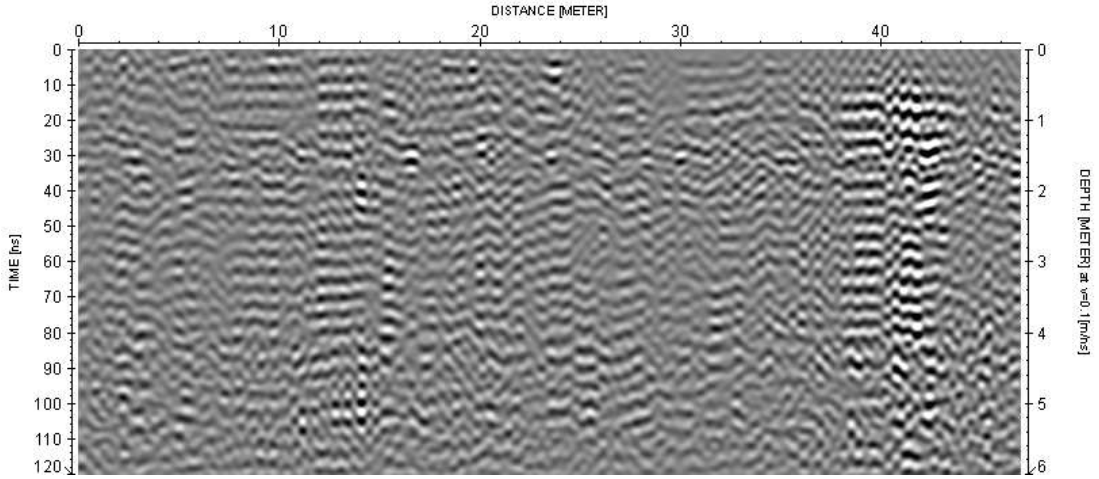

Profile 49

Appendices

- **Site 3:**

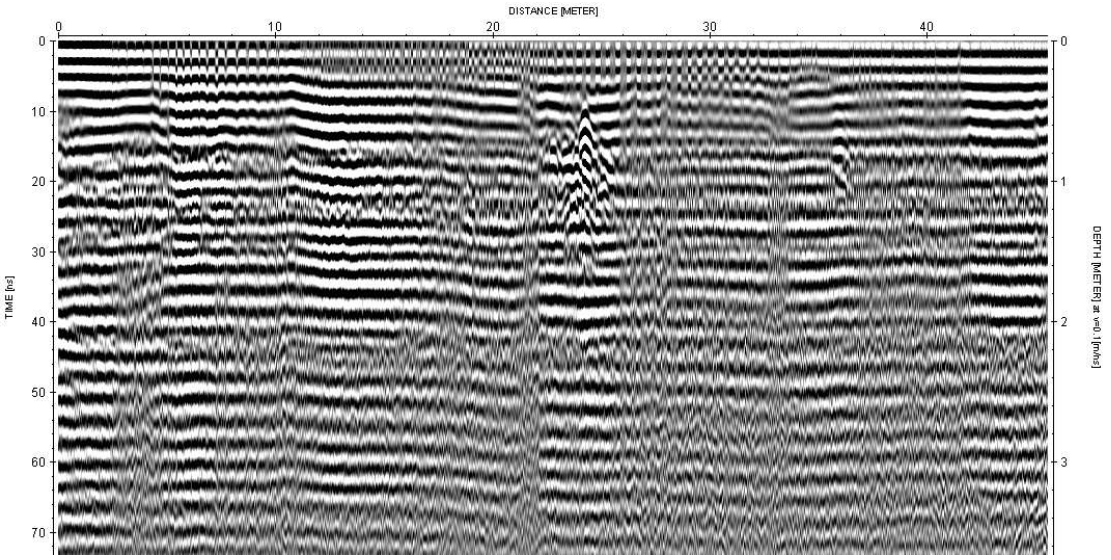

Profile 53

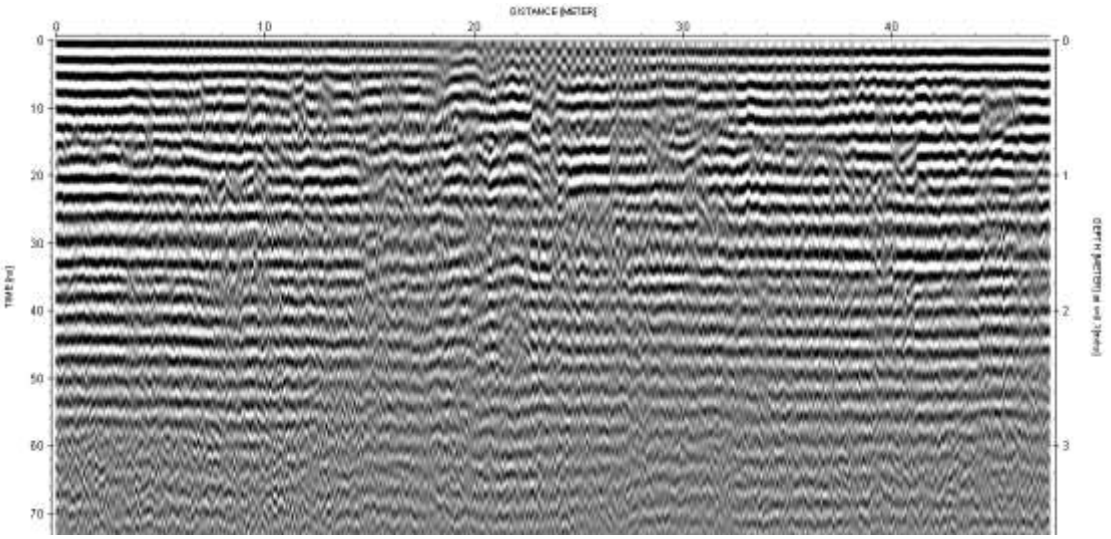

Profile 54

- **Site 4:**

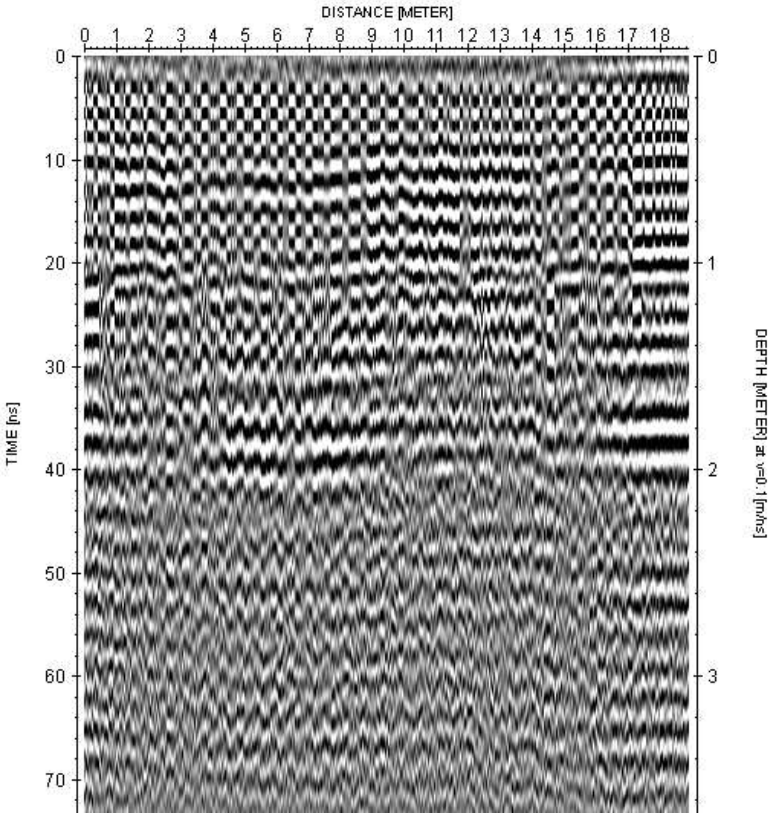

Profile 59

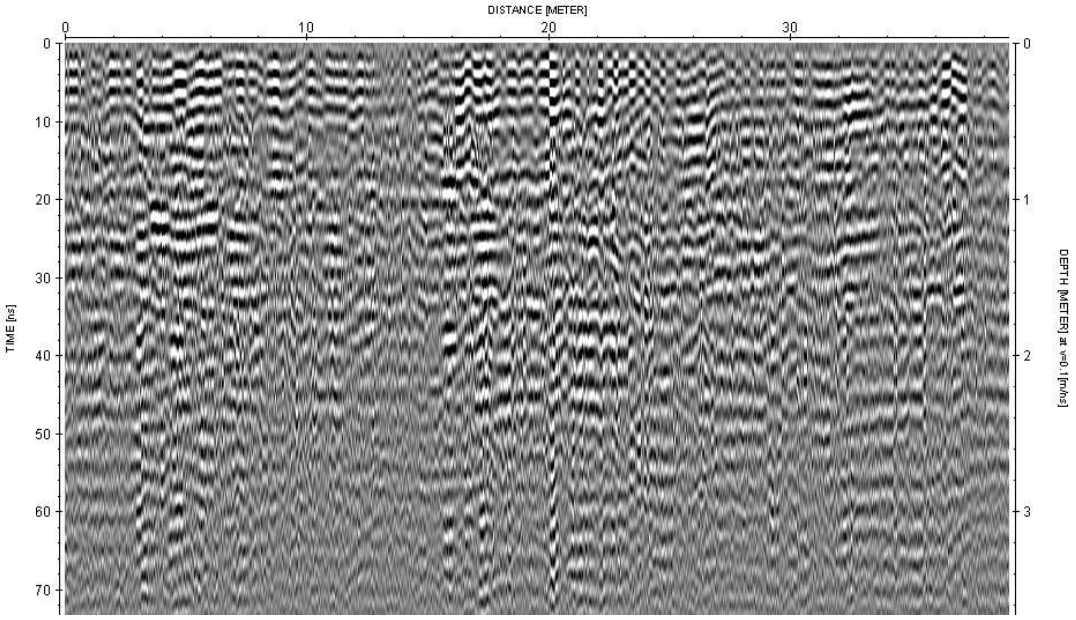

Profile 61

Appendices

Site 5:

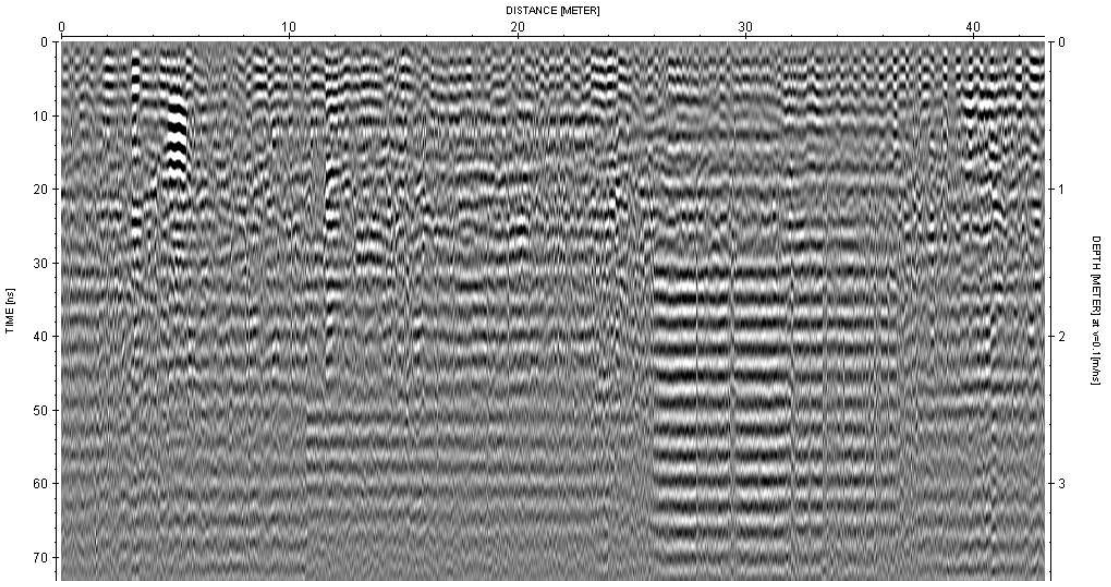

Profile 66

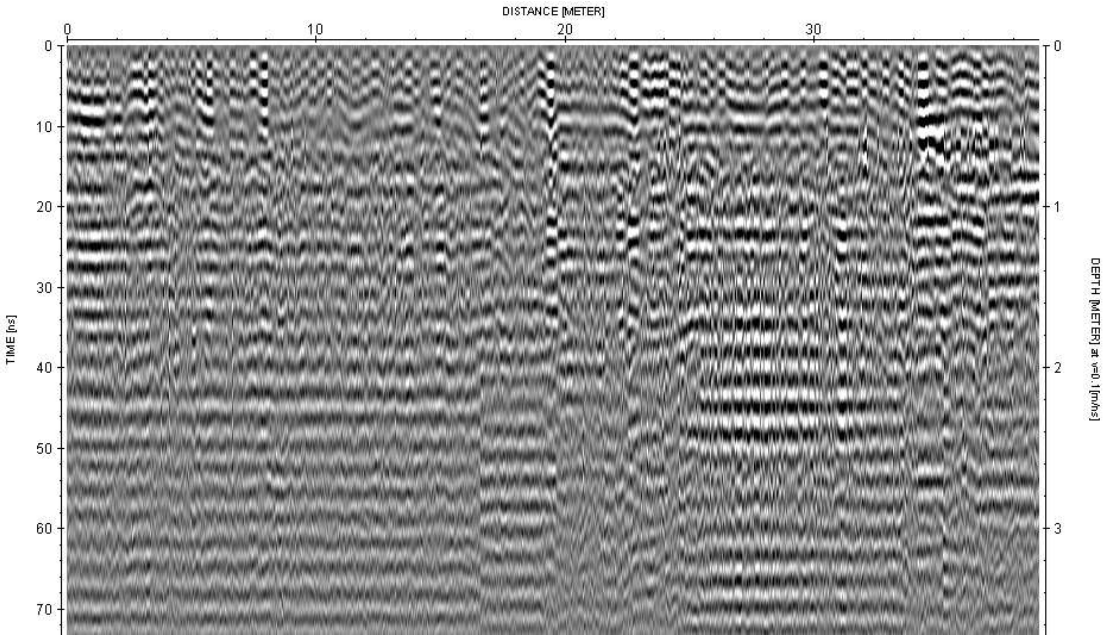

Profile 68

Appendices

المستخلص

تم استخدام تقنية رادار الاختراق الأرضي (GPR) في مدينة الفلوجة بمحافظة الأنبار كطريقة غير مدمرة وسريعة وذات تكلفة منخفضة وقوية في اكتشاف أي تغيير في مكونات المواد الجوفية التي يمكن بالتالي تطبيقها في المناطق الحضرية والانشائية. الهدف الرئيسي من هذه الدراسة هو محاكاة بيانات GPR الخاصة بمسبار الهندسة الضحلة التي تم الحصول عليها بواسطة هوائيات 250MHzو 500. تم تنفيذ هذا العمل في خمسة مواقع مختلفة ، في كل موقع تم اختيار 5 مسارات متوازية ، وتختلف أطوال المسارات واتجاهاتها من موقع إلى آخر ، والمسافة بين كل مسار واخر هي 5 أمتار. تم استيراد بيانات GPR التي تم جمعها ومعالجتها باستخدام برنامج ReflexW^{TM} وهو برنامج حزمة مستقل يمكنه استيراد مجموعة من أنواع البيانات المختلفة ومعالجتها. اعتمادًا على نوع الهوائي ، يتراوح عمق الاختراق من 3 إلى 6 أمتار في منطقة الدراسة. تم اكتشاف العديد من الأجسام المدفونة ومناطق الضعف والفجوات في الأعماق الضحلة. ومناطق الضعف تتمثل في هشاشة التربة وضحالة المياه الجوفية مما يؤثر على أسس الأبنية في المدينة.

بعد معالجة بيانات الرادار ،تبين وجود العديد من الشواذ في كل موقع مسح , نظرًا للتلامس الضحل والتباين الكبير بين طبقات التربة الرخوة والمضغوطة ، يكون الجزء الاعلى اكثر وضوحا في جميع البروفايلات في الهوائي 250MHz , والهوائي 500MHz. وبعد تفسير بيانات GPR تظهر انعكاسات مميزة ايضا ويعتقد أنها تمثل أجسامًا مدفونة بالقرب من السطح, بالاضافة الى وجود العديد من الانعكاسات المميزة والتي تكون واضحة في اغلب البروفايلات المعالجة وتكون ناتجة عن شذوذ يمثل مصدر الانعكاسات. بسبب ضحالة المياه الجوفية وصعودها بالقرب من السطح ، تظهر العديد من مناطق الضعف متمثلة في الفراغات والمتواجدة في اغلب البروفايلات المعالجة.

جمهورية العراق

وزارة التعليم العالي والبحث العلمي

جامعة الانبار

كلية العلوم

قسم الجيولوجيا التطبيقية

التطبيقات الهندسية لطريقة رادار الاختراق الارضي في مدينة الفلوجة

رسالة مقدمة الى مجلس كلية العلوم / جامعة الانبار

وهي جزء من متطلبات نيل شهادة الماجستيرفي الجيولوجيا التطبيقية

من قبل

زياد ناجح عبد الحميد

بكالوريوس جيولوجيا تطبيقية ٢٠١٩

باشراف

أ.د. علي مشعل عبد

د. حيدر عبدالزهرة الدباغ

١٤٤٤هـ **٢٠٢٢م**